

ISOCYANATE FUNCTIONALIZATION OF NANO-BOEHMITE
FOR THE SYNTHESIS OF POLYURETHANE
ORGANIC-INORGANIC HYBRID MATERIALS

A THESIS SUBMITTED TO
THE GRADUATE SCHOOL OF NATURAL APPLIED SCIENCE
OF
MIDDLE EAST TECHNICAL UNIVERSITY

BY

GÜLDEN EROĞLU

IN PARTIAL FULFILLMENT OF THE REQUIREMENTS
FOR
THE DEGREE OF MASTER OF SCIENCE
IN
POLYMER SCIENCE AND TECHNOLOGY

JANUARY 2011

Approval of the thesis:

**ISOCYANATE FUNCTIONALIZATION OF NANO-BOEHMITE
FOR THE SYNTHESIS OF POLYURETHANE
ORGANIC-INORGANIC HYBRID MATERIALS**

submitted by **GÜLDEN EROĞLU** in partial fulfillment of the requirements for the degree of **Master of Science in Polymer Science and Technology Department, Middle East Technical University** by,

Prof. Dr. Canan Özgen _____
Dean, Graduate School of **Natural and Applied Sciences**

Prof. Dr. Necati Özkan _____
Head of Department, **Polymer Science and Technology**

Prof. Dr. Güngör Gündüz _____
Supervisor, **Chemical Engineering Dept., METU**

Prof. Dr. Üner Çolak _____
Co-Supervisor, **Nuclear Energy Engineering Dept., HU**

Examining Committee Members:

Prof. Dr. Leyla Aras _____
Chemistry Dept., METU

Prof. Dr. Güngör Gündüz _____
Chemical Engineering Dept., METU

Prof. Dr. Necati Özkan _____
Central Laboratory, METU

Prof. Dr. Cevdet Kaynak _____
Metallurgical and Materials Engineering Dept., METU

Instructor Dr. Cevdet Öztin _____
Chemical Engineering Dept., METU

Date: 28/01/2011

I hereby declare that all information in this document has been obtained and presented in accordance with academic rules and ethical conduct. I also declare that, as required by these rules and conduct, I have fully cited and referenced all material and results that are not original to this work.

Name, Last name: Gülden Erođlu

Signature :

ABSTRACT

ISOCYANATE FUNCTIONALIZATION OF NANO-BOEHMITE FOR THE SYNTHESIS OF POLYURETHANE ORGANIC-INORGANIC HYBRID MATERIALS

Erođlu, Glden

M.Sc., Department of Polymer Science and Technology

Supervisor: Prof. Dr. Gngr Gndz

Co-Supervisor: Prof. Dr. ner olak

January 2011, 119 pages

In this study, organic-inorganic hybrid materials were prepared from polyurethane and boehmite. It was achieved by polymerizing monomers in the presence of functional nano-particles of boehmite with cyanate groups. The produced polyurethane organic-inorganic hybrid materials with enhanced mechanical properties were used for coating applications. Plate-like boehmite nano-particles were produced by hydrothermal process from aluminum hydroxide which was first ground in a high energy ball-mill, and then, processed hydrothermally under pressure and high temperature in a reactor. The surface morphology and crystal structure of boehmite were investigated by Scanning Electron Microscopy and X-Ray Diffraction

analyses, respectively. The molecular structures of boehmite particles were investigated by Fourier Transform infrared spectroscopy. Furthermore, Brunauer-Emmett-Teller analysis and Photon Correlation Spectroscopy analysis were carried out to determine the surface area and the size of particles. Then, plate-like boehmite nano-particles were functionalized by the reaction of their hydroxyl groups with 1,6-hexamethylene diisocyanate and 4,4'-methylene diphenyl diisocyanate. Scanning Electron Microscopy, Fourier Transform Infrared Spectroscopy, Differential Thermal Analysis-Thermal Gravimetric Analysis, and elemental analysis were performed for both functionalized and non-functionalized particles to confirm the functionalization of the particles. The polyester polyol used in the production of polyurethane was synthesized from 1,4-butanediol and adipic acid (PE-PO-1), and phthalic anhydride (PE-PO-2). Molecular structure of the polyester polyols was confirmed by Fourier Transform Infrared Spectroscopy analysis and molecular weight of the polymers were determined by end group analysis. Then, the produced functionalized nano-particles and polyester polyols were used for producing polyurethane organic-inorganic hybrid materials. Furthermore, polyurethane polymer and polymer-nonfunctionalized boehmite organic-inorganic hybrids were also synthesized for property comparison. Hardness, impact resistance, scratch resistance, abrasion resistance, and gloss property of the samples were determined.

It was observed that mechanical properties of organic-inorganic hybrid materials improved significantly. The hardness of the PU produced with PE-PO-1 increased from 82 to 98 Persoz, and the hardness of the PU produced with PE-PO-2 increased from 52 to 78

Persoz when one weight percentage functionalized boehmite was used. The impact resistance of the coatings was found to depend on the type of the polyols used in PU but not in the inorganic component. Therefore PE-PO-2 used PU has higher impact resistance than PE-PO-1 used PU. Scratch resistance of the coatings improved from 2B to 2H when using functionalized boehmite. Abrasion resistance of PUs produced with PE-PO-1 increased from 2 to 10 l/μm and abrasion resistance of PUs produced with PE-PO-2 increased from 12 to 20 l/μm by addition of functionalized boehmite.

Key words: boehmite nano-particle, hydrothermal, functional boehmite, polyurethane, organic-inorganic hybrid materials.

ÖZ

POLİÜRETAN ORGANİK-ANORGANİK HİBRİT MALZEMELERİNİN SENTEZİNDE KULLANILMAK ÜZERE NANO-BÖHMITİN İZOSİYANAT İLE İŞLEVSELLEŞTİRİLMESİ

Erođlu, Gülden

Yüksek Lisans, Polimer Bilim ve Teknolojisi Bölümü

Tez Yöneticisi: Prof. Dr. Güngör Gündüz

Ortak Tez Yöneticisi: Prof. Dr. Üner Çolak

Ocak 2011, 119 sayfa

Bu çalışmada poliüretan ve siyanat grupları içeren işlevselli böhmit kullanarak organik-anorganik hibrit malzemeler üretilmiştir. Mekanik özellikleri geliştirilmiş poliüretan organik-anorganik hibrit malzemeler kaplama uygulamalarında kullanılmıştır. Başlangıç malzemesi olarak kullanılan alüminyum hidroksit öğütme işleminden sonra basınç ve yüksek sıcaklık altında hidrotermal işleminden geçirilerek tabakamsı böhmit nano-parçacıkları üretilmiştir. Böhmit parçacıklarının yüzey biçimi ve kristal yapısı Taramalı Elektron Mikroskopisi ve X-Işını Kırınım analizleri ile incelenmiştir. Böhmitin molekül yapısı Fourier Dönüşümlü Kızılötesi Spektroskopisi analizi ile doğrulanmıştır. Bunun yanında parçacıkların yüzey alanlarını ve boyutlarını belirlemek için sırasıyla Brunauer-Emmett-Teller ve Foton Korelasyon Spektroskopisi

analizleri yapılmıştır. Sonrasında tabaka yapılı böhmit parçacıkları yüzeylerindeki hidroksillerle 1,6-hekzametilen diizosiyanatın ya da 4,4'-metilen difenil diizosiyanatın tepkimeye sokulmasıyla işlevselleştirilmiştir. İşlevselleştirme işleminin başarılıp başarılmadığını anlamak için hem böhmit hem de işlevselleştirilmiş böhmit parçacıklarına Fourier Dönüşümlü Kızılötesi Spektroskopisi, Taramalı Elektron Mikroskopisi, Diferansiyel Termal Analizi-Termal Ağırlık Analizi ve elementel analizi yapılmıştır. Poliüretan sentezinde 1,4-bütandiol ve adipik asit (PE-PO-1) ile fitalik anhidrit (PE-PO-2) kullanılmıştır. Üretilen poliester poliollerin molekül yapısını doğrulamak için Fourier Dönüşümlü Kızılötesi Spektroskopisi analizi yapılmıştır ve poliollerin molekül ağırlıkları son grup analizi ile belirlenmiştir. Sonrasında işlevselleştirilmiş nano-parçacıklar ve poliester poliölü kullanılarak poliüretan organik-anorganik hibrit malzeme üretimi yapılmıştır. Ayrıca özelliklerini karşılaştırmak için poliüretan ve polimer nano-kompozit üretimi de yapılmıştır. Örneklerin sertlik, esneklik, çarpma direnci, aşınma direnci ve parlaklık özelliklerine bakılmıştır.

Organic-anorganik hibrit malzemelerin mekanik özelliklerinin önemli ölçüde iyileştiği görülmüştür. Ağırlıkça yüzde bir işlevselleştirilmiş böhmit kullanıldığında, PE-PO-1 kullanılarak sentezlenen PU'nın sertliği 82 Persozdan 98 Persoza çıkarken, PE-PO-2 ile sentezlenen PU'nın sertliği 52 Persozdan 72 Persoza çıkmıştır. Kaplamaların darbe direncinin anorganik bileşenine değil kullanılan poliölün çeşidine bağlı olduğu belirlenmiştir. Bu nedenle PE-PO-2 ile üretilen PU'nun darbe direnci PE-PO-1 ile üretilenden daha yüksektir. İşlevselleştirilmiş böhmit kullanıldığında kaplamaların çizilme direnci 2B'den 2H'ye kadar artmıştır. İşlevselleştirilmiş böhmit kullanıldığında, PE-PO-1 kullanılarak

sentezlenen PU'nun dayanma direnci 2 l/ μm 'den 10 l/ μm 'ye çıkarken, PE-PO-2 ile sentezlenen PU'nun aşınma direnci 12 l/ μm 'den 20 l/ μm 'ye çıkmıştır.

Anahtar Sözcükler: böhmit nano-parçacığı, hidrotermal, işlevselleştirilmiş böhmit, poliüretan, organik-anorganik hibrit.

To Eylül

ACKNOWLEDGEMENTS

I would like to express my special thanks to my supervisor Prof. Dr. Gngr Gndz for his endless help, encouragement and valued guidance. As my supervisor; he guided me on my thesis and my life, especially in personal matters.

I also wish to express my thank to my co-supervisor Prof. Dr. ner olak for his understanding, support, suggestions, help, and his motivating speeches during my thesis period.

I would like to thank Assist. Prof. Dr. Bora Mavi for his invaluable suggestions, support and encouragement throughout this study.

My deepest gratitude is to my parent abettin Erođlu and Hazel Erođlu, my brother Engin Erođlu and his wife Sevil Erođlu for their very special care, understanding, and for their faith in me. At every step of my life, they were just beside me with their endless love, patience, and encouragement. Among them, special thanks to my nephew, Eyll Erođlu due to her existence to my life. She is the most precious thing for my life and her existence is enough to make me feel better and motivated.

I am also very thankful to my second parents Nursel zcan and Ahmet zcan for their endless support during my education life.

My special thanks go to Simge ınar, Sevin Kahya and Berna Burcu Topuz for being my family in Ankara.

I wish to express my sincere thanks to İrem Vural, Korhan Sezgiker, Lale Ayhan, Ahmet Güdelođlu, Rezan Erdoğan, Münire Tülü, and Güven Öğüş for their friendship, help and patience in whole period of my thesis.

I thank especially to Boğaçhan Buğra Kaya for being my friend and every beautiful thing in my life.

I thank to members of the Institute of Natural and Applied Sciences especially Aslı Aras Taşkın, Ceren Bora, and Fulya Karahan Dağ for their help, encouragement and motivation throughout this study.

The friendship of Ümit Sayiner, Seçkin Kıntaş, Serkan Şahin, Selin Çiftçi, Nagehan Keskin, Serdar Asmaođlu, Seçil Zekih, Barış Açıkalin, Mehmet Emin Yılmaz, Burçay Engüzel, and Anisa Çoniku is much appreciated.

I would also thank to Ali Sinan Dike, Olcay Mert, Osman Yaslıtaş, and Biology Group for helping me throughout this study.

Financial support of TÜBİTAK (Project No 108M204) and ODTÜ BAP Koordinatörlüğü (Project No BAP-03-04-2009-01) is acknowledged.

TABLE OF CONTENTS

ABSTRACT	iv
ÖZ	vii
ACKNOWLEDGEMENTS	xi
TABLE OF CONTENTS	xiii
LIST OF TABLES	xvii
LIST OF FIGURES.....	xix
LIST OF SYMBOLS AND ABBREVIATIONS	xxiii
CHAPTERS	
1. INTRODUCTION	1
2. LITERATURE REVIEW	9
2.1. PRODUCTION OF BOEHMITE NANO-PARTICLES BY HYDROTHERMAL PROCESS	9
2.2. FUNCTIONALIZATION OF BOEHMITE NANO-PARTICLES	16
2.3. POLYESTER POLYOL SYNTHESIS.....	20
2.4. POLYURETHANE PRODUCTION.....	23
2.5. ORGANIC-INORGANIC HYBRID MATERIAL PRODUCTION...	25
3. EXPERIMENTAL PROCEDURE.....	31
3.1. MATERIALS.....	31
3.2. PROCEDURE.....	32

3.2.1. PRODUCTION OF FUNCTIONALIZED BOEHMITE NANO-PARTICLES	33
3.2.1.1. GRINDING OF ALUMINUM HYDROXIDE	33
3.2.1.2. THE PRODUCTION OF BOEHMITE NANO-PARTICLES BY HYDROTHERMAL PROCESS	33
3.2.1.2.1. PREPARATION OF SOLUTION	34
3.2.1.2.2. THE PRODUCTION PROCESS	34
3.2.1.3. FUNCTIONALIZATION OF BOEHMITE NANO-PARTICLES	36
3.2.2. POLYESTER-POLYOL SYNTHESIS	39
3.2.3. PRODUCTION OF POLYURETHANE ORGANIC-INORGANIC HYBRID MATERIALS	40
3.2.3.1. POLYURETHANE POLYMER SYNTHESIS	40
3.2.3.2. POLYURETHANE COMPOSITE PRODUCTION	41
3.2.3.3. POLYURETHANE ORGANIC-INORGANIC HYBRID MATERIAL PREPARATION	42
3.3. CHARACTERIZATION METHODS	43
4. RESULTS AND DISCUSSION	44
4.1. FUNCTIONALIZATION OF BOEHMITE NANO-PARTICLES	44
4.1.1. GRINDING OF ALUMINUM HYDROXIDE	44
4.1.2. BOEHMITE PRODUCTION BY HYDROTHERMAL PROCESS	46
4.1.2.1. TRANSFORMATION OF ALUMINUM HYDROXIDE TO BOEHMITE NANO-PARTICLES	47
4.1.2.2. EFFECT OF EXPERIMENTAL PARAMETERS ON BOEHMITE NANO-PARTICLES	49

4.1.2.3. EFFECTS OF ULTRASONIC MIXING.....	54
4.1.3. FUNCTIONALIZATION OF PLATE-LIKE BOEHMITE NANO-PARTICLES	56
4.2. POLYESTER-POLYOL SYNTHESIS	62
4.3. POLYURETHANE PRODUCTION.....	63
4.4. MECHANICAL TESTS	67
4.4.1. PENDULUM HARDNESS	67
4.4.2 IMPACT RESISTANCE	70
4.4.3. SCRATCH RESISTANCE	71
4.4.4 ABRASION RESISTANCE.....	73
4.4.5 GLOSS	75
4.4.6 ADHESION TEST	75
5. CONCLUSIONS.....	77
REFERENCES	80
APPENDICES	
A. PROPERTIES OF USED MATERIALS IN THE EXPERIMENTS	100
B. CALCULATIONS OF THE EXPERIMENTS	104
B.1. PRE-GRINDING CALCULATION	104
B.2. GAP SOLUTION PREPARATION	105
C. ACID NUMBER DETERMINATION	106
D. DIBUTYLAMINE BACK TITRATION	107
E. MOLECULAR WEIGHT CALCULATION OF POLYESTER-POLYOL	109

F. INSTRUMENTAL INFORMATION	110
F.1. SEM (SCANNING ELECTRON MICROSCOPY) ANALYSIS....	110
F.2. FTIR (FOURIER TRANSFORM INFRARED) SPECTROSCOPY	110
F.3. XRD (X-RAY DIFFRACTION) ANALYSIS	110
F.4. PCS (PHOTON CORRELATION SPECTROSCOPY).....	111
F.5. BET (BRUNAUER-EMMET-TELLER) ANALYSIS.....	111
F.6. ELEMENTAL ANALYSIS.....	112
F.7. DTA-TGA (DIFFERENTIAL THERMAL ANALYSIS-THERMAL GRAVIMETRIC ANALYSIS)	112
F.8. MECHANICAL TESTS.....	113
F.8.1. FILM APPLICATION	113
F.8.2. PENDULUM HARDNESS TEST.....	113
F.8.3. IMPACT RESISTANCE TEST	114
F.8.4. SCRATCH RESISTANCE TEST	116
F.8.5. ABRASION RESISTANCE TEST	116
F.8.6. SPECULAR GLOSS.....	117
G. MECHANICAL TESTS RESULTS.....	118

LIST OF TABLES

TABLES

Table 1.1	Stability behavior of colloids with changing zeta potential.	3
Table 3.1	Experiments of boehmite production by hydrothermal process.	35
Table 3.2	Functionalization experiments with HDI.	37
Table 3.3	Functionalization experiments with MDI.	38
Table 3.4	Polyester-Polyol synthesis experiments.	40
Table 3.5	Polyurethane production experiments.	42
Table 4.1	Particle size results of $\text{Al}(\text{OH})_3$ and ground $\text{Al}(\text{OH})_3$. ..	46
Table 4.2	Surface area, mean particle size by IMAGE-J and PCS, aspect ratio, and zeta potential of plate-like boehmites.	52
Table 4.3	Elemental analysis.	61
Table 4.4	Impact resistance of PUs.	71
Table 4.5	Scratch resistance values of synthesized PUs.	72
Table 4.6	Adhesion of synthesized PUs.	76
Table A.1	List of chemicals.	101
Table A.1	List of chemicals (continued).	102

Table A.1	List of chemicals (continued).	103
Table G.1	Hardness values of synthesized PUs.	118
Table G.2	Abrasion resistance values of synthesized PUs.	119

LIST OF FIGURES

FIGURES

Figure 1.1	Organic-inorganic hybrid materials.	2
Figure 1.2	Variation of zeta potential with pH.	4
Figure 1.3	Zeta potential and double layer of the negatively charged particles.	5
Figure 1.4	Polyurethane applications.	7
Figure 2.1	Molecular structure of boehmite.	9
Figure 2.2	Hydrothermal process for the production of boehmite nano-particles.	12
Figure 2.3	Proposed mechanism of functionalization.	17
Figure 2.4	Reaction mechanism of boehmite and diisocyanate.	19
Figure 2.5	Reaction mechanism of polyester-polyol synthesis.	21
Figure 3.1	Flow diagram.	32
Figure 3.2	Experimental setup for hydrothermal process.	35
Figure 3.3	Experimental setup for functionalization.	37
Figure 3.4	Experimental setup for polyester-polyol synthesis.	39

Figure 3.5	Experimental setup of the polyurethane production...	41
Figure 4.1	SEM micrographs of (a) aluminum hydroxide ($\times 3000$), (b) ground aluminum hydroxide ($\times 3000$).	45
Figure 4.2	FTIR spectrum of boehmite nano-particles	48
Figure 4.3	XRD graphs of boehmite nano-particles and aluminum hydroxide.	49
Figure 4.4	SEM micrographs of produced boehmite in (a) HT-1 ($\times 40000$), (b) HT-2 ($\times 100000$), (c) HT-3 ($\times 100000$), (d) HT-4 ($\times 100000$).	51
Figure 4.5	Variation of particle distribution with particle size.	53
Figure 4.6	TGA/DTA graphs of boehmite nano-particles.	54
Figure 4.7	Boehmite productions by hydrothermal process (a) without ultrasonic mixing ($\times 10000$), (b) with ultrasonic mixing ($\times 10000$).	55
Figure 4.8	SEM micrographs of (a) MDI functionalized nano-boehmites ($\times 100000$), (b) HDI functionalized nano-boehmites ($\times 100000$).	56
Figure 4.9	FTIR spectra of MDI functionalization experiments.	57
Figure 4.10	FTIR spectra of HDI functionalization experiments.	57

Figure 4.11 FTIR spectra of MDI and HDI functionalize boehmites, MDI, HDI, and dry boehmite.	58
Figure 4.12 Effect of MDI functionalization temperature.....	59
Figure 4.13 TGA/DTA graphs of HDI functionalized boehmite nano-particles.	60
Figure 4.14 TGA/DTA graphs of MDI functionalized boehmite nano-particles.	60
Figure 4.15 FTIR spectra of produced polyester polyols.	63
Figure 4.16 FTIR spectra of PUs.....	64
Figure 4.17 Photographs of produced PU coatings.....	66
Figure 4.18 SEM micrographs of, (a) PU polymer (b) organic-inorganic hybrids with functionalized boehmite.	67
Figure 4.19 The change of hardness of PU organic-inorganic hybrid materials with the amount of functionalized boehmite.....	69
Figure 4.20 Chain extender and PE-PO effects on the hardness of PU organic-inorganic hybrid materials.	69
Figure 4.21 Effect of functionalized boehmite on the abrasion resistance of hybrid materials.....	74
Figure 4.22 Effect of chain extender and PE-PO on the abrasion resistance of hybrid materials.....	74

Figure F.1	Pendulum hardness tester and persoz pendulum.	114
Figure F.2	Impact resistance tester.....	115
Figure F.3	(a) Transfer of impact, (b) result of impact.....	115
Figure F.4	Abrasion resistance tester.....	116

LIST OF SYMBOLS AND ABBREVIATIONS

AA	Acetic acid
Ad.Ac.	Adipic acid
AMM	Ammonia solution
Al(OH) ₃	Aluminum hydroxide
BD	1,4-Butanediol
BH	Boehmite
DBTDL	Dibutyltin dilaurate
FB	Functionalized boehmite
HDI	1,6-Hexamethylene diisocyanate
HT	Hydrothermal condition
IPA	Isopropyl alcohol
IPDI	Isophrone diisocyanate
MDI	4,4'-methylene diphenyl diisocyanate
PE-PO	Polyester polyol
PU	Polyurethane
US	Ultrasonic mixing

CHAPTER 1

INTRODUCTION

Polymers have been used in a wide range of applications due to their low density, mechanical strength, and lack of susceptibility to corrosion [1-3]. However, they are usually easily affected from abrasion and scratching. Reinforced polymer composites have become very popular due to their desired scratch and abrasion characteristics [1-2]. And the scope of this study is the production of polyurethane (PU) organic-inorganic hybrid materials to improve mechanical properties of PU's.

Organic-inorganic hybrid materials are prepared by combination of organic and inorganic building blocks with chemical-bonding [4]. Perfect flexibility, toughness, moldability, and adhesiveness are the most important properties of polymeric materials. Besides, inorganic materials show high elastic modulus, heat resistance, corrosion resistance, weather resistance, UV resistance, electric conductivity, fire retardancy, solvent resistance, and desired mechanical properties against scratch and abrasion. However, they have poor moldability and high brittleness [5-10]. Functionalized inorganic nano particles form covalent bonds with the bulk polymer. It, in turn, highly improves mechanical properties. Thus, suitable combination of nano-particles and polymer is critical for producing desired organic-inorganic hybrid materials [10-24]. A

representative example of organic-inorganic hybrid materials is shown in Figure 1.1.

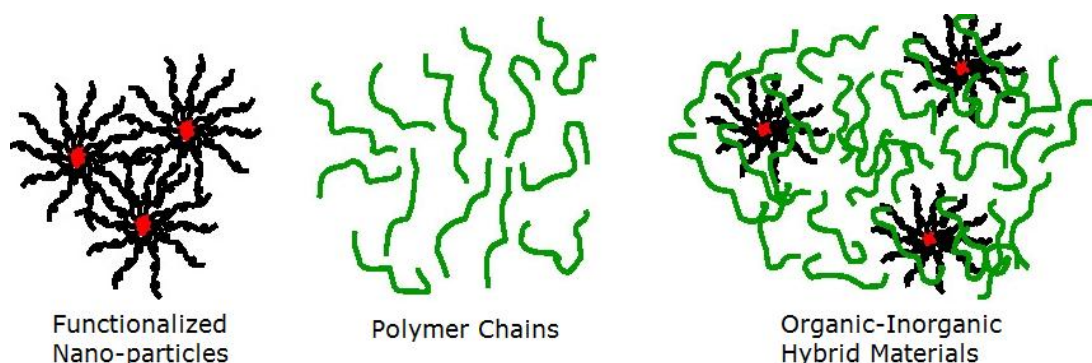


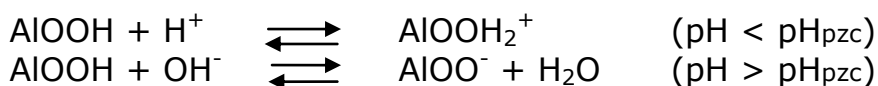
Figure 1.1 Organic-inorganic hybrid materials [25].

With recent interest in organic-inorganic hybrid materials, nano-silica, and aluminum oxide based materials such as nano-alumina and boehmite have received considerable attention to enhance scratch and abrasion characteristics because of their high surface to volume ratio, high hardness, high strength, and good wear resistance [26-28]. Boehmite is cheaper and has the ability to be functionalized for organic-inorganic hybrid material fabrication as compared with other nano-materials [9, 29-30]. In coating applications, siloxanes derived from tetra ethoxy silane (TEOS) are generally used to improve the scratch resistance of the coatings. However, the high cost of TEOS puts a burden to its wide use. Therefore, the use of a low cost starting material like aluminum hydroxide can provide an economical solution.

Surface control of the nano-particles is very crucial in organic-inorganic hybrid material applications. Nano-particles exhibit high

tendency to aggregate with each other due to their surface energy. Hydroxyl groups on the surface of boehmite nano-particles prevent dispersion in organic solvents or in plastics. Achieving a balance between the surface forces can accomplish redispersion [7, 31-32].

The acidity (e.g. pH) of the medium strongly affects the surface properties of boehmite. The surface is charged positively when the pH of the medium is lower than pH_{PZC} (PZC is 'the point of zero charge', the pH value at which the net surface charge is zero, $\sigma_s=0$). On the other hand, the surface is charged negatively when the pH of the medium is higher than pH_{PZC} [33].



The zeta potential designates the degree of repulsion between similarly charged adjacent particles in dispersion. The repulsion between the particles and their dispersion decrease as the value of zeta potential goes to zero. Thus, colloids with high zeta potential (negative or positive) are electrically stabilized while colloids with low zeta potentials tend to agglomeration as outlined in Table 1.1.

Table 1.1 Stability behavior of colloids with changing zeta potential.

Zeta Potential (mV)	Stability behavior of colloids
0 ↔ ±5	Rapid agglomeration
±10 ↔ ±30	Incipient instability
±30 ↔ ±40	Moderate stability
±40 ↔ ±60	Good stability
<-60 or >+60	Excellent stability

The isoelectric point (IEP) is the pH at which the negative and positive charges on the molecule or surface are equal. An example of the change of pH with zeta potential is shown in Figure 1.2.

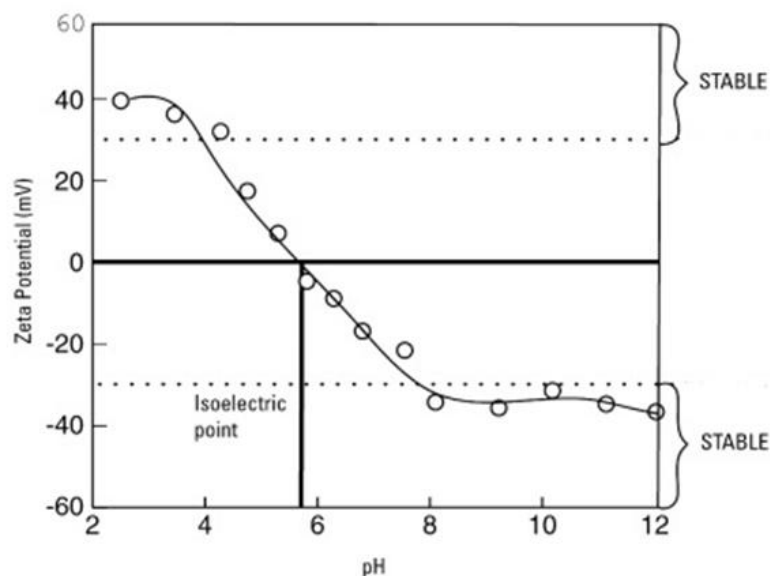


Figure 1.2 Variation of zeta potential with pH [34].

The PZC of boehmite is between 7 and 10. Therefore, the surface of boehmite particle is charged negatively in more basic medium. Electrical double layer occurs due to the electrostatic interaction between the negatively charged boehmite surface and ions of an opposite charge present in the solution [33].

Surface potential is defined as the electrostatic potential energy of surface confined charges. The development of a net charge at the particle surface affects the distribution of ions in the surrounding interfacial region, resulting in an increased concentration of counter

ions close to the surface. Thus an electrical double layer exists around each particle. The liquid layer surrounding the particle exists as two parts; an inner region, called the stern layer, where the ions are strongly bound and an outer, diffuse, region where they are less firmly attached. Within the diffuse layer there is a notional boundary inside which the ions and particles form a stable entity. When a particle moves due to gravity, ions within the boundary move with it, but any ions beyond the boundary do not travel with the particle. This boundary is called the surface of hydrodynamic shear or slipping plane. The potential that exists at this boundary is known as the zeta potential [35]. Negatively charged particles such as boehmite and its behavior in the solution are exhibited in Figure 1.3.

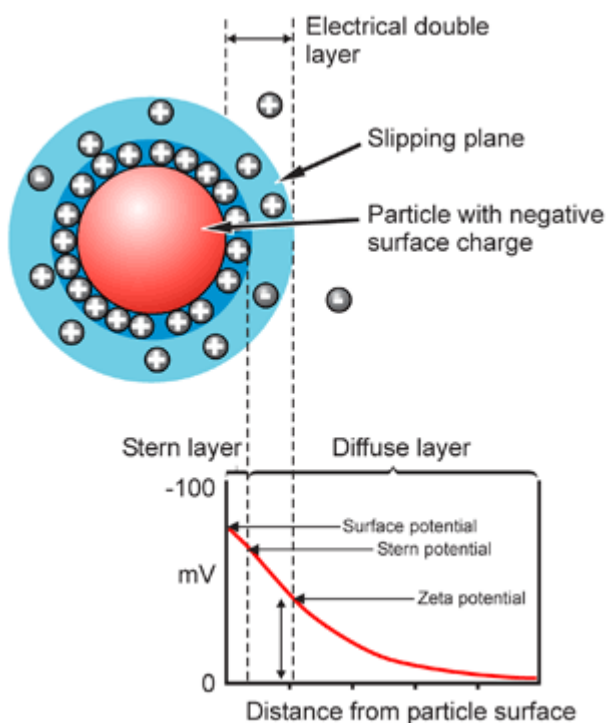


Figure 1.3 Zeta potential and double layer of the negatively charged particles [36].

Adhesion which is defined as the interatomic and intermolecular interaction between two surfaces is controlled by the chemical groups at or near the interface between polymer surface and coating layer [37]. Good adhesion at the interface between inorganic nano-particles and polymer matrix, and homogenous and effective dispersion of nano-particles in the organic components are the most important points to obtain high performance hybrid materials. The main problem here is the incompatibility of hydrophilic ceramic oxide fillers and hydrophobic polymer matrix which yields organic-inorganic hybrids with poor properties [18, 22, 38]. Therefore, new methods to control size, morphology, shape, and dispersion in organic molecules need to be developed for nano-particles, and control and manipulation of the surface properties of the particles are of crucial importance [5, 16, 22].

Nano-particle aggregates are dispersed in a polymeric matrix mainly by mechanical methods [20, 39]. Besides, surface modification or functionalization of the nano-particles is required for controlling surface properties. Therefore, it is possible to prevent agglomeration of nano-particles and improve stabilization and dispersion in the polymer matrix, and chemical and mechanical properties of the polymer are enhanced [39-43]. In our study, boehmite nano-particles were produced hydrothermally and surface of the boehmite nano-particles were modified for the production of PU organic-inorganic hybrid materials.

Coating is applied by means of a brush or spraying to change the surface properties such as color, gloss, and mechanical properties. The surface coating industry has been dominated by alkyd resins until the last few decades due to their excellent gloss, chemical

resistance, and fast drying. However, polyurethanes have gained great importance due to their excellent chemical and mechanical properties [44-48]. Excellent abrasion resistance, toughness, tear strength, low temperature flexibility, extraordinary processibility, good chemical and mechanical resistance, gloss stability, elasticity and moisture sensitivity are the main characteristics of polyurethane paints [49-52].

Polyurethanes (PU) are used for highly diverse purposes in such as fibers, foams, coatings, sealants, and adhesives due to their unique properties [17, 53-56]. Appearance, lifespan, scratch, and corrosion resistance of the products are improved by applying polyurethane coatings onto the surface of products [54]. Applications of the polyurethane polymer and used chemicals in the polyurethane production are briefly given in Figure 1.4.

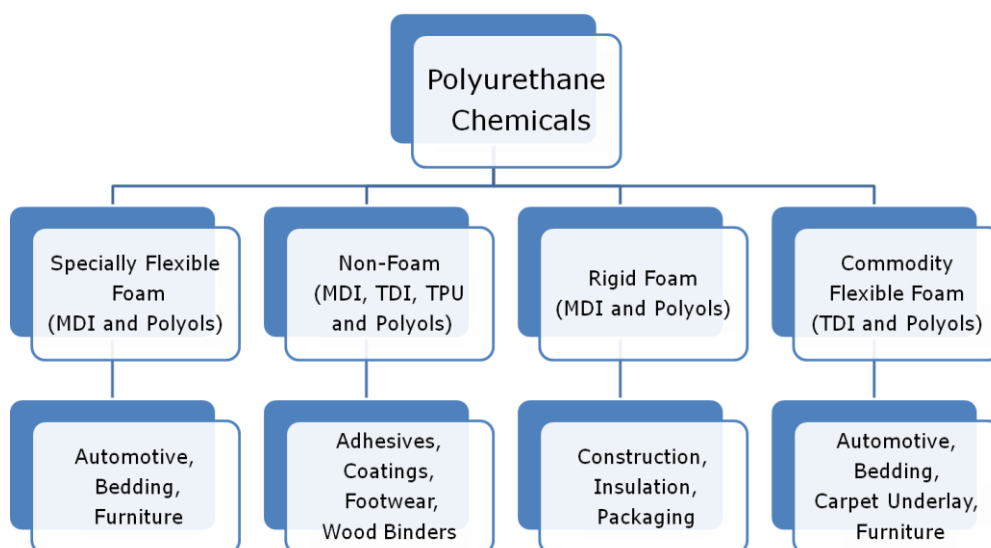


Figure 1.4 Polyurethane applications.

The properties of polyurethanes are improved either by changing microstructure of polyurethane or by dispersing inorganic particles within the polyurethane matrix [49, 56].

The main objective of this work is to produce polyurethane organic-inorganic hybrid material with enhanced mechanical properties such as scratch resistance by using isocyanate functionalized nano-boehmite particles. Boehmite nano-particles were produced under hydrothermal conditions from aluminum hydroxide which needs to be ground first in a ball-mill. Plate-like boehmite nano-particles was obtained by changing pH, concentration of powder, concentration of acid and base, and time in hydrothermal process. Dispersion is practically obtained by ultrasonic mixing before and after the reaction. 4,4'-methylene diphenyl diisocyanate (MDI) and 1,6-hexane diisocyanate (HDI) were used in the functionalization of plate-like boehmite nano-particles. While one of the cyanate groups is expected to react with surface OH groups of nano-boehmite particles, the other one would remain free which can react with the prepolymer. The results indicated that isocyanate functionalized nano-particles can be used to improve functional properties of PU coatings. Polyester-polyol were synthesized by using 1,4-butanediol and phthalic anhydride or adipic acid. Polyurethane organic-inorganic hybrid materials were produced by reacting the functionalized nano-boehmite particles with the synthesized polyester polyol. The mechanical properties of the polyurethane organic-inorganic hybrid materials were determined, and the properties of the produced polyurethane organic-inorganic hybrid materials were compared.

CHAPTER 2

LITERATURE REVIEW

2.1. PRODUCTION OF BOEHMITE NANO-PARTICLES BY HYDROTHERMAL PROCESS

Boehmite (γ -AlO(OH)) is used as a precursor for the production of advanced catalysts, adsorbents, various optical and electrical devices, alumina, alumina-derived ceramics, membranes, materials with photo luminescent properties, and coatings because of its low cost, high dispersibility, catalytic properties, and high surface area [23, 57-64].

Boehmite has a layered structure with adjacent layers being bound by hydrogen bonds [57]. Boehmite crystal structure (orthorhombic) is connected by hydrogen bonds between hydroxyl ions, and they stay parallel. The OH groups remain on the surface of the boehmite. The crystals of boehmite exhibit excellent cleavage perpendicular to the general direction of the hydrogen bonding [18]. The crystal structure is shown in Figure 2.1.

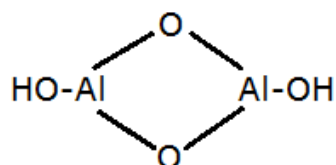


Figure 2.1 Molecular structure of boehmite [18].

Conventionally, boehmite is produced by solution methods such as spray pyrolysis, hydrolysis reactions of aluminum salts, and also by thermal processes [57, 60, 65-66]. The latter can be divided into three groups, which are (i) solvothermal, (ii) glycothermal, and (iii) hydrothermal processes. In all these processes, the product materials are synthesized in solvents at high temperatures [67-69]. The only difference between them is the type of solvent used in the reaction medium. Water, glycol, and organic solvents are used in hydrothermal, glycothermal, and solvothermal processes, respectively. Aluminum salts or aluminum hydroxide ($\text{Al}(\text{OH})_3$) are used as a starting material [65]. The chemical and physical properties, morphology, monodispersibility and particle size of boehmite depend on the experimental conditions such as type of precursor substance, pH, temperature, pressure, and time of aging [17, 70-73].

Hydrothermal process is the most popular one among the methods mentioned above. This method is used to produce metal hydroxyoxides from the aqueous solutions of metal salt through heating [74]. Powders form directly from the solution. Depending on reaction temperature, the powders come out to be anhydrous, crystalline, or amorphous. It is possible to control particle size and shape by controlling reaction temperature and selecting the proper precursor material [23, 69]. The hydrothermal process is one of the most effective procedures due to its low temperature, simple process control, and synthesis of high quality products [58, 75-76]. On the other hand, the irregular fragmentation of the particles and the problems associated with drying of the gel are the two important problems of production of boehmite in other methods. Moreover, production of aluminum alkoxide to be used as precursor

material is an expensive route to produce alumina ceramics with high quality. Therefore, boehmite synthesis from inorganic salts has become more common in recent years [60].

Aluminum nitrate, aluminum acetate, aluminum chloride, aluminum hydroxide, or aluminum sulfate have been used as starting materials in many studies on boehmite production by hydrothermal process [57, 61, 75-85]. Hydrothermal process is achieved at high temperatures (100-400°C) and pressures (10-40 MPa) with different reaction time (0-168h) [61, 79-86].

Typically, boehmite is prepared by precipitation of amorphous aluminum hydroxides and the pH of the starting solution is changed between 0.9 to 12.1 using acids or bases such as nitric acid and acetic acid or ammonia, ammonium hydroxide solution, urea, potassium hydroxide, potassium iodide, and sodium hydroxide [61, 78, 81-84]. Experimental parameters, such as type of acid or alkali, temperature, time and drying conditions, highly affect boehmite morphology when aluminum hydroxide is used as the starting material [60]. Needle-like boehmites are produced under acidic conditions, whereas plate-like and cubic-like boehmites are produced in basic conditions. The general procedure of boehmite production by hydrothermal process is shown in Figure 2.2.

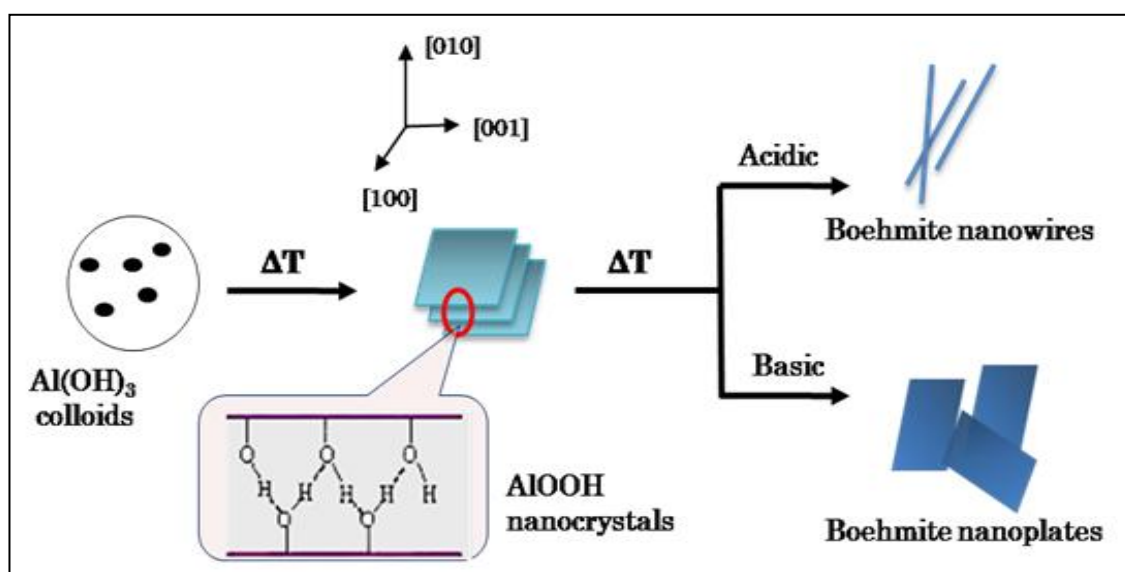


Figure 2.2 Hydrothermal process for the production of boehmite nano-particles.

Moreover, the presence of the salts in the starting solution is one of the crucial factors that affect the crystallization process and the growth of the boehmite nano-wire bundles. The chemical potential of the solution increases with the increase of the amount of salt, and 1-D nano-structure growth occurs due to high chemical potential. Therefore, the addition of the salt solution into the reaction medium can increase the ionic strength evidently, which reversely decreases the repulsion between nano-wires and favors the formation of agglomeration [80].

Surfactant (surface active organic additives) such as cetyltrimethyl ammonium bromide (CTAB) and polyethylene oxide (PEO) was also used in hydrothermal process to control the morphology of the boehmite particles and to obtain desired shape and dispersion of particles [82, 85]. The surfactant micelles interact with the

hydroxyl groups on the surface of boehmite particles through hydrogen bonding [85]. The tendency of layer combination through hydrogen bonds decreases due to bonding between CTAB molecules and hydroxyl groups on the surface of γ -AlO(OH) layer [61, 75]. However, purification of impurities in nano-particles is very difficult.

The effects of the parameters of hydrothermal process such as concentration of starting material, pH of the starting solution, temperature, and pressure on particle size of boehmite were investigated in the past [77]. The particle size increased with an increase in the reaction temperature and the amount of $\text{Al}(\text{NO}_3)_3$ concentration whereas it decreased with the increase of pH of the starting solution. Furthermore, broadening of particle size distribution was achieved as pressure was increased from 25 MPa to 40 MPa [77].

Music et al. [60] investigated the morphology of hexagonal boehmite when hydrothermal process was carried out by using aluminum nitrate and ammonia solution at 200°C for 2h.

In another research work aqueous aluminum chloride salt solution was prepared, and the pH was increased to 11 using sodium hydroxide solution. It was treated hydrothermally at 160 °C for different periods of time. The increase of reaction time from 24 to 168 hours resulted in the formation of very long boehmite fibers [23]. The size plate-like boehmite particles got bigger as the reaction time was increased from 6.0 to 24.0 h [86].

It was observed that, flower-like boehmites morphology was observed at higher concentrations of AlCl_3 . The addition of ethanol decreased the rate of boehmite crystal growth and controlled boehmite crystal growth was thus achieved. Moreover, the addition of CTAB is very crucial for acquiring uniform boehmite nano-sheets [61].

Fiber-like morphology highly depends on the type of surfactant, the type of starting material, and the pH value of the starting solution [75]. Fiber-like boehmite forms when the crystal growth direction of boehmite is perpendicular to the (002) planes. As the reaction proceeds the nano-rods formed begin to arrange along the axis of the [001] direction to form nano-strips, possibly via an oriented-attachment process [79].

Rhombic plates were produced at relatively low temperature and low concentration. On the other hand, hexagonal plates were obtained at higher temperature or high concentration. The particle size varies with temperature and pressure. However, it is not affected by the initial concentration of solution above 623 K [72].

Zhu et al. [85] reported that hydrothermal treatment at high temperatures provided significant improvement in the morphology of the particles. The aspect ratio decreased with the increase in the pH of the reaction mixture.

In the literature, boehmite particles were synthesized under hydrothermal treatment of the solutions with changing initial pH values. Needle-like boehmite morphology was obtained under highly acidic conditions (pH=2). Particle dispersion is very difficult

due to the tendency of agglomeration under these conditions. The degree of agglomeration is decreased by increasing the pH of the starting solution from 2 to 6. The particle morphology then changed from needle-like to hexagonal boehmites, and the aspect ratio decreased with the increase of pH (pH=8 or 10). It is also understood that the balance of attractive and repulsive interaction forces between the sol particles would play a very important role in the process of boehmite particle growth. In addition, the particle size increased with the increase of reaction temperature [84].

Boehmite was also synthesized from aluminum isopropoxide by means of a hydrothermal treatment without any additives in a study [66].

Mousavand et al. [32] studied the boehmite production and its modification in a hydrothermal reactor starting with $\text{Al}(\text{NO}_3)_3$ aqueous solution. Modifiers were added to the solution in order to modify the surface of the nano-particles during hydrothermal treatment [32].

In our current study, we synthesized boehmite by a hydrothermal process at 180°C and at 5 or 10 h of duration. Aluminum hydroxide ($\text{Al}(\text{OH})_3$) was used as the starting material. Before adding into the reactor, $\text{Al}(\text{OH})_3$ was ground to decrease the size of the particles, because no mixing is done in the reactor. Both acetic acid and ammonia solution were used in reaction medium. $\text{Al}(\text{OH})_3$ particles were peptized by the effects of acetic acid and ammonia solution added subsequently; the latter makes the medium basic. Acetic acid increases the distance between the plates and also covers the hydroxyl groups on the surface of boehmite particles. Therefore,

the direction of the boehmite crystal growth is affected. At the end of the reaction, the produced nano-particles had plate-like morphology and complete conversion of aluminum hydroxide to boehmite was obtained. Moreover, dispersion was accomplished by means of ultrasonic mixing of the particles before and after the hydrothermal process. In other words, (i) using both acid and base in the starting solution, (ii) grinding of $\text{Al}(\text{OH})_3$ to decrease the size of the particles, and (iii) ultrasonic mixing for providing dispersion are three main differences of this study from those given in the literature.

2.2. FUNCTIONALIZATION OF BOEHMITE NANO-PARTICLES

In our study, boehmite nano-particles were functionalized to provide chemical bonding between polymer and inorganic particles. In this section, functionalization of inorganic particles was explained and studies about surface modification were discussed.

The introduction of functional groups onto the surface of the inorganic particles can provide chemical bonding between the particles and the polymer matrix. Therefore, the interaction between the two components is enhanced and the organic-inorganic hybrid may gain improved mechanical strength [15]. The sequence of the strongest to weakest interactions between inorganic particles and polymer matrix are covalent bonding, hydrogen bonding, dipole dipole and van der Waals interactions. Covalent bonding between two phases promotes adhesion and dispersion of the organic-inorganic hybrids, allows better mechanical load transformation to the particles and also enhances

toughness of the organic-inorganic hybrid materials [7, 9, 22]. A proposed mechanism of functionalization is shown in Figure 2.3.

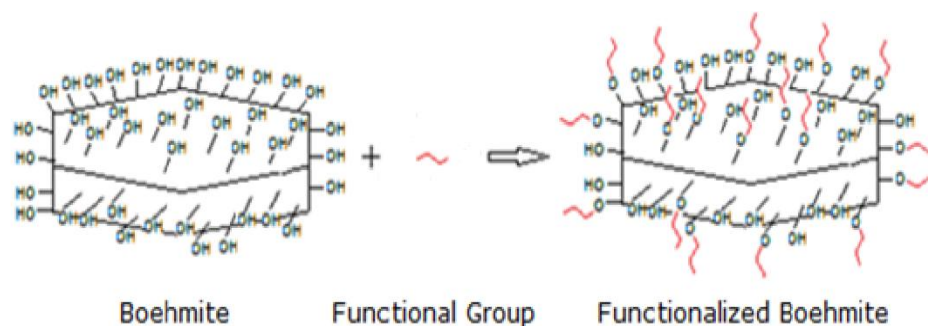


Figure 2.3 Proposed mechanism of functionalization.

Actually, there are two methods to functionalize the surface of inorganic particles. The first one is surface absorption or reaction with small molecules (covalent modification) [17-19, 87-88], such as silane coupling agent or side-wall covalent attachment of functional groups [21, 88]. In surface modification, silane coupling agents enhance dispersion, adhesion, and compatibility [16, 18-19]. The second way is to rely on graft polymers by covalent bonding onto the hydroxyl groups at the surface of the inorganic particles [16-18, 43, 89].

Surface modification was applied on many different materials such as nano-silica particles, kaolin, boehmite, nano-alumina, and carbon nano-tubes [40-41, 88-91].

In the literature, amino groups could be easily introduced onto nano-alumina surface by treatment with amino-silane coupling

agents. In addition, Michael addition reaction is used as a general modification method for modifying the surface of amino-alumina [28].

Furthermore, the attachment of the reactive groups onto nanoparticles such as the alumina surfaces was achieved by the reaction of the silane groups that are γ -methacryloxypropyl trimethoxy silane, vinyltri(2-methoxyethoxy) silane, vinyltrimethoxy silane, 3-mercaptopropyl trimethoxysilane, 3-aminopropyl triethoxysilane, 3-glycidoxypropyl trimethoxysilane, tetraethoxyorthosilane (TEOS) and aminopropyl-methyldiethoxysilane with the hydroxyl groups onto the alumina surfaces. Then, graft polymerization reactions were performed [16-18, 43, 64, 91-95]. The reaction using the alkoxy silane gives stable covalent bonding via siloxane bond on aluminum oxide [89].

In addition, dendritic carboxylic acids were used for the functionalization of nano-alumina [40]. The product is also called carboxylate-alumoxane [41]. Lysine is also used for the modification of alumoxane [22, 96]. Amino acid alumoxane was produced by using amino acids [97].

Isocyanate functionalization of the materials was carried out in many researches because isocyanate group is very reactive [98-100]. It can easily react with $-OH$, $-COOH$, $-NH_2$, etc groups [51, 98]. The reaction between the isocyanate group and the hydroxyl group on the surface of boehmite was attributed to the additional reaction of the double bond between C and N in the isocyanate group. The reaction between boehmite and diisocyanate is given in Figure 2.4.

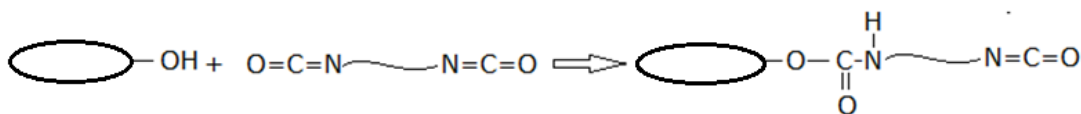


Figure 2.4 Reaction mechanism of boehmite and diisocyanate.

Functionalization of different materials with diisocyanate was reported in the literature. In one study, isocyanate functionalization of kaolin was accomplished. There are two steps in the functionalization of kaolin, these are (i) isocyanate functionalization and (ii) reaction of functionalized kaolin with polyethylene glycol [8]. In another study, perfluoroalkyl isocyanate was attached onto the hydroxyl groups of the aluminum surfaces [30]. Isocyanate functionalization of carbon nano-tubes was also carried out [88]. Generally, isocyanate functionalization reaction was carried out in a dry nitrogen atmosphere at 50-100°C for 1-24h [15, 88, 100].

Complex amine structures were also attached on surfaces such as silicon wafer surface through grafting. Silica layer was first modified by 10-isocyanatodecyl-trichlorosilane. Then, amine substrates were attached to the wafer surface through urea linkage through the reaction of isocyanate groups [42].

Li et al [15] studied modification of nano-alumina particles with diisocyanate. Diphenylmethane 4-4'-diisocyanate (MDI) was used as surface grafting agent to react with hydroxyl groups on nano-alumina. Acetone was used as a solvent and the reaction temperature was kept at 60°C. It was observed that the reaction between the diisocyanate group and the hydroxyl group on the surface of α -alumina nano-particles took place. Functionalization

was carried out by additional reaction of the double bond between C and N in the isocyanate group [15].

In our study, boehmite nano-particles were functionalized with MDI and HDI in toluene due to its quite higher boiling point than that of acetone. Thus, it was possible to keep the reaction temperature at 80°C. To our knowledge, there is no study reporting boehmite functionalization with diisocyanates in the literature. The closest study is functionalization of alumina particles with MDI in the medium of acetone.

2.3. POLYESTER POLYOL SYNTHESIS

In our study, polyester polyol was synthesized to use it in making PU organic-inorganic hybrid material. In this section, properties, applications, and production of polyester-polyol were discussed.

In the literature, polyols that have polyethers, polyesters, polycaprolactone or polycarbonate origin are used in polyurethane production. Polyester polyols have some advantages over polyether polyols [101]. Generally, polyester polyols increase abrasion resistance and adhesion property of polyurethane. On the other hand, ether based polyols have low-temperature flexibility, and low viscosity [50, 102]. In addition, polyether polyols are composed of limited monomer composition such as propylene oxide, ethylene oxide, and butylene oxide in industry. Besides, ester containing polyols are synthesized with many organic acids and alcohols in industry. Therefore, polyester polyols are prepared by different

combinations of monomers and this gives versatility for PU products [50].

Polyester polyols are prepared by the reaction of a polycarboxylic acid or anhydride with a polyhydric alcohol. At the beginning a stoichiometric excess of polycarboxylic acid or anhydride was used. After removing 90 to 95 % of water of esterification polyhydric alcohol was added to adjust the stoichiometry of the reaction. The reaction is stopped when polyester polyol was synthesized with the desired acid number. The polyester polyols are synthesized at 120-230°C under nitrogen atmosphere and non-stop stirring. A condenser is used to remove the water produced in the esterification reaction [50-51, 103-107]. The reaction mechanism of diol and diacid for the synthesis of polyester-polyol synthesis is given in Figure 2.5.

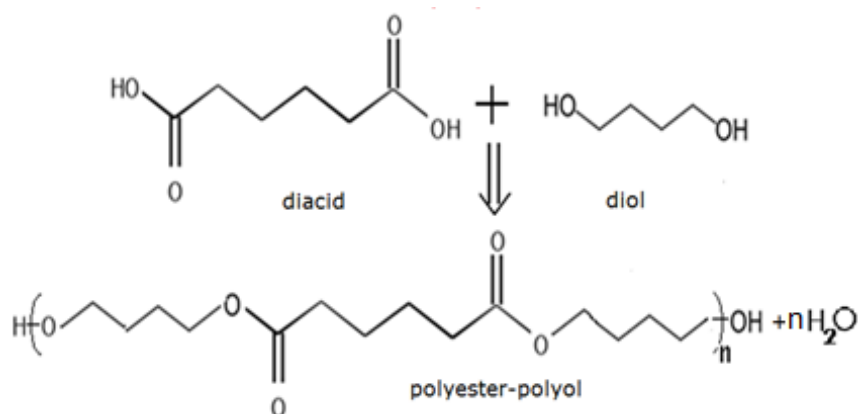


Figure 2.5 Reaction mechanism of polyester-polyol synthesis.

Generally, adipic acid, phthalic anhydride, ricinoleic acid, or oleic acid are used as diacid; and ethylene glycol, linseed oil, castor oil

or 1,4-butanediol are used as a diol for the production of polyester polyols [103, 105-108].

Linear or slightly branched polyester polyols are used in polyurethane production [101]. Aliphatic polyester polyols give flexibility to the polyurethane chain. Hardness and heat resistance property of the polyurethane is improved when phthalic anhydride or isophthalic acid is used. The molecular weight of the polyester polyol to be used is in the range of 500-2000 g/mol, and its acid number is 1-4. To avoid the side reactions in the polyurethane production, water that comes out from the reaction must be removed away [51].

Generally, hydroxyl-terminated polyesters can promote organic-inorganic hybrid coatings with great solvent resistance and adhesion to metals. Both aliphatic and aromatic diacids are used to synthesize polyester resins for coating applications. Isophthalic acid and adipic acid are widely used as aromatic dibasic acid and aliphatic diacid, respectively, in coatings. Glass transition temperature (T_g), hardness and chemical resistance of the polyester polyols can be improved by using substances with phenyl group. However, aromatic group absorbs UV light and decreases the photo oxidative stability [50-51].

In this study, polyester polyol was synthesized by esterification reaction of 1,4-butanediol and adipic acid or phthalic anhydride under nitrogen atmosphere. *p*-Toluenesulfonic acid was used as catalyst. Stoichiometric ratio is very important during the synthesis. The diol to acid or anhydride molar ratio was kept 1.3 in order to produce hydroxyl ended polyester. Polyester polyol

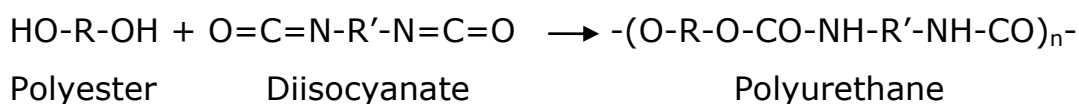
produced with adipic acid had higher flexibility than the one produced using phthalic anhydride, simply because, aromatic groups give rigidity to the polyester polyol chain.

2.4. POLYURETHANE PRODUCTION

In this study, polyurethane was produced in the presence of functionalized boehmite nano-particles for acquiring organic-inorganic hybrid materials. In addition, PU polymer was also synthesized to compare the properties of them. In this part, properties, applications, and production of PU polymer were discussed.

The condensation polymerization reaction of diols with diisocyanates is used to produce urethane polymer was pioneered in 1937 [50-51, 109-110]. Polyurethanes contain urethane linkages in the main polymer chain [51, 55]. Polyurethane elastomers consist of soft segments derived from polyols, and hard segments from isocyanates and chain extenders [45, 52, 109-110]. Generally, raw materials are stirred mechanically for about 2-6 h at 60-80 °C under nitrogen atmosphere. The molar amount of diisocyanate must be two times greater than polyol [104-105, 111-112].

There are a number of methods available for the preparation of polyurethanes, but the most widely used one is the reaction of hydroxyl terminated polyesters with diisocyanates [51, 108-110] as shown below.



Linear polyurethanes are produced when only difunctional reactants are used. Branched or crosslinked polyurethanes form when hydroxyl or diisocyanate functionality is higher than two. The properties of various types of polyurethanes depend primarily on molecular weight, degree of crosslinking, effective intermolecular forces, stiffness of chain segments, and crystallinity.

Polyurethane has very high flexibility, scratch resistance, and high toughness properties. It has many applications in surface coatings, leather and textile industry, and glue production [51].

Typically, polyurethanes have excellent elastomeric properties and can be synthesized as thermoplastics when linear polyester polyols, diphenylmethane-4,4'-diisocyanate (MDI), and glycol chain extenders (with a 1:1 ratio of NCO and OH groups) are used [104]. Polyurethane coatings were synthesized with varying types of isocyanates such as HDI isocyanurate and IPDI trimer. The coatings crosslinked with HDI isocyanurate have better resistance against water, acids, alkalis, and solvents than the coatings crosslinked with IPDI trimer [50].

In this study, two different types of polyurethanes were produced. In the first one polyester polyol produced from adipic acid and 1,4-butanediol, and MDI were used. In the second one polyester polyol having phthalic anhydride and 1,4-butanediol in the backbone, and MDI were used. In both cases dibutyl tin dilaurate was used as catalyst. The synthesis of prepolymer was stopped when the

percent of NCO from dibutylamine back titration was 1-5. Then chain extender and crosslinker were added to produce polyurethane.

2.5. ORGANIC-INORGANIC HYBRID MATERIAL PRODUCTION

In this section, literature studies about organic-inorganic hybrid materials were discussed.

Polymer nano-composites are produced by mixing nano-particles and polymer [1-2, 13]. There are many procedures for the preparation of polymer nano-composites, such as, (i) mixing nano-particles and polymers directly, (ii) in situ generation of nano-particles in a polymer matrix, (iii) polymerization of monomers in the presence of nano-particles, and (iv) a combination of polymerization and formation of nano-particles [2, 21].

In the literature generally polyurethane and inorganic particles were purchased, then polymer composites were produced by mixing them [1, 113-115]. Mixture of polymer and inorganic particles are coated on the substrates by spin coating method [1]. At the end of the coating, hardness, scratch, abrasion, and corrosion tests were done for measuring the mechanical and chemical properties of the composites [1, 53]. Mechanical and chemical properties of the polymer were generally enhanced [1].

In the literature, there are many research studies on nano-composites produced with silica particles. For instance, poly(methyl metacrylate) (PMMA)-silica hybrid copolymer was prepared by

surface modification of silica particles and copolymerization reaction with mixing silica particles and methyl metacrylate (MMA) monomers [11]. Apart from that, silica based organic-inorganic hybrid coatings was modified by using silane coupling agents to functionalize the inorganic particles [12]. In another research, nano-silica particles were modified with polyurethane by melt grafting method. Then modified particles were used for the preparation of polypropylene masterbatches and composites by reactive compatibilization between polypropylene and functionalized particles [27]. In another study, nano-silica particles were modified with silane coupling agent and then hybrid nano-composites were produced by polymerization [43]. Moreover, silicon carbide nano-particles or nano-layered silicates were dispersed in polyurethane, and the properties of the composites were measured. The results showed that the tensile strength of the composite increased with the increased particle loading [21]. According to Türünç et al. [10], silica nano-particles with changing particle size were synthesized by sol gel method. Particles were modified with cyclic carbonate functional organoalkoxysilane. Polyurethane-silica nano-composite coatings were produced by direct addition of functionalized silica particles into carbonated soybean oil and polypropylene glycol resin mixture by means of nonisocyanate route. The results showed that the abrasion resistance and thermal stability of the polymer increased. In another study, silica nano-particles were grafted with silane coupling agents. In the organic-inorganic hybrid material production, silica nano-particles were well dispersed in polyol or polypropylene glycol. Then, TDI and toluene solvent were introduced into the mixture for prepolymerization carried out at 55-

85°C for 3-5 h. Finally, 1-4, butanediol was added as a chain extender and stirred at 80°C for one hour [17, 95].

There are many studies on clay-polymer nano-composites in the literature. In the study of Choi et al. [49], organifier were synthesized and then organoclay was prepared by the reaction of organifier and clay. Finally organoclay, polyol, and diisocyanate were used for the production of polyurethane/clay nano-composites. In another study, polyurethane was synthesized and then mixed with the clay. The cured nano-composites exhibited excellent mechanical and adhesive properties, and thermal stability compared to pristine polyurethane [53]. Apart from that, organophilic nano-clay was previously dispersed in solvent. Then, different concentrations of polyurethane and organophilic nano-clay were added. It was shown that, the presence of clay additives enhanced both modulus, strength, and toughness of coating materials [39].

In the study of Zilg et al. [56], organophilic fluoromica was prepared with bis(2-hydroxyethyl) methyl dodecyl ammonium chloride and synthetic mica. Then, organophilic fluoromica, polyol and diisocyanate were mixed and polyurethane nano-composite was produced.

In the literature, functionalized carbon nano-tubes also were used for the production of polyurethane nano-composites. Modified particles were dispersed in polyurethane polymer. Carbon nano-tubes are responsible for the considerable enhancement of mechanical properties of the polyurethane [116]. According to Yang et. al. [117], multiwalled carbon nano-tubes were

functionalized with carboxylic acid. Carboxylated carbon nano-tubes react with chloride, diaminoethanol, and toluene diisocyanate. Then, diaminoethanol and diisocyanate reaction continued step by step and hyperbranched polyurethane functionalized multiwalled carbon nano-tubes were produced.

In many studies reported in the literature, boehmite and polyurethane were purchased and boehmite particles were dispersed in polyurethane. The polyurethane nano-composite properties were tested [20, 118]. In one research study, polymer was synthesized, and then, alumina nano-particles were added at different concentrations. Mechanical methods were used to obtain dispersed polymer-particle mixture. The results showed that the corrosion and UV resistance, and mechanical properties of coatings were enhanced with increasing concentration of alumina particles. In other words, addition of alumina particles in coating mixture has a positive effect on the properties of coating [6].

Singh et al. [119] stated that polymer nano-composite preparation has three important stages. Firstly, alumina particles were produced. Then, isocyanate functionalization of alumina particles was done. Finally, the polymer was synthesized and polymer and modified particles were mixed. The results showed that the impact resistance of the polymer doubled.

Chemically functionalized alumina nano-particles (carboxylated alumoxane) were also used as the inorganic part of the organic-inorganic hybrid materials. Organic hydroxides or amines in the functionalized particles directly react with epoxide resins to provide covalent bonding of the nano-particles to the polymer, and form

hybrid materials. The results exhibited that there was a significant increase in thermal stability and tensile strength of the polymers [7, 9]. Mistry et al. stated that [97], amino acid alumoxanes and polypropylenefumarate were used to synthesize polymer nanocomposites.

There are studies in the literature reporting boehmite nanoparticles grafted with silane coupling agents. Then, the grafted particles blended with polymers such as low density polyethylene and polyurethane. Homogenous dispersion and good interfacial adhesion between inorganic particles and polymer matrix improved mechanical properties [16, 64]. Similarly, alumina particles grafted with silane coupling agent was used in the preparation of alumina/polystyrene composite nanoparticles through emulsion polymerization [94].

In this study, functionalized boehmite particles were used as the inorganic part of the polyurethane organic-inorganic hybrid materials. MDI on the boehmite surface react with hydroxyl groups at the end of the polyester polyol chain. However, the amount of MDI on the boehmite surface was not sufficient to establish strong bonding. Therefore, after the reaction between MDI on the functionalized boehmite and hydroxyl groups of the polyester polyol, some more MDI was added to the medium. This was done to form polyurethane network in the bulk. When the percent NCO from dibutylamine back titration reached the expected value the synthesis of prepolymer was stopped. Chain extender and crosslinker were then added to make polyurethane organic-inorganic hybrid materials. The mechanical properties of the PU

organic-inorganic hybrid materials were determined through several tests.

CHAPTER 3

EXPERIMENTAL PROCEDURE

In this chapter, the materials used in the experiments were given. In addition, all the steps of the procedure for producing polyurethane organic-inorganic hybrid materials were explained in detail. The characterization methods are also described.

3.1. MATERIALS

- Aluminum Hydroxide
- Isopropyl Alcohol
- Acetic Acid
- Ammonia Solution
- 4,4'-Methylene Diphenyl Diisocyanate
- 1,6-Hexamethylene Diisocyanate
- Dibutyltin Dilaurate
- Toluene
- Adipic Acid
- Phthalic Anhydride
- 1,4-Butanediol
- P-Toluenesulfonic Acid
- Diaminoethanol
- Hexamethylenetetramine

Properties of the materials used in this study were tabulated in Appendix A.

3.2. PROCEDURE

In this study, the experiments were carried out in six steps; these are (i) grinding of aluminum hydroxide particles, (ii) boehmite production by hydrothermal process, (iii) functionalization of boehmite nano-particles, (iv) polyester-polyol synthesis, (v) production of polyurethane organic-inorganic hybrid materials, and (vi) mechanical tests for the characterization of hybrid materials. The flow diagram of these steps is shown in Figure 3.1.

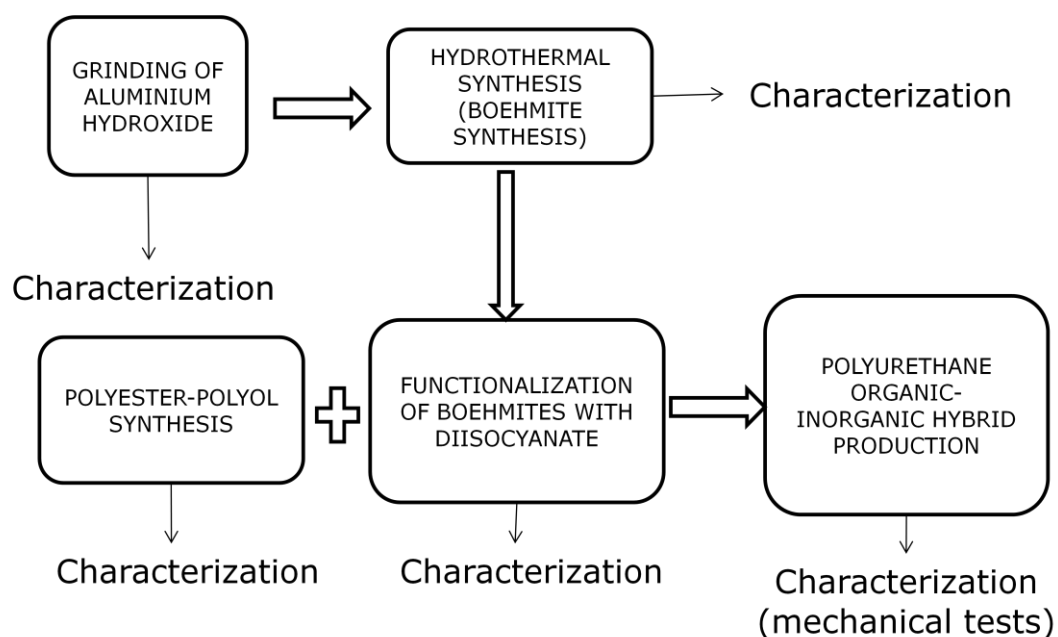


Figure 3.1 Flow diagram.

3.2.1. PRODUCTION OF FUNCTIONALIZED BOEHMITE NANO-PARTICLES

In this part, the experiments were divided into three stages, these are grinding of aluminum hydroxide, production of boehmite nano-particles by hydrothermal process, and functionalization of boehmite nano-particles. The functionalized boehmite nano-particles were used for hybrid material production.

3.2.1.1. GRINDING OF ALUMINUM HYDROXIDE

In this step, isopropyl alcohol was used as wetting agent. Initially, the solution was prepared by using 0.67 mol aluminum hydroxide and 0.37 mol isopropyl alcohol (pure). The solution was mixed approximately for one hour by a magnetic stirrer. After the dispersion of the particles in the solution was achieved, the solution was poured into a jar where it is mixed by a mechanical stirrer for 30 minutes at 500 rpm. Then, the particles were washed with isopropyl alcohol (technical grade) and distilled water. Later, centrifugation was done at 6000 rpm for ten minutes, and the particles were dried at 60°C in an oven for one day. The ground $\text{Al}(\text{OH})_3$ particles were used for boehmite production.

3.2.1.2. THE PRODUCTION OF BOEHMITE NANO-PARTICLES BY HYDROTHERMAL PROCESS

Boehmite production procedure has two main steps, (i) preparation of solution, and (ii) hydrothermal reaction in a reactor.

3.2.1.2.1. PREPARATION OF SOLUTION

In this part, ground Al(OH)_3 was mixed with distilled water and stirred for 1-2 hour. Then, acetic acid was added for peptization of the Al(OH)_3 plates, and ultrasonic mixing was done at two minute periods (3-4 times) and 35-40 % of full power. Then, it was stirred by a magnetic stirrer for one day, and ammonia solution was added for increasing the pH to about 10-11. Later, it was stirred ultrasonically with two minute periods (3-4 times) and 35-40 % of full power. Finally, the solution was kept stirred for one day.

3.2.1.2.2. THE PRODUCTION PROCESS

The glass jar containing the prepared solution was placed into the reactor. A solution with the same composition was poured into the reactor for filling the volume surrounding the glass jar. It somehow saturated the atmosphere with ammonia, and prevented the loss of ammonia from the contents of the jar. The experimental set up is shown in Figure 3.2 and the experimental parameters are tabulated in Table 3.1. Time and temperature was adjusted by controllers to 5-10 h, and 180°C , respectively. After the reaction is over, and the reactor cooled, the particles were washed with isopropyl alcohol and diionized water, and then centrifuged at 7000 rpm for ten minutes. Then the particles were dried at 60°C in an oven for 1-3 days.

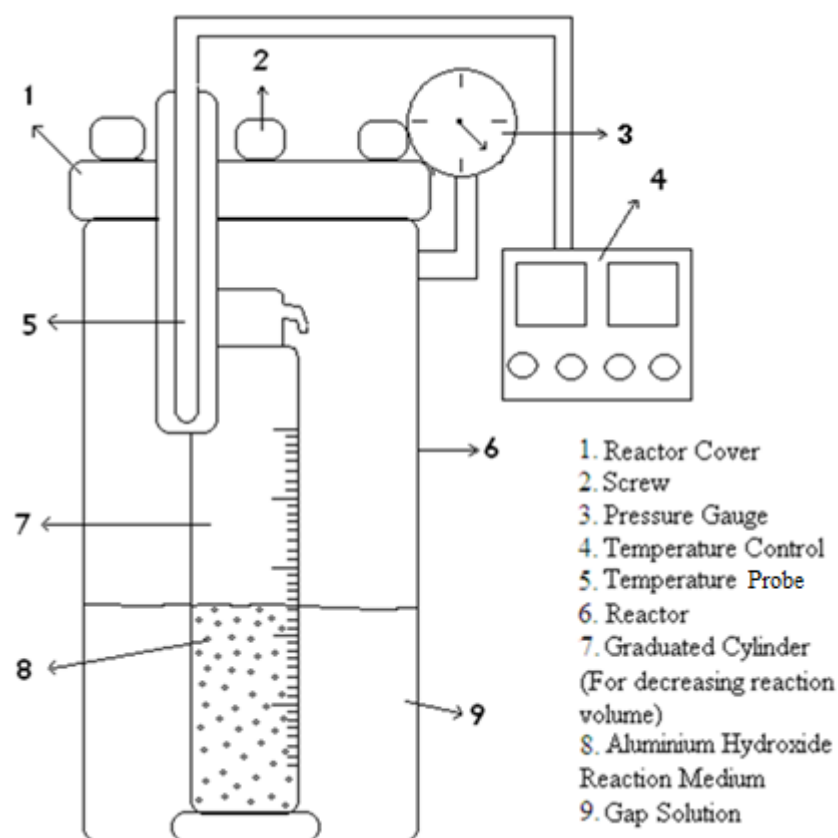


Figure 3.2 Experimental setup for hydrothermal process.

Table 3.1 Experiments of boehmite production by hydrothermal process.

	t (h)	AA (mol)	NH ₃ (mol)	H ₂ O (mol)	Al(OH) ₃ (mol)	AA (mol) %	NH ₃ (mol) %	Morphology
HT1	5	0.21	0.70	5.59	0.17	3.19	10.47	Cubic-like
HT2	5	0.39	0.85	5.49	0.17	5.70	12.37	Plate-like
HT3	10	0.39	0.85	5.49	0.17	5.70	12.37	Plate-like
HT4	5	0.49	0.93	4.80	0.17	7.69	14.58	Plate-like

-T=180 °C
 -P=14-16 bar

The produced boehmite nano-particles have two different morphologies; these are plate-like and cubic-like. Plate-like boehmite nano-particles were functionalized for PU organic-inorganic hybrid materials due to their high aspect ratio.

3.2.1.3. FUNCTIONALIZATION OF BOEHMITE NANO-PARTICLES

The experiments were conducted under nitrogen atmosphere. Plate-like boehmite nano-particles were dried at 110°C in vacuum oven to remove free water. HDI or MDI was dissolved in toluene and ultrasonic mixing was carried out at two-minute periods (3-4 times) and 35-40 % of full power. Then, the dried boehmite and toluene were mixed and ultrasonic mixing was done at two-minute periods (3-4 times) and 35-40 % of full power. Then, boehmite and catalyst (DBTDL) were added into the solution, and the temperature was raised to 80°C and the solution was stirred continuously. Five hours later, heating and nitrogen feeding were turned off and the solution was kept stirring for one day. Then, the functionalized boehmite nano-particles were washed out with toluene and acetone, and centrifuged at 7000 rpm for ten minutes. Finally, the functionalized nano-particles were dried at 60°C in an oven for 1-3 days. The experimental setup for functionalization is shown in Figure 3.3, and the parameters of the experiments were tabulated in Table 3.2 and Table 3.3.

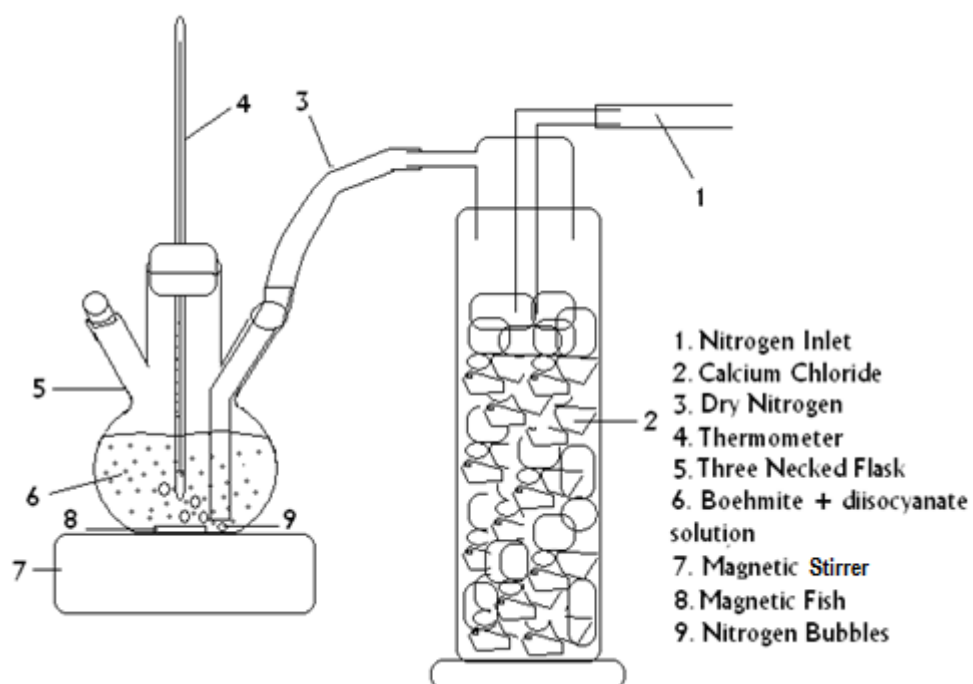


Figure 3.3 Experimental setup for functionalization.

Table 3.2 Functionalization experiments with HDI.

	V_{solvent} (ml)	Boehmite (mol)	HDI (mol)	mol Boehmite /mol HDI	Catalyst (wt %)
HDI-1	50	0.02	0.01	2.00	4.0
HDI-2	<u>50</u>	<u>0.02</u>	<u>0.02</u>	<u>1.00</u>	<u>2.6</u>
HDI-3	50	0.02	0.01	2.00	5.1
HDI-4	80	0.02	0.04	0.50	0.7
HDI-5	80	0.02	0.08	0.25	0.4
HDI-6	120	0.02	0.16	0.13	0.2
HDI-7	80	0.02	0.01	2.00	10.2
HDI-8	80	0.02	0.02	1.00	5.2

-T= 45°C

-Solvent: Toluene

-Time: 5 hour

Table 3.3 Functionalization experiments with MDI.

	T (°C)	Time (h)	V_{solvent} (ml)	Boehmite (mol)	MDI (mol)	mol BH/ mol MDI	Catalyst (wt %)
MDI-1	80	5	50	0.02	0.004	5.0	-
MDI-2	80	5	50	0.02	0.006	3.3	-
<u>MDI-3</u>	<u>80</u>	<u>5</u>	<u>50</u>	<u>0.02</u>	<u>0.004</u>	<u>5.0</u>	<u>2.7</u>
MDI-4	80	7	50	0.02	0.004	3.3	2.7
MDI-5	80	5	120	0.02	0.04	0.5	0.5
MDI-6	100	5	50	0.02	0.004	5.0	2.7
MDI-7	80	5	80	0.02	0.004	5.0	5.4
MDI-8	80	5	80	0.02	0.004	5.0	10.8
MDI-9	90	5	80	0.02	0.012	1.7	2.7
MDI-10	80	5	120	0.02	0.012	1.7	2.7
MDI-11	70	5	120	0.02	0.012	1.7	2.7
MDI-12	60	5	120	0.02	0.012	1.7	2.7
MDI-13	50	5	120	0.02	0.012	1.7	2.7
MDI-14	40	5	120	0.02	0.012	1.7	2.7

-Solvent : Toluene

The functionalized boehmites were used in PU organic-inorganic hybrid material production. HDI-2 and MDI-3 are the best functionalization experiments in this study. Results are discussed in detail in chapter 4.

3.2.2. POLYESTER-POLYOL SYNTHESIS

The experiments were performed under nitrogen atmosphere. 1,4-butanediol was poured into five-necked flask, and the temperature was raised to 80°C. Then adipic acid or phthalic anhydride and p-toluenesulfonic acid (catalyst) were added. Temperature was increased and kept at 130-150°C while stirring the solution continuously. The acid number was determined during the reaction (~8-10 times). The used amount of polyols during determining the acid number was neglected (~0.1 g), because the samples taken out were too small in quantity. When the acid number reached down to an expected value the reaction was stopped. The experimental setup for polyester-polyol synthesis is shown in Figure 3.4 and the parameters of the experiments are tabulated in Table 3.4.

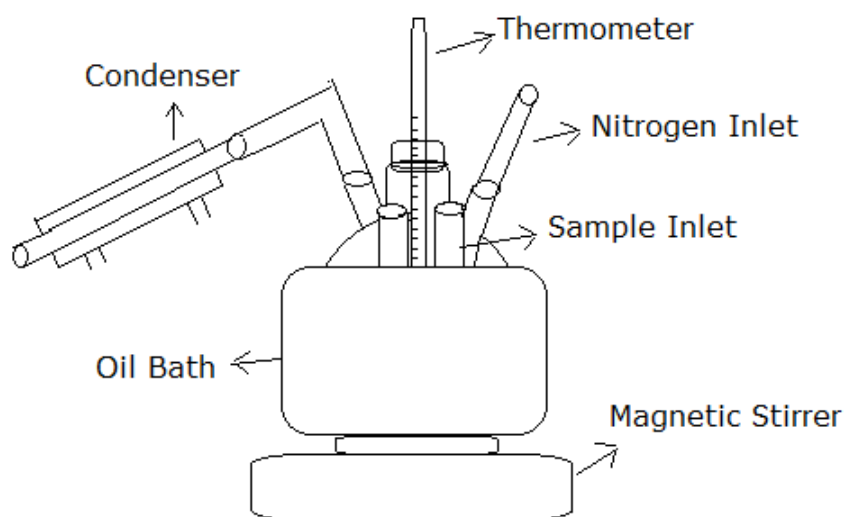


Figure 3.4 Experimental setup for polyester-polyol synthesis.

Table 3.4 Polyester-Polyol synthesis experiments.

	M1	M2	Catalyst wt %	mole M1	mole M2	Acid #	MWt (g/mol)
PE-PO_1	BD	Ad. Ac.	0.5	1.3	1.0	16	1000
PE-PO_2	BD	Ph. An.	0.5	1.3	1.0	13	1000

-T : 130-150 °C

-Catalyst : p-toluene sulfonic acid

3.2.3. PRODUCTION OF POLYURETHANE ORGANIC-INORGANIC HYBRID MATERIALS

In this step, polyurethane was produced in three different ways. In the first part, polyurethane synthesis was done by using polyol and diisocyanate. In the second part, polyurethane composite was prepared by dispersing boehmite nano-particles in polyurethane under mechanical stirring. Finally, inorganic-organic hybrid material was produced by carrying out polymerization of 'polyol-MDI-functionalized boehmite' all together. Experiments were conducted under nitrogen atmosphere. Experimental setup for polyurethane production is shown in Figure 3.5.

3.2.3.1. POLYURETHANE POLYMER SYNTHESIS

Polyester-polyol and solvent (toluene) were introduced into a five-necked reactor. The temperature was raised to 70°C by means of a hot water circulator. Then, MDI or HDI and dibutyl tin dilaurate (catalyst) were added, and the solution was stirred mechanically. After about five hours when %NCO became to be around 7-8, diaminoethanol (chain extender) and hexamethylene tetramine (crosslinker) were added and stirred for one more hour.

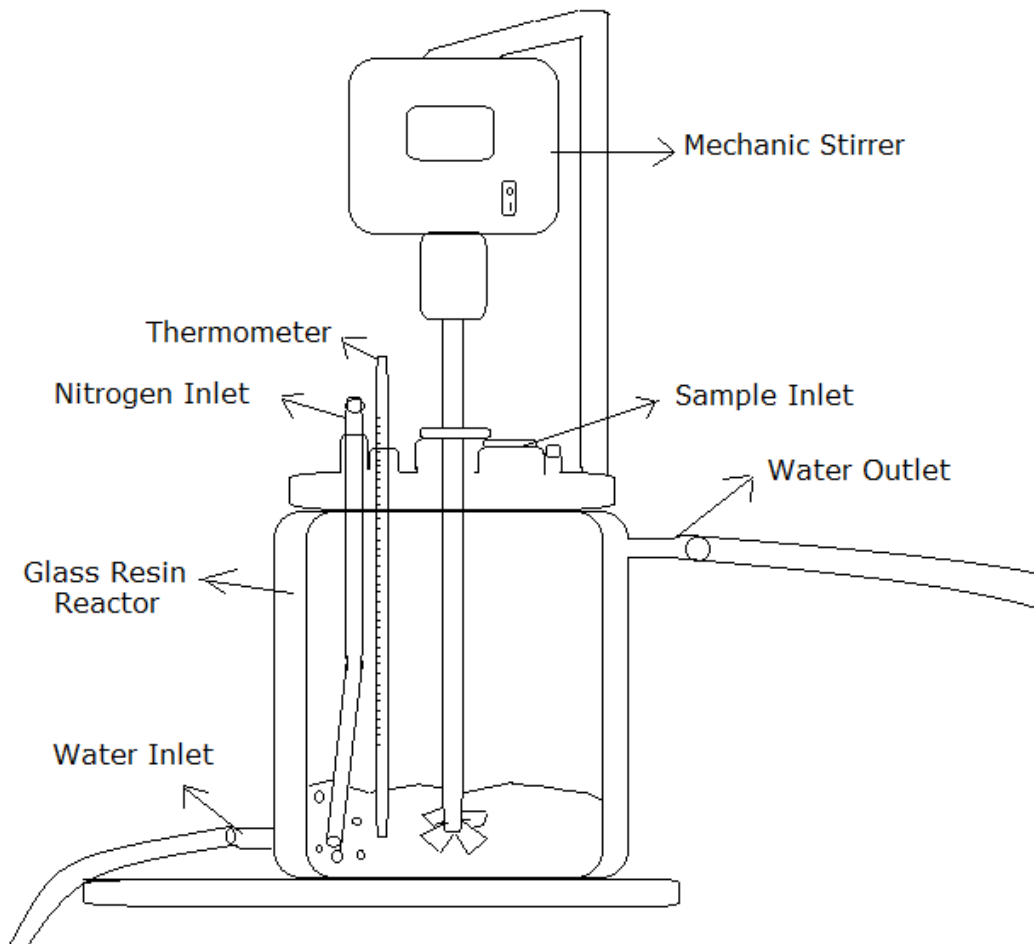


Figure 3.5 Experimental setup of the polyurethane production.

3.2.3.2. POLYURETHANE COMPOSITE PRODUCTION

After the production of polyurethane, boehmite was mixed with polyurethane and the solution was stirred mechanically for one hour.

3.2.3.3. POLYURETHANE ORGANIC-INORGANIC HYBRID MATERIAL PREPARATION

Polyester-polyol and solvent (toluene) were introduced into a reactor, and the temperature was raised to 70°C by means of a circulator. Then, MDI functionalized boehmite and dibutyl tin dilaurate (catalyst) were added and the solution as stirred mechanically. After one hour MDI was added to the medium, and the solution was stirred about four hours until %NCO is around 7-8. Then, diaminoethanol (chain extender) and hexamethylene tetraamine (crosslinker) were added and stirred one more hour.

The parameters of the experiments were tabulated in Table 3.5.

Table 3.5 Polyurethane production experiments.

	Monomer 2	Boehmite Type	Boehmite wt %	Chain Extender	NCO %
PU-1	Polyol (Ad.Ac.)	-	-	Diaminoethanol	4
PU-2	Polyol (Ph.An.)	-	-	Diaminoethanol	3
PU-3	Polyol (Ad.Ac.)	BH	1	Diaminoethanol	3
PU-4	Polyol (Ph.An.)	BH	1	Diaminoethanol	4
PU-5	Polyol (Ad.Ac.)	FB	1	Diaminoethanol	4
PU-6	Polyol (Ph.An.)	FB	1	Diaminoethanol	3
PU-7	Polyol (Ph.An.)	FB	3	Diaminoethanol	5
PU-8	Polyol (Ph.An.)	FB	5	Diaminoethanol	4
PU-9	Polyol (Ph.An.)	-	-	1,4-Butanediol	3
PU-10	Polyol (Ad.Ac.)	-	-	1,4-Butanediol	5
PU-11	Polyol (Ad.Ac.)	FB	1	1,4-Butanediol	5
PU-12	Polyol (Ad.Ac.)	FB	3	1,4-Butanediol	3

-Monomer 1: MDI

-Catalyst (DBTL) wt %: 0.5

-mol M1/mol M2/mol chain extender: 2/1/1

3.3. CHARACTERIZATION METHODS

In this study, different characterization methods were used for determining the structure, morphology, and the properties of the materials. They are SEM (Scanning Electron Microscopy), FTIR (Fourier Transform Infrared) Spectroscopy, XRD (X-ray Diffraction), PCS (Photon Correlation Spectroscopy), BET (Brunauer-Emmet-Teller analysis), elemental analysis, DTA-TGA (Differential Thermal Analysis-Thermal Gravimetric Analysis), hardness test, scratch resistance test, abrasion resistance test, bending test, impact test, and gloss meter. Some information was given about the instruments in Appendix F.

CHAPTER 4

RESULTS AND DISCUSSION

In this study, the results were grouped in four parts; these are (i) functionalization of boehmite nano-particles, (ii) synthesis of polyester polyol, (iii) production of PU organic-inorganic hybrid materials, and (iv) mechanical tests.

4.1. FUNCTIONALIZATION OF BOEHMITE NANO-PARTICLES

In this section, the results were divided into three parts; these are (i) grinding of aluminum hydroxide, (ii) boehmite production by hydrothermal process, and (iii) functionalization of boehmites.

4.1.1. GRINDING OF ALUMINUM HYDROXIDE

In this part, the effects of grinding were discussed. Aluminum hydroxide was used as the starting material in hydrothermal process. It was ground in a ball mill before subjected to hydrothermal treatment in order to decrease the particle, because, there is no mixing part in the reactor.

Dissociation and recrystallization reactions occur in boehmite production. Therefore, decreasing the particle size of the starting material was very crucial for complete conversion of aluminum

hydroxide to boehmite without agglomeration. SEM micrographs of ground $\text{Al}(\text{OH})_3$ particles were given in Figure 4.1.

IPA (iso propyl alcohol) was selected as a wetting agent in a ball-milling process as a grinding aid for size reduction.

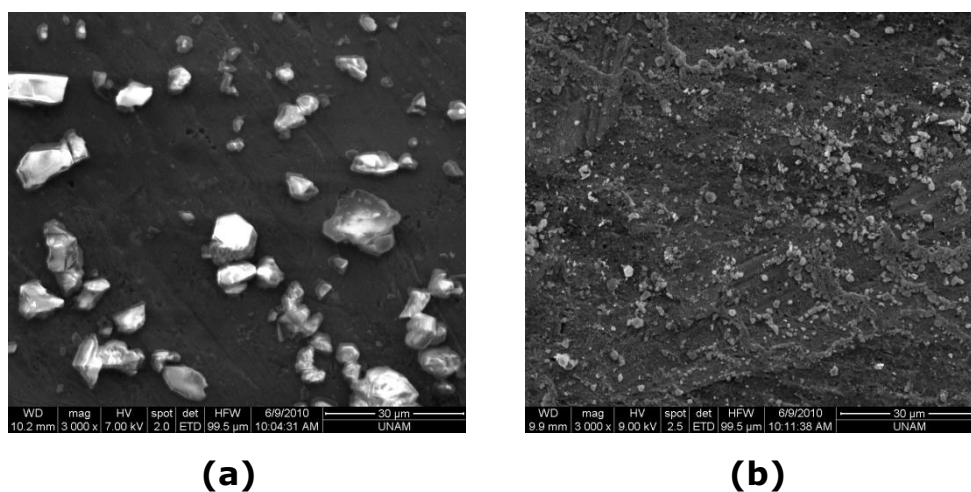


Figure 4.1 SEM micrographs of **(a)** aluminum hydroxide ($\times 3000$), **(b)** ground aluminum hydroxide ($\times 3000$).

The mean particle sizes of $\text{Al}(\text{OH})_3$ and ground $\text{Al}(\text{OH})_3$ were measured by Image-J program from SEM micrographs and also by PCS technique. The measurements done by using Image-J program showed that the ground $\text{Al}(\text{OH})_3$ particles were approximately ten fold smaller than the original $\text{Al}(\text{OH})_3$ particles. The particle size measurements of ground particles using PCS and Image-J program showed that both measurements were almost equal. However, the size of initial $\text{Al}(\text{OH})_3$ particles couldn't be determined by using PCS technique due to small measurement range of size (1nm to $5\mu\text{m}$)

of the device. The results of measurements were tabulated in Table 4.1.

Table 4.1 Particle size results of $\text{Al}(\text{OH})_3$ and ground $\text{Al}(\text{OH})_3$.

	Mean Particle Size (SEM) (μm)	Mean Particle Size (PCS) (μm)
$\text{Al}(\text{OH})_3$	6.04	-
Ground $\text{Al}(\text{OH})_3$	0.66	0.75

4.1.2. BOEHMITE PRODUCTION BY HYDROTHERMAL PROCESS

The morphology of boehmite particles produced change with the pH of the medium. Needle-like particles were produced at low pH, and cubic-like and plate-like particles were produced at high pH. Therefore, pH had to be adjusted while preparing the solution. In literature, plate-like boehmite particles were produced in high pH by adding alkaline solution. However, this method failed to give a satisfactory result in this research. In our study, although the solution pH was basic in plate-like boehmite production, solution preparation was different than other studies. Firstly, the distance between plate-like boehmite layers was increased (peptization) with acetic acid addition. Then, solution pH was increased to 10.3-10.7 by addition of ammonia solution.

4.1.2.1. TRANSFORMATION OF ALUMINUM HYDROXIDE TO BOEHMITE NANO-PARTICLES

Molecular structure of produced boehmite nano-particles, and crystal structure of $\text{Al}(\text{OH})_3$ and produced boehmite nano-particles were investigated in order to prove complete transformation of $\text{Al}(\text{OH})_3$ to boehmite. The molecular structure of particles was determined by FTIR spectroscopy, and the crystal structure was evaluated by XRD analysis.

Boehmite showed FTIR absorption bands at 641, 737, 1071, 1161, 1640, 1974, 2100, 3092 and 3300 cm^{-1} which were reported in the literature [27, 64, 66-67, 77, 86, 88]. The FTIR spectra of boehmite nano-particles produced with different parameters were shown in Figure 4.2. The bands in the range 500-750 cm^{-1} corresponds to the vibration modes of boehmite while other bands in the range of 1071-3300 cm^{-1} characterize the OH^- bonds in the boehmite lattice. The intense band at 1070 and the shoulder at 1160 cm^{-1} are ascribed to $\gamma\text{-AlO}(\text{OH})$ symmetric and asymmetric bending vibrations in the boehmite lattice. Two weak bands at 2100 and 1974 cm^{-1} can be assigned to combination bands. Two strong but well-separated absorption bands at 3092 and 3300 cm^{-1} assigned to $\gamma\text{-AlO}(\text{OH})$ asymmetric and symmetric stretching vibrations and this indicated that the $\text{Al}(\text{OH})_3$ was converted to crystalline boehmite particles. In addition the shoulder at 1640 cm^{-1} can be assigned to the bending mode of adsorbed water [65-66].

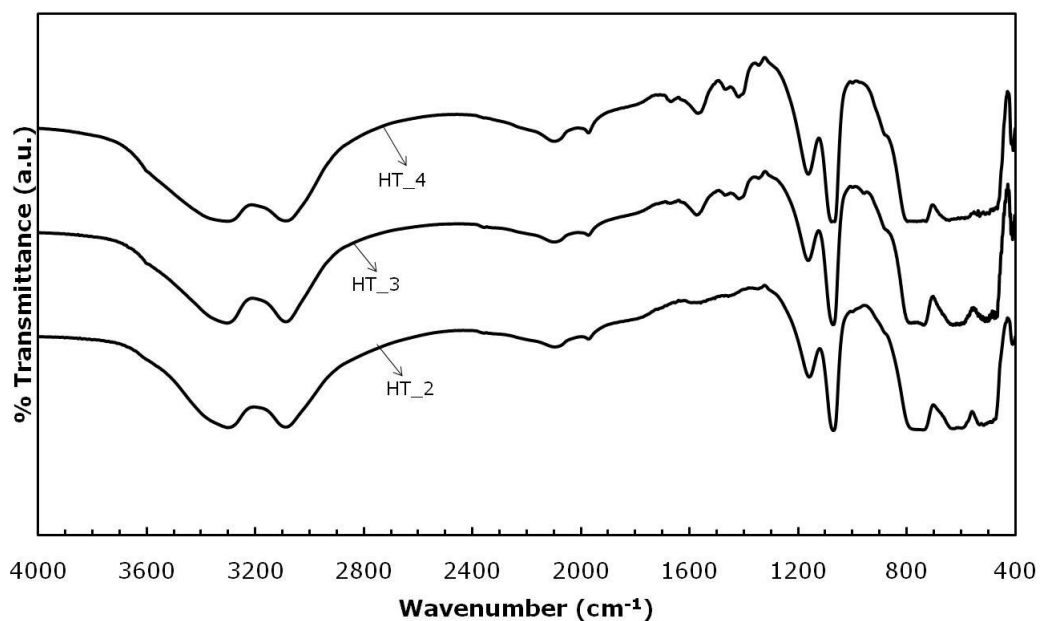


Figure 4.2 FTIR spectrum of boehmite nano-particles

Figure 4.3 shows the XRD spectrum of $\text{Al}(\text{OH})_3$ and boehmite. The (020), (120), (031), (131), (051), (200), (220), (151), (080), (231) and (002) peaks were reported to be the characteristic peaks of boehmite particles [57, 61, 72]. The very sharp peaks indicate high crystallinity of the synthesized product.

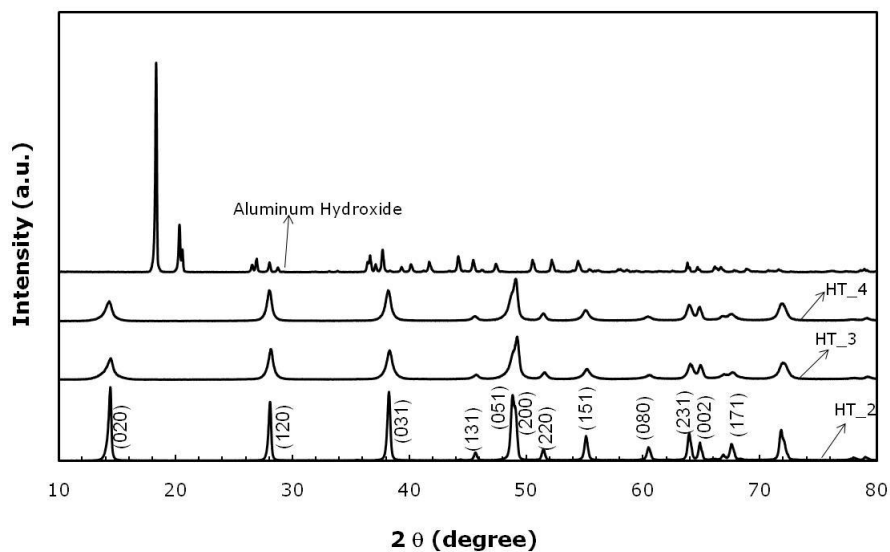


Figure 4.3 XRD graphs of boehmite nano-particles and aluminum hydroxide.

4.1.2.2. EFFECT OF EXPERIMENTAL PARAMETERS ON BOEHMITE NANO-PARTICLES

In this study, plate-like boehmite particles with high aspect ratio was aimed to produce to achieve relatively high mechanical properties when used in polyurethane organic-inorganic hybrid materials. So the effects of pH, the amount of acid and base, and the reaction time on the morphology of particles were investigated. It was observed that plate-like structures couldn't be achieved in highly basic medium, when only ammonia solution was used in solution preparation. So the pH of the medium was first made highly acidic to separate the layers from each other. After this peptization step, ammonia solution was added for increasing the pH 10.3-10.7. Then hydrothermal treatment was started. Despite all these, the amount of acetic acid was not enough for peptization

in the first experiment (HT-1), and the morphology of the particles came out to be cubic-like (Figure 4.4 (a)). Thus, the amount of acetic acid was increased in the second set of experiment (HT-2), and the morphology of the particles turned out to be plate-like (Figure 4.4 (b)).

In order to increase the aspect ratio of the particles, two different experiments were also conducted. Aging time of the experiments was increased from 5 to 10 h in the third experiment (HT-3). The amount of acid and base were increased while the pH of the medium was kept constant at 10.3-10.7 in the fourth experiment (HT-4). Consequently, the aspect ratio of the particles increased both in the third and fourth experiments as seen from Figure 4.4 (c) and Figure 4.4 (d), respectively. Figure 4.4 (c) shows that the aspect ratio of boehmite particles increased with the increase of the aging time. The particle size of boehmites decreased as the amount of acid and base increased as seen in Figure 4.4 (d). However, morphology of the boehmite was getting worse with increasing acid and base amount. It is easily seen in SEM micrographs, HT-3 has better morphology, size and aspect ratio than others.

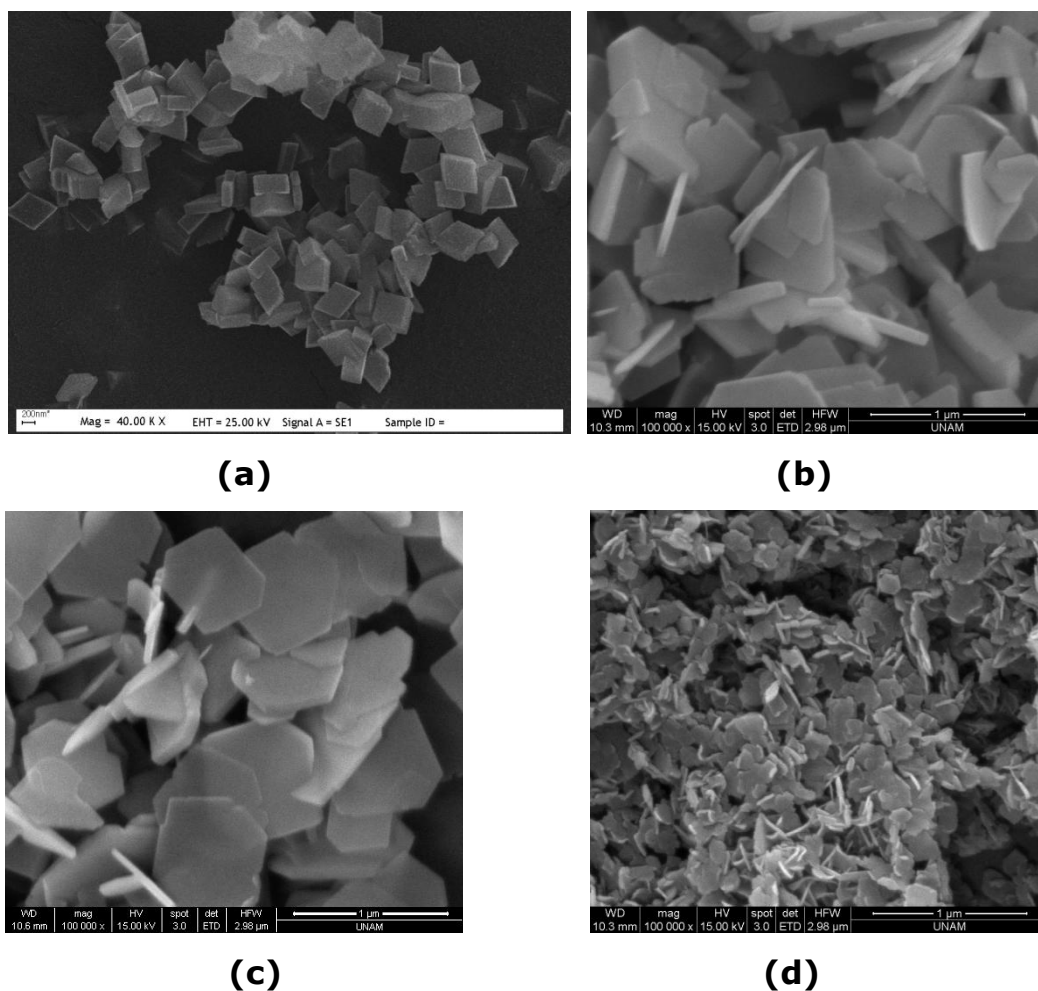


Figure 4.4 SEM micrographs of produced boehmite in **(a)** HT-1 (x40000), **(b)** HT-2 (x100000), **(c)** HT-3 (x100000), **(d)** HT-4 (x100000).

The produced plate-like boehmite nano-particles were used in making PU organic-inorganic hybrid coating material. High particle surface area was preferred in organic-inorganic hybrid coatings. Therefore, surface area of the boehmite particles was measured by BET (Brunauer-Emmet-Teller), and the results were tabulated in Table 4.2. It is seen that HT-3 has the highest surface area.

In addition, the size of the particles was measured by PCS technique, and from SEM micrographs using IMAGE-J program. In PCS technique, particles are assumed to be spherical. Therefore, the measurements taken from PCS were less accurate than those found from SEM micrographs.

Moderate stability is provided when the zeta potential between 30-40 mV as given in the introduction part. Therefore, the zeta potentials found from PCS show that the dispersion of boehmites produced by HT process was almost accomplished.

The surface area, size, aspect ratio and zeta potential of the boehmite nano-particles were tabulated in Table 4.2.

Table 4.2 Surface area, mean particle size by IMAGE-J and PCS, aspect ratio, and zeta potential of plate-like boehmites.

	BET (m²/g)	IMAGE-J (nm)	PCS (nm)	Aspect Ratio (SEM)	Zeta Potential (mV)
HT1	-	439/213	257	2.06	37.5
HT2	13.82	582/60	595	9.65	35.0
HT3	90.95	675/27	607	25.45	30.0
HT4	80.69	127/7	266	18.62	42.2

The particle size distribution of boehmites varies between 100 to 700 nm. The size distribution of HT-2 and HT-3 obtained from PCS measurements showed that the distribution changed between 500 to 700 nm, and the size distribution of HT-1 and HT-4 changed

from 100 to 500 nm. In addition, high particle sizes were also observed in HT-4 experiment. In this case, because, particles were too small and surface attraction was very high, so particles had high tendency to agglomerate.

Al(OH)₃ particles have two different size ranges. One of them changed between 200 to 500 nm and the other one changed between 700 to 1500 nm. Because of these two different ranges, two different distributions occurred in Al(OH)₃ curve as seen in Figure 4.5.

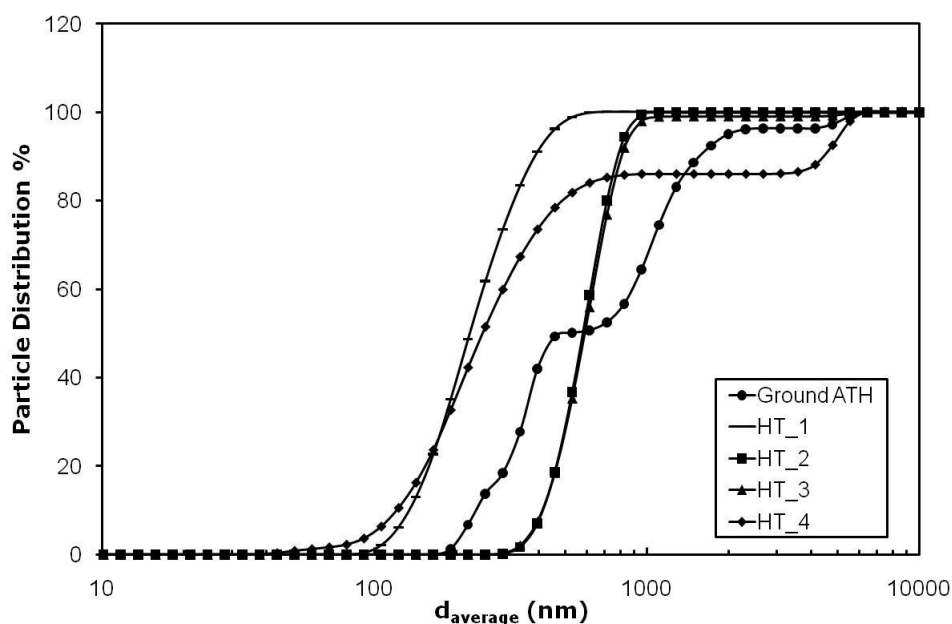


Figure 4.5 Variation of particle distribution with particle size.

The thermal behavior of the boehmite was studied by DTA-TGA. Because of thermal transformations of boehmite powder, three distinguishable steps in DTA-TGA curve were reported in the

literature [58]. However, in Figure 4.6, TGA/DTA curve has two steps in the temperature range of 20°C - 800°C. Therefore, α -Al₂O₃ phase formation which occurred at around 950°C did not show up in Figure 4.6. Two weight loss regions are observed at the ranges of 45-150°C and 400-510°C. The first endothermic peak at 70°C is due to desorption of physically sorbed water, while the second endothermic peak is attributed to transformation of boehmite to γ -Al₂O₃ phase at 480°C.

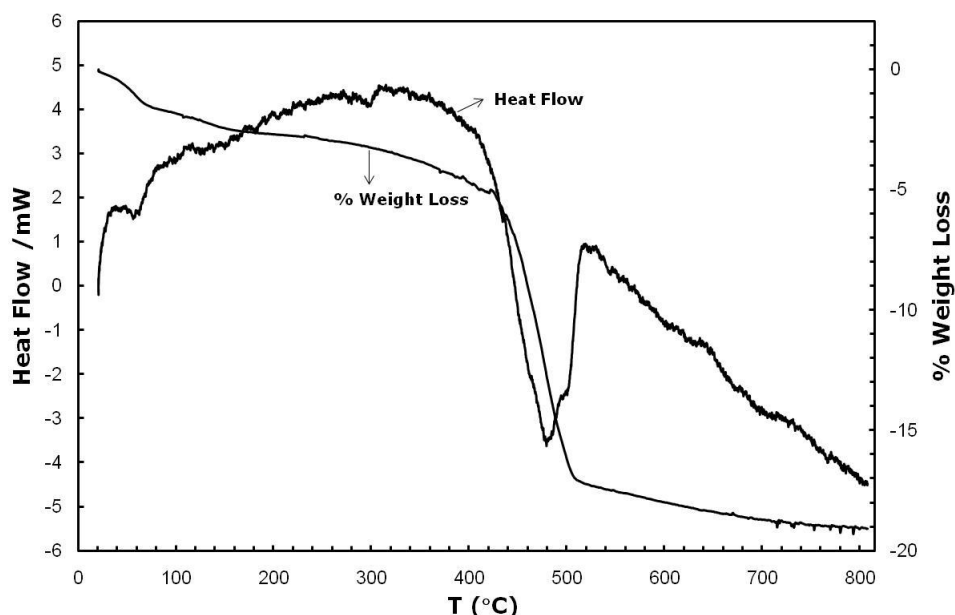


Figure 4.6 TGA/DTA graphs of boehmite nano-particles.

4.1.2.3. EFFECTS OF ULTRASONIC MIXING

Dispersed functionalized boehmite nano-particles are required for the production of PU organic-inorganic hybrid materials. Therefore, dispersion of the particles in all steps is very crucial in order to

produce PU coatings with enhanced mechanical properties. In the literature survey, dispersion was provided by using surfactant in hydrothermal process. However, the resultant boehmite particles include impurities due to use of surfactants. Moreover, using surfactants increase the cost of the production. Therefore, ultrasonic mixing was applied before and after hydrothermal treatment, in the functionalization of boehmite particles, and just before making PU organic-inorganic hybrid materials. Ultrasonic mixing was done at two minute periods (3-4 times) and 35-40 % of full power.

The difference between with and without ultrasonic mixing before and after hydrothermal process is shown in Figure 4.7. It is clear that ultrasonic mixing is a necessity.

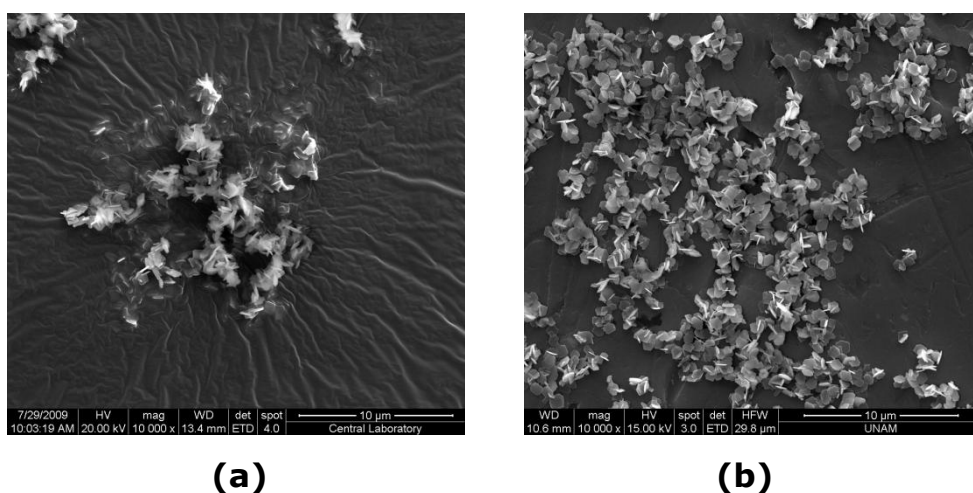


Figure 4.7 Boehmite productions by hydrothermal process **(a)** without ultrasonic mixing (x10000), **(b)** with ultrasonic mixing (x10000).

4.1.3. FUNCTIONALIZATION OF PLATE-LIKE BOEHMITE NANO-PARTICLES

The SEM micrographs of MDI and HDI functionalized boehmite nano-particles are shown in Figure 4.8.

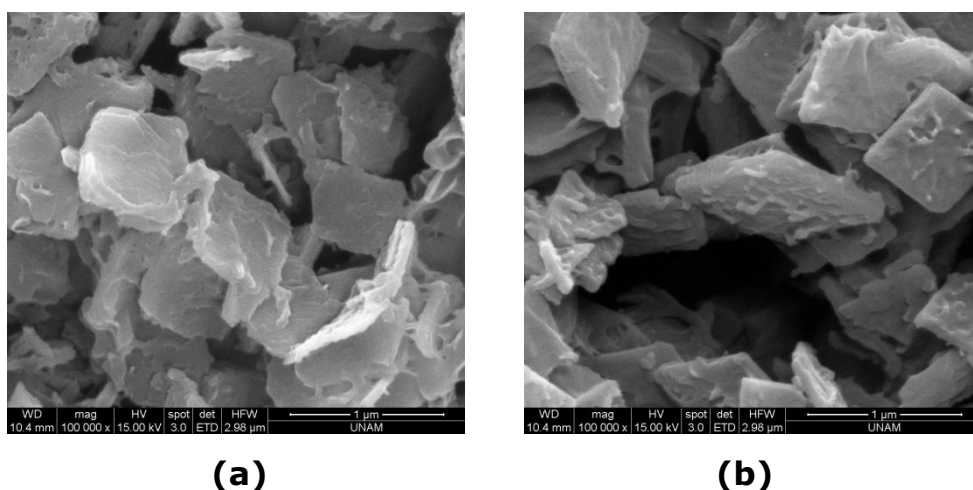


Figure 4.8 SEM micrographs of (a) MDI functionalized nano-boehmites (x100000), (b) HDI functionalized nano-boehmites (x100000).

According to FTIR spectra as seen in Figure 4.9 and Figure 4.10, the most effective functionalization experiments are HDI-2 and MDI-3. The highest ratio of cyanate peak at 2277 cm^{-1} to boehmite peak at 3300 cm^{-1} was observed at HDI-2 and MDI-3 experiments.

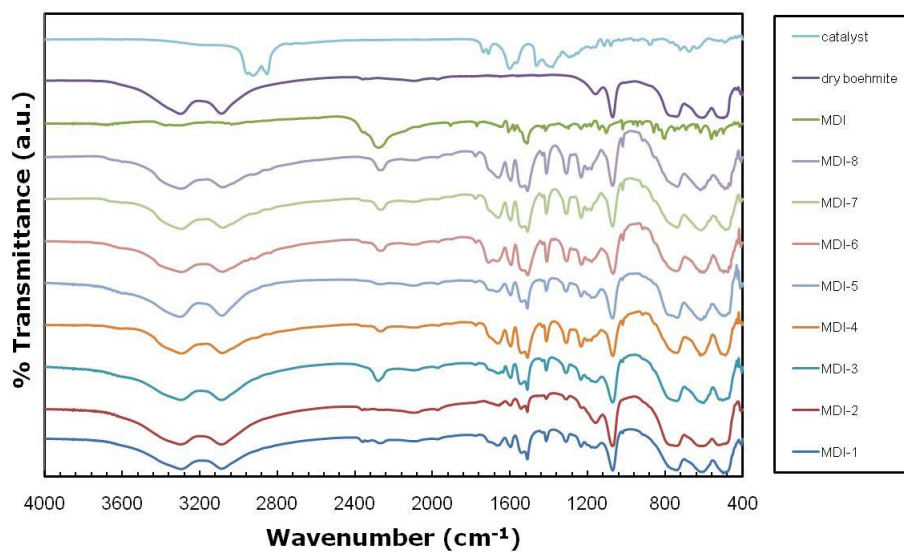


Figure 4.9 FTIR spectra of MDI functionalization experiments.

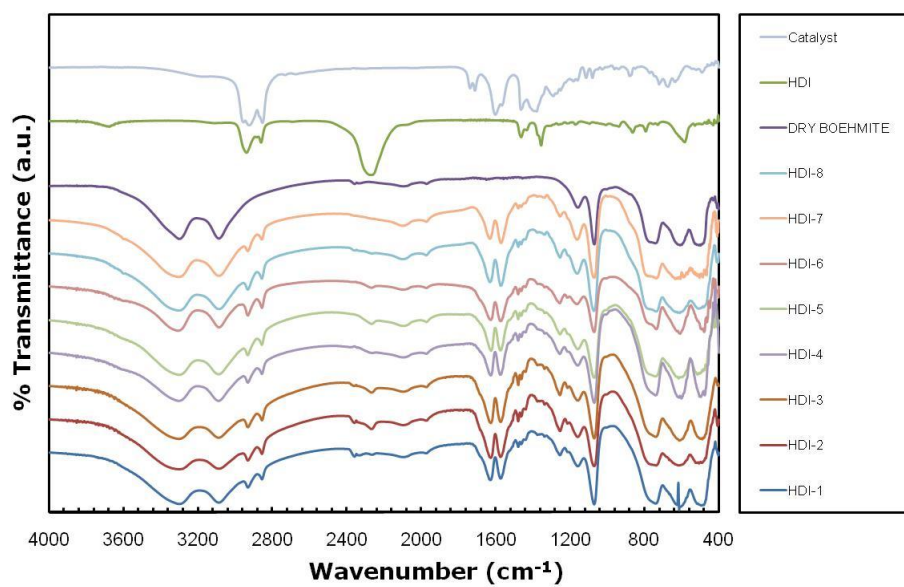


Figure 4.10 FTIR spectra of HDI functionalization experiments.

The infrared spectra of the MDI and HDI grafted boehmite shows new absorptions at 3313, 2277, 1540, 1510, 1600, 1640, 1230, 2900, and 2825 cm^{-1} . The absorption peaks at 3313 and 2270 cm^{-1} are respectively attributed to the stretching vibration of $-\text{NH}$ groups, asymmetric stretching vibrations of $-\text{NCO}$ groups, and the 1540 and 1510 cm^{-1} correspond to bending vibration of $-\text{CNH}$ groups. The absorption peaks at 1600 and 1640 cm^{-1} occurred due to $\text{C}=\text{O}$ stretching vibrations. Stretching vibrations of $\text{C}-\text{N}$ groups was observed at 1640 cm^{-1} . The peaks at 2900 and 2825 cm^{-1} are attributed to symmetric and asymmetric vibrations of methyl groups, respectively. The FTIR spectra of HDI, MDI, dry boehmite, MDI functionalized boehmite, and MDI functionalized boehmite are shown in Figure 4.11.

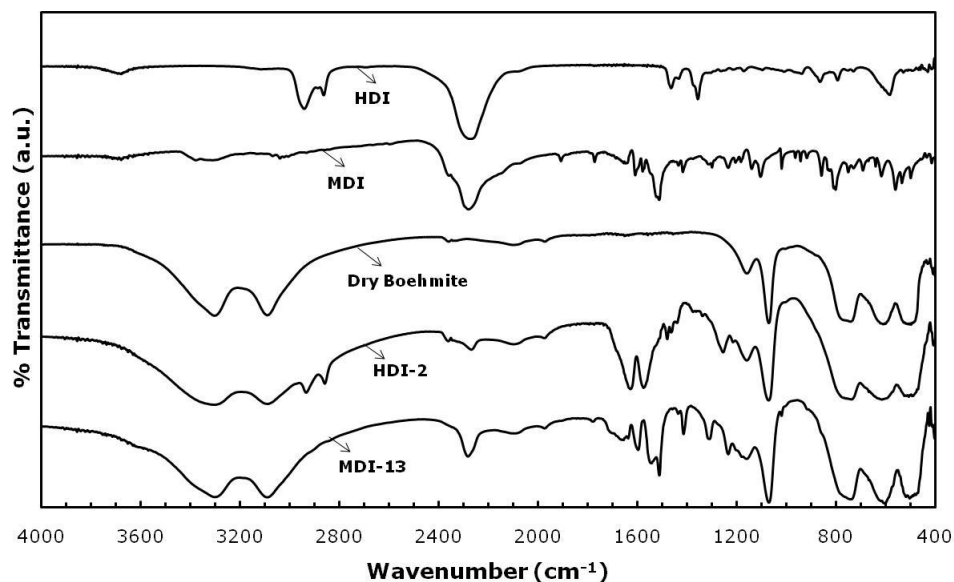


Figure 4.11 FTIR spectra of MDI and HDI functionalize boehmites, MDI, HDI, and dry boehmite.

The functionalization of boehmite nano-particles with MDI was conducted at different temperatures to determine the most effective functionalization temperature. The FTIR spectra of the products obtained at different temperatures are shown in Figure 4.12. It is easily seen that the highest ratio of cyanate peak at 2277 cm^{-1} to boehmite peak at 3300 cm^{-1} was observed at $80\text{ }^{\circ}\text{C}$. Therefore, the most effective functionalization occurred at $80\text{ }^{\circ}\text{C}$.

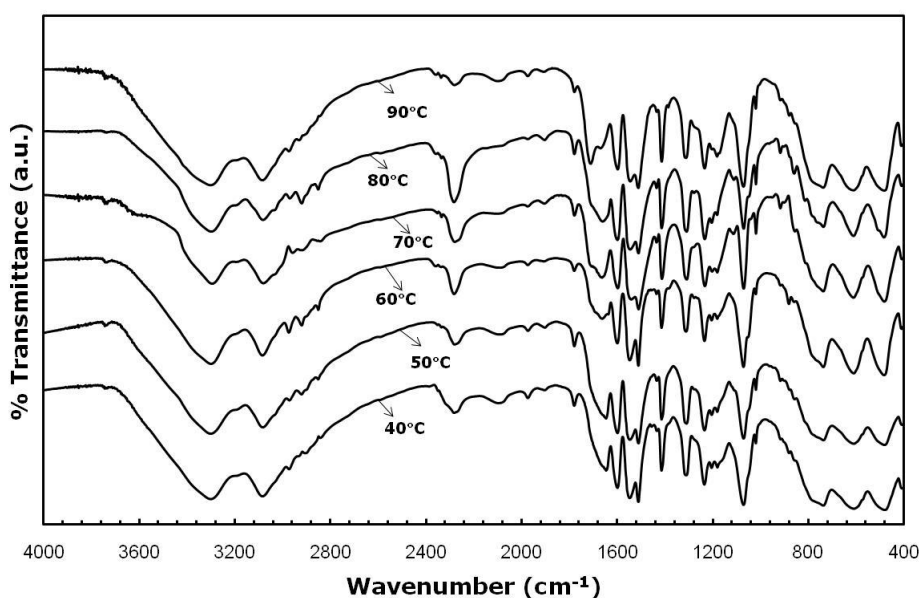


Figure 4.12 Effect of MDI functionalization temperature.

The DTA-TGA results of HDI and MDI functionalized boehmite nano-particles are given in Figure 4.13, and Figure 4.14, respectively. The comparison of these figures with Figure 4.6 indicates that the functionalized specimens display weight loss due to their organic matter content between $300\text{-}350\text{ }^{\circ}\text{C}$.

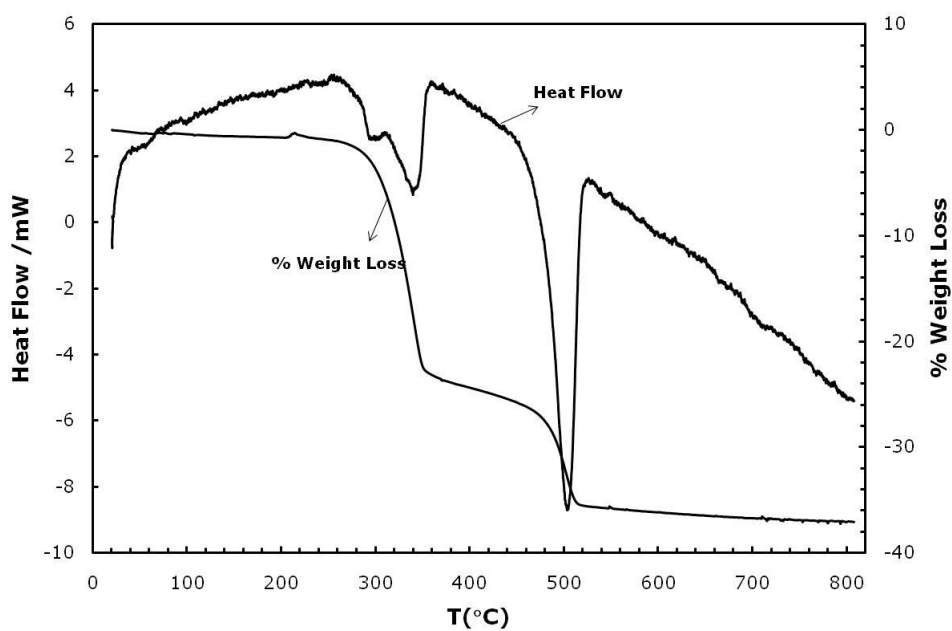


Figure 4.13 TGA/DTA graphs of HDI functionalized boehmite nano-particles.

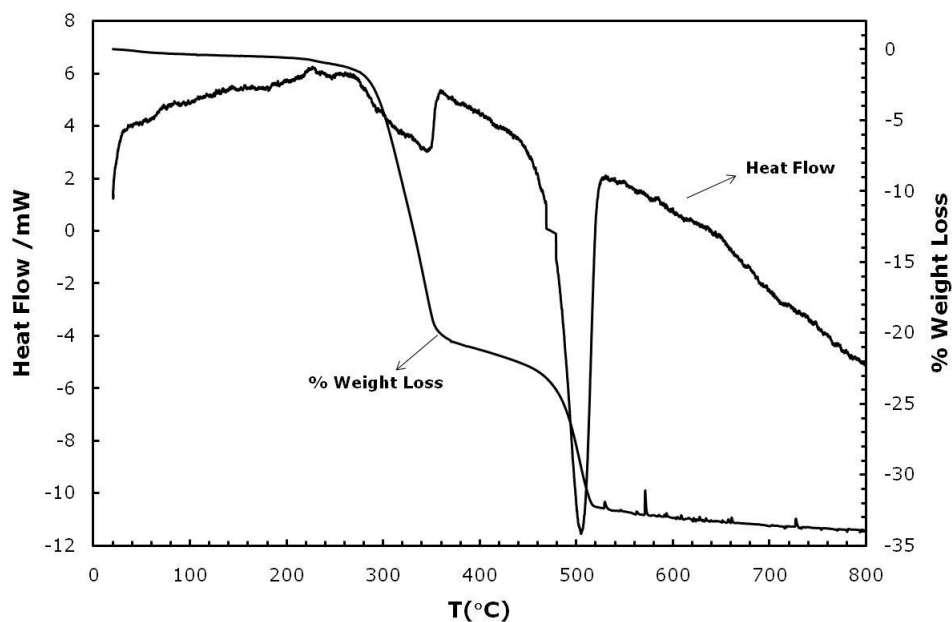


Figure 4.14 TGA/DTA graphs of MDI functionalized boehmite nano-particles.

The functionalized boehmite particles were further characterized by elemental analysis to determine the amounts of C, H, and N in the structure. The results of elemental analysis of boehmite and functionalized boehmites are given in Table 4.3. Boehmite has 0.29 % C which might be due to carbon dioxide absorbed from air, and it does not contain any nitrogen. On the other hand, HDI and MDI functionalized boehmites involve carbon and nitrogen. This proves that the functionalization of the particles was accomplished.

The results show that, the amount of C, H, and N in the HDI functionalized boehmite was higher than in MDI functionalized boehmite. However, MDI functionalization showed better results than HDI functionalization in FTIR spectra when free NCO peaks of functionalized boehmites to characteristic peak of boehmite at 3300 cm^{-1} ratio was compared. The high amount of C, N, and H in HDI functionalized boehmites could occur due to the polymerization of HDI on the boehmite surface. Therefore, PU organic-inorganic hybrids were produced by using MDI functionalized boehmites.

Table 4.3 Elemental analysis.

Sample Name	% C	% H	% N
Boehmite	0.29	2.20	-
HDI-2	54.36	4.67	8.59
MDI-13	16.38	2.96	2.93

4.2. POLYESTER-POLYOL SYNTHESIS

Two types of polyols were synthesized and the mechanical properties of produced PUs with these polyols were compared. Both adipic acid and phthalic anhydride used polyols have molecular weight of 1000 g/mol.

The FTIR spectra of two different polyols are given in Figure 4.15. In FTIR spectrum, the OH stretching band at 3520, 3430, and 3320 cm^{-1} in polyols with adipic acid and 3600, 3525, 3410, and 3100 cm^{-1} in polyols with phthalic anhydride indicate the presence of free hydroxyl groups in all polyols. Furthermore, typical ester C=O peak was observed at 1730 cm^{-1} and this proved that esterification reaction took place. The absorption peaks at 2800-3000 cm^{-1} are attributed to $-\text{CH}_2$ symmetric and asymmetric stretching vibrations. 1240-1167 and 1105 cm^{-1} correspond to $-(\text{C}-\text{C}(=\text{O})-\text{O})$ and $-\text{O}-\text{C}-\text{C}$ vibrations, respectively. The absorption peaks at 1590, 1577, 1476, 1445, and 1287-1274 cm^{-1} show vibrations of aromatic rings from phthalic anhydride.

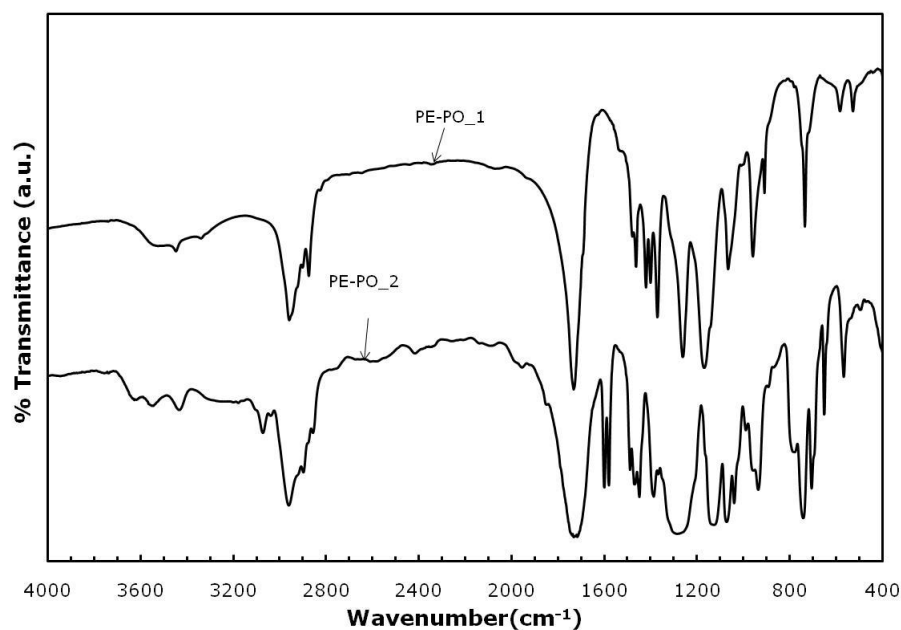


Figure 4.15 FTIR spectra of produced polyester polyols.

4.3. POLYURETHANE PRODUCTION

The FTIR spectra of produced PUs are shown in Figure 4.17. In FTIR spectrum, the characteristic -NH/OH stretching vibrations peaks of polyurethane appeared at 2970-2870, 1730, 1704, 1620, and 1460 cm^{-1} . The absorption peak at 2970-2870 cm^{-1} is attributed to the stretching vibration of -CH groups. Asymmetric stretching vibrations of -NCO groups at 2270 cm^{-1} was disappeared due to the reaction of cyanate and hydroxyl groups. The formation of the urethane group can be determined by examining the absorption peak at 1730 cm^{-1} . The absorption peaks at 1620 and 1460 cm^{-1} correspond to -NH stretching vibrations and -CH_2 scissoring vibrations, respectively. The peak at 1040 cm^{-1} is attributed to the O-C=O stretching of urethane/ester group.

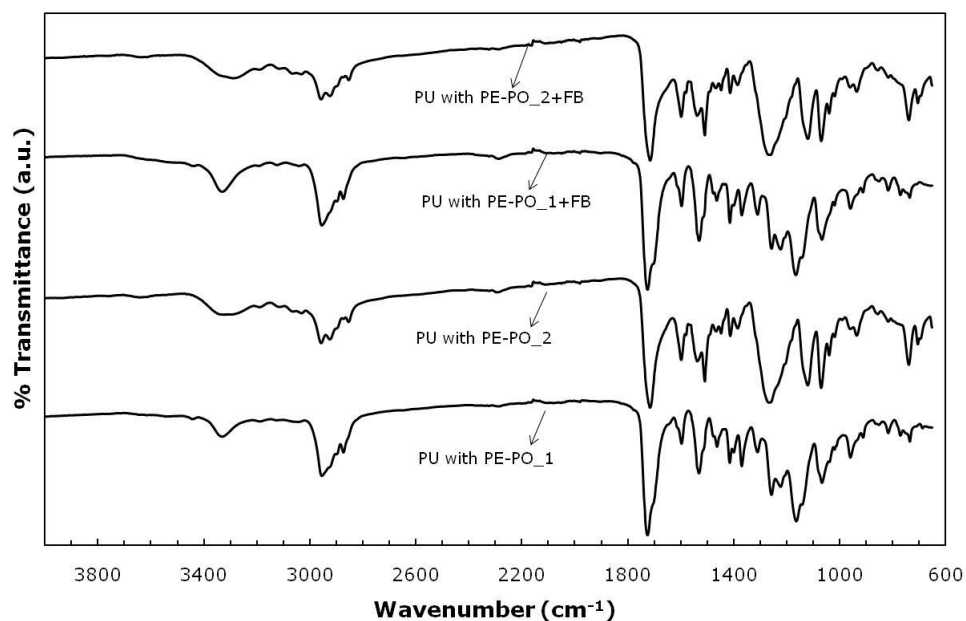


Figure 4.16 FTIR spectra of PUs.

The pictures of PU coatings are shown in Figure 4.19. Coatings were taken photos by using camera (Canon, 10.0 mega pixels). It is easily seen that dispersion was not achieved when non-functionalized boehmites used in PU organic-inorganic hybrid materials (PU-3 and PU-4). Cracks occurred in PU coating produced with PE-PO_2 due to the high amount of functionalized boehmite in the coating.



PU-1



PU-2



PU-3



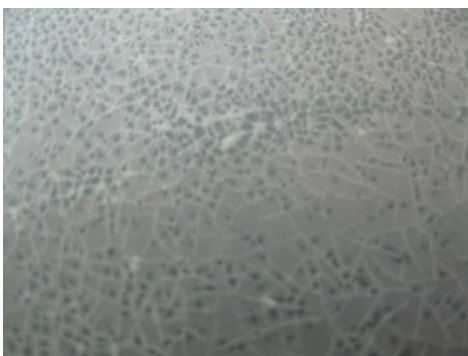
PU-4



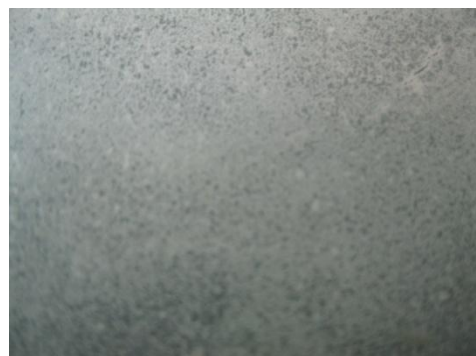
PU-5



PU-6



PU-7



PU-8

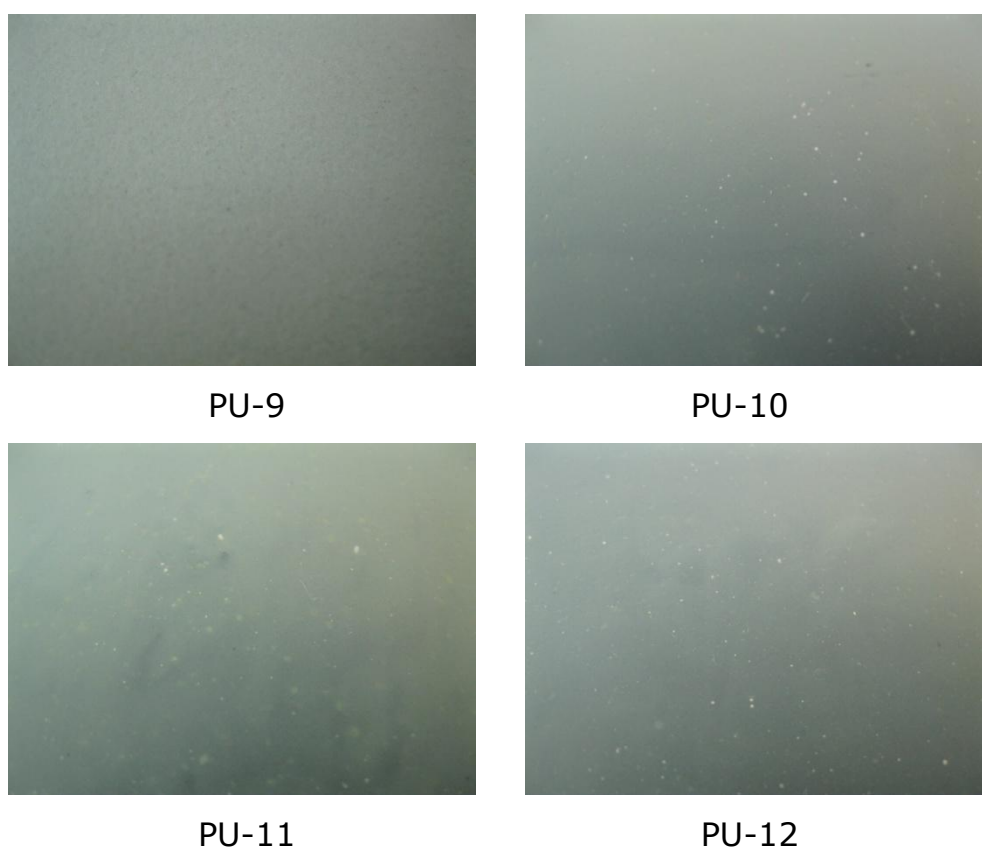


Figure 4.17 Photographs of produced PU coatings.

SEM micrographs of PU polymer and PU organic-inorganic hybrid materials are shown in Figure 4.20. It is easily seen that good dispersion of the functionalized boehmite was achieved in the PU.

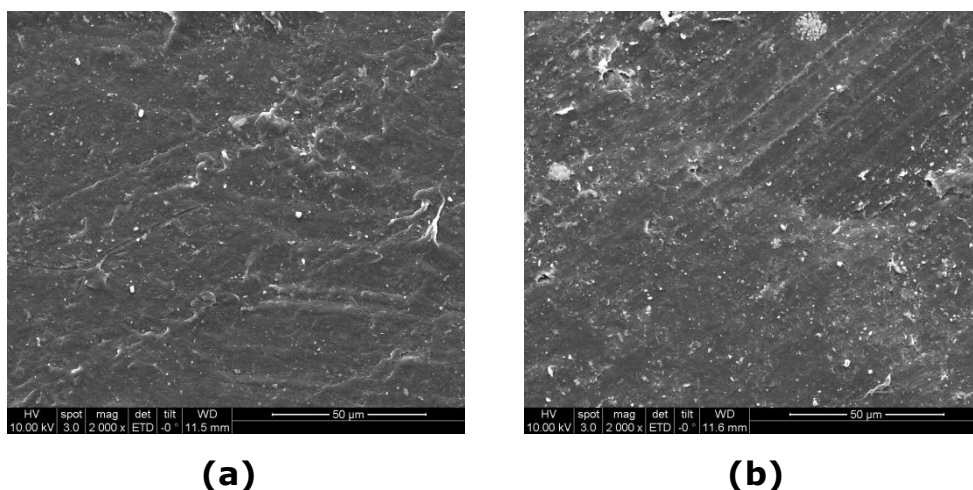


Figure 4.18 SEM micrographs of, **(a)** PU polymer **(b)** organic-inorganic hybrids with functionalized boehmite.

4.4. MECHANICAL TESTS

4.4.1. PENDULUM HARDNESS

The increase in the amount of functionalized boehmite increased the hardness of the PU organic-inorganic hybrid materials. Little amount of functionalized boehmite was enough for increasing the hardness of the PU due to low particle size and high surface area. Therefore, one weight percentage of boehmite in the PU gave the best mechanical properties. Three weight percentages loading also improved hardness property of PUs but not as much as one percentage. The hardness of PU produced with PE-PO-1 increased from 82 to 98 Persoz and the hardness of PU produced with PE-PO-2 increased from 52 to 78 Persoz when one weight percentage of functionalized boehmite is used in the production.

Actually, the hardness of produced PUs must increase with an increase in the amount of functionalized boehmite. In persoz

hardness measurements, the surface of the coating should be smooth to observe accurate results in this study. In other words, the hardness of PUs decreased with the addition of functionalized boehmite higher than 1 %, due to decreasing smoothness of the coating surface.

In addition, hardness was also changed with the types of polyols and chain extenders. When PE-PO_1 was used in the PU production, the hardness of PU organic-inorganic hybrid materials increased twice (40 to 82 Persoz) by using 1,4-butanediol instead of diaminoethanol.

Moreover, hardness of PU with PE-PO_2 was thirty percent (40 to 52 Persoz) higher than PU with PE-PO_1 when diaminoethanol was used for chain extender instead of 1,4-butanediol.

In addition, hardness value of the experiment PU-3 and PU-4 are not accurate due to rough surface of the PU-3 and PU-4 coatings.

The hardness values of the synthesized PUs were given in Appendix G and shown in Figure 4.21 and Figure 4.22.

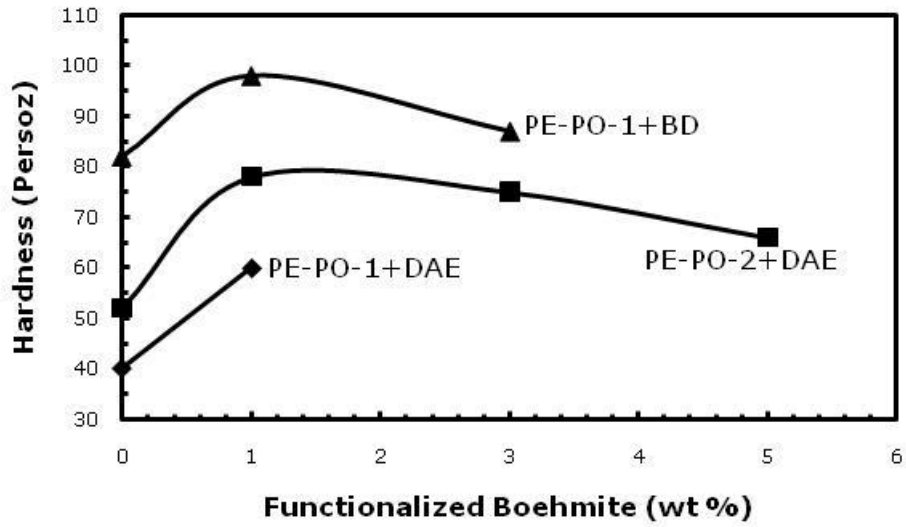


Figure 4.19 The change of hardness of PU organic-inorganic hybrid materials with the amount of functionalized boehmite.

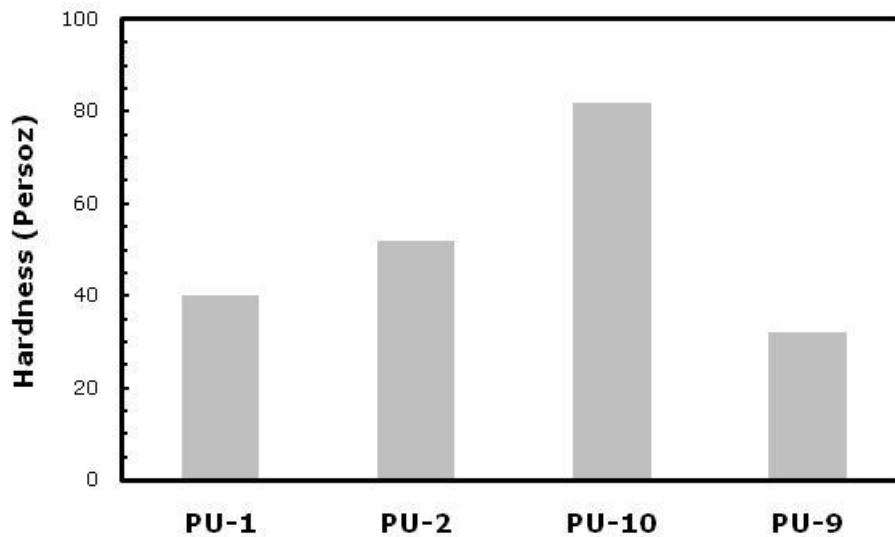


Figure 4.20 Chain extender and PE-PO effects on the hardness of PU organic-inorganic hybrid materials.

4.4.2 IMPACT RESISTANCE

The impact resistance is the relative susceptibility of polymers to fracture under a sudden force applied by a specific weight dropped from a specific height. Impact tests are carried to find out the required minimum potential energy for creating cracks on the surface. The maximum height and weight are 1m and 2 kg, respectively. Therefore the maximum potential energy is 19.6 J. Table 4.7 shows the impact resistance of the specimens tested.

The results show that the PUs with polyols containing phthalic anhydride have very low impact resistance. It should be due to the aromatic content which imparts rigidity, and makes the hybrid material highly brittle. In other words, the impact resistance of the coatings does not depend on the inorganic component but on the type of the polyols used in PU. In addition, the impact resistance of PUs with polyols containing adipic acid was very high due to the flexibility of the polyols.

Moreover, 1,4-butanediol gave flexibility to the PU chains. Thus, diaminoethanol used PU organic-inorganic hybrid materials was more rigid than 1,4-butanediol used PU.

PU-3 and PU-4 could not be applied onto the metal surface due to the dispersion problems. Therefore, impact resistance of PU-3 and PU-4 were not measured.

Table 4.4 Impact resistance of PUs.

Sample	Potential Energy (J)
PU-1	19.6
PU-2	Very Low
PU-3	-
PU-4	-
PU-5	19.6
PU-6	Very Low
PU-7	Very Low
PU-8	Very Low
PU-9	4.9
PU-10	19.6
PU-11	19.6
PU-12	19.6

4.4.3. SCRATCH RESISTANCE

The scratch resistance of the samples was determined by the hardness of the indenter. The pencils with different hardness (2B, B, HB, H, 2H, 3H, 4H and 5H) were used as an indenter. The results are tabulated in Table 4.8.

The results show that the scratch resistance highly depends on the types of polyols used. Polyols with adipic acid gave flexibility to the PUs produced. Therefore, the synthesized PUs were quite soft and scratched easily. To conclude that the scratch resistance of polyols

with adipic acid used PU was 2B, whereas the scratch resistance of polyol with phthalic anhydride used PU was 2H.

In addition, using functionalized boehmites also affected the scratch resistance property of PU. The scratch resistance of PU produced with PE-PO-1 increased from 2B to 2H when diaminoethanol was used as chain extender, 2B to B when 1,4-butanediol was used as chain extender. The scratch resistance of PU produced with PE-PO-2 increased from 2H to 5H when diaminoethanol was used in the production.

Table 4.5 Scratch resistance values of synthesized PUs.

Sample	Scratch Resistance
PU-1	2B
PU-2	2H
PU-3	B
PU-4	5H
PU-5	2H
PU-6	5H
PU-7	5H
PU-8	2H
PU-9	H
PU-10	2B
PU-11	B
PU-12	B

4.4.4 ABRASION RESISTANCE

Functionalized boehmite in the coatings increases the resistance against abrasion as seen from Figure 4.23. The abrasion resistance of coating increased from 2 to 10 $l/\mu\text{m}$ when functionalized boehmite was used in PU produced with PE-PO-1 and 12 to 20 $l/\mu\text{m}$ when functionalized boehmite was used in PU produced with PE-PO-2. In addition, the results show that abrasion resistance is directly related with rigidity of the polymers. Therefore, abrasion resistance of PU produced with phthalic anhydride used polyol is six times higher than the other ones as seen from Figure 4.24. Abrasion resistance of PU was also tabulated in Appendix G.

Moreover, chain extender changed the abrasion resistance when it was used in the production of PU with PE-PO-2. The results showed that abrasion resistance of PU was 3 times higher than when diaminoethanol was used instead of 1,4-butanediol.

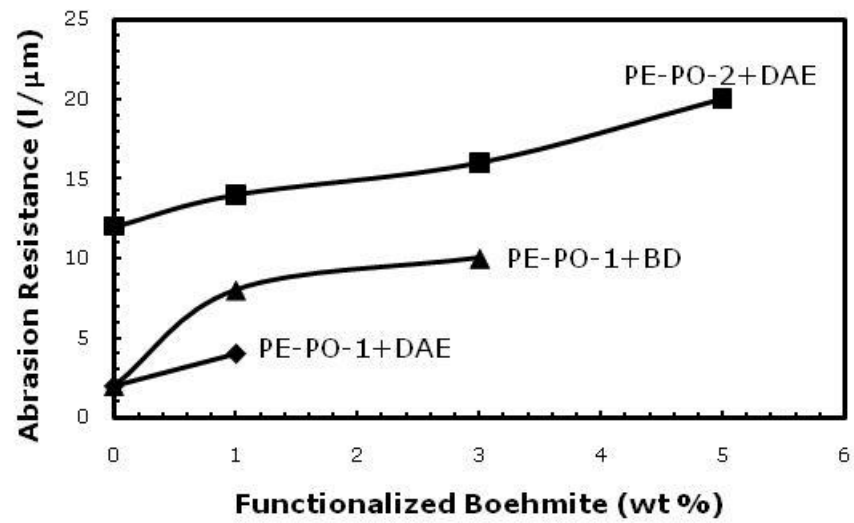


Figure 4.21 Effect of functionalized boehmite on the abrasion resistance of hybrid materials.

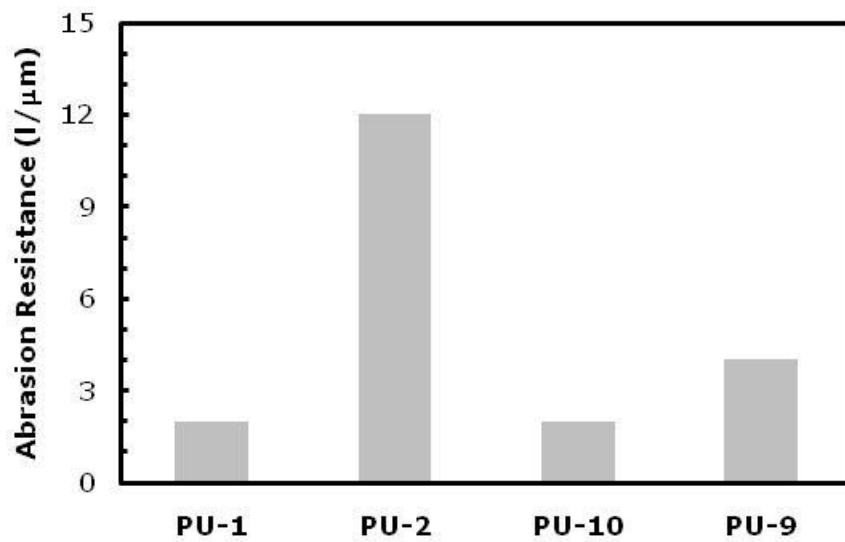


Figure 4.22 Effect of chain extender and PE-PO on the abrasion resistance of hybrid materials.

4.4.5 GLOSS

The gloss values of the synthesized PUs applied on glass plate were measured at three different angles of incidence as 20°, 60°, and 85°. According to standards, resins which have gloss values at 60° higher than 70 are considered as high gloss range. Therefore, the gloss of the PU coatings was neglected due to very small values between 2 to 10.

4.4.6 ADHESION TEST

Adhesion properties of the synthesized PUs applied on glass plate were measured by adhesion tester. Information about test application was given in Appendix F. The cross-cut adhesion of the synthesized PUs was tabulated in Table 4.8.

The results show that the PUs with polyols containing phthalic anhydride have very low adhesion property. It should be due to the aromatic content which imparts rigidity, and makes the hybrid material highly brittle and this causes some cracks on the coating. Moreover, 1,4-butanediol increased adhesion of the PU coatings produced with PE-PO-1.

Table 4.6 Adhesion of synthesized PUs.

Sample	Adhesion Property
PU-1	1
PU-2	1
PU-3	-
PU-4	-
PU-5	0
PU-6	2
PU-7	4
PU-8	4
PU-9	1
PU-10	0
PU-11	0
PU-12	0

CHAPTER 5

CONCLUSIONS

1. Nano-boehmite production with aluminum hydroxide by hydrothermal process was achieved.
2. Time, pH and concentration of acid and base were controlled. Aspect ratio of the plate-like boehmites increased with increasing the reaction time. The morphology of the particles was determined by pH adjustment. Plate-like boehmite particles were produced by controlling the concentration of acid and base.
3. Dispersion of nano-boehmite particles was very difficult due to the surface forces of the boehmite nano-particles. Even so, complete dispersion was almost achieved by grinding of $\text{Al}(\text{OH})_3$ and ultrasonic mixing at every step of the experiments.
4. The width of the produced plate-like boehmite particles changes between 10-50nm and the height between 400-500 nm.
5. MDI and HDI were used for the functionalization of plate-like boehmite nano-particles. FTIR, SEM, DTA-TGA and

Elemental analyses results prove functionalization of nano-boehmites.

6. Functionalization with MDI was carried out more successfully than HDI functionalization. In FTIR analysis, cyanate peak to boehmite peak ratio in MDI is higher in HDI.
7. Polyester-polyols with different diacid source (adipic and phthalic) were synthesized to be used in PU organic-inorganic hybrid materials. Polyester polyols produced with phthalic anhydride gave rigidity of the PU due to the phenyl groups in the chains.
8. PU organic-inorganic hybrid materials were produced by polymerization of monomers in the presence of functionalized boehmite nano-particles. Produced PU organic-inorganic hybrid materials were used for coating applications.
9. The hardness of PU produced with PE-PO-1 increased from 82 to 98 Persoz and the hardness of PU produced with PE-PO-2 increased from 52 to 78 Persoz when one weight percentage of functionalized boehmite is used in the production.
10. The scratch resistance of PU produced with PE-PO-1 increased from 2B to 2H when diaminoethanol was used as chain extender, from 2B to B when 1,4-butanediol was used as chain extender. The scratch resistance of PU produced

with PE-PO-2 increased from 2H to 5H when diaminoethanol was used in the production.

11. The abrasion resistance of coating increased from 2 to 10 $l/\mu\text{m}$ when functionalized boehmite was used in PU produced with PE-PO-1, and from 12 to 20 $l/\mu\text{m}$ when functionalized boehmite was used in PU produced with PE-PO-2.

REFERENCES

1. Wang, Y., Lim, S., Luo, J.L., and Xu, Z.H., *Tribological and Corrosion Behaviors of Al₂O₃/Polymer Nanocomposite Coatings*. *Wear*, 2006. **260**(9-10): p. 976-983.
2. Friedrich, K., Fakirov, S., and Zhang, Z., *Polymer Composites from Nano-to Macro-Scale*. 1 ed. Application of Non-Layered Nanoparticles in Polymer Modification, ed. K. Friedrich. 2005, New York: Springer Science+Business Media.
3. Galip, H., Hasipoğlu, H., and Gündüz, G., *Flame-Retardant Polyester*. *Journal of Applied Polymer Science*, 1999. **74**(12): p. 2906-2910.
4. *Definitions and Categories of Hybrid Materials*, Retrieved from <http://www.azom.com/Details.Asp?Articleid=4845>, Last Visited on 19/01/2011.
5. Yanagisawa, K., Gushi, D., Onda, A., and Kajiyoshi, K., *Hydrothermal Synthesis of Boehmite Plate Crystals*. *Journal of the Ceramic Society of Japan*, 2007. **115**(12): p. 894-897.
6. Dhoke, S., Mangal Sinha, T., and Khanna, A., *Effect of Nano-Al₂O₃ Particles on the Corrosion Behavior of Alkyd Based Waterborne Coatings*. *Journal of Coatings Technology and Research*, 2009. **6**(3): p. 353-368.

7. Vogelson, C.T., Koide, Y., Alemany, L.B., and Barron, A.R., *Inorganic–Organic Hybrid and Composite Resin Materials Using Carboxylate-Alumoxanes as Functionalized Cross-Linking Agents*. *Chemistry of Materials*, 2000. **12**(3): p. 795-804.
8. Molphy, M., Laslett, R.L., Gunatillake, P.A., Rizzardo, E., and Mainwaring, D.E., *Surface Modification of Kaolin. 1. Covalent Attachment of Polyethylene Glycol Using a Urethane Linker*. *Polymer International*, 1994. **34**(4): p. 425-431.
9. Shahid, N., Villate, R.G., and Barron, A.R., *Chemically Functionalized Alumina Nanoparticle Effect on Carbon Fiber/Epoxy Composites*. *Composites Science and Technology*, 2005. **65**(14): p. 2250-2258.
10. Türünç, O., Kayaman-Apohan, N., Kahraman, M., Menceloğlu, Y., and Güngör, A., *Nonisocyanate Based Polyurethane/Silica Nanocomposites and Their Coating Performance*. *Journal of Sol-Gel Science and Technology*, 2008. **47**(3): p. 290-299.
11. Sugimoto, H., Daimatsu, K., Nakanishi, E., Ogasawara, Y., Yasumura, T., and Inomata, K., *Preparation and Properties of Poly(Methylmethacrylate)-Silica Hybrid Materials Incorporating Reactive Silica Nanoparticles*. *Polymer*, 2006. **47**(11): p. 3754-3759.
12. Mammeri, F., Bourhis, E.L., Rozes, L., and Sanchez, C., *Mechanical Properties of Hybrid Organic-Inorganic Materials*. *Journal of Materials Chemistry*, 2005. **15**(35-36): p. 3787-3811.

13. Gläsel, H.J., Hartmann, E., Wennrich, L., Höche, T., and Buchmeiser, M.R., *Novel Nanosized Aluminium Carboxylates: Synthesis, Characterization and Use as Nanofillers for Protective Polymeric Coatings*. *Macromolecular Materials and Engineering*, 2007. **292**(1): p. 70-77.
14. *Functionalized Alumina Particles for Polymer Composites*, U.S.D.o.t. Interior, Editor. 2007: USA. p. 1-8.
15. Li, H., Yan, Y., Liu, B., Chen, W., and Chen, S., *Studies of Surface Functional Modification of Nanosized [Alpha]-Alumina*. *Powder Technology*, 2007. **178**(3): p. 203-207.
16. Brostow, W., Datashvili, T., Huang, B., and Too, J., *Tensile Properties of LDPE + Boehmite Composites*. *Polymer Composites*, 2009. **30**(6): p. 760-767.
17. Chen, S., Sui, J., and Chen, L., *Positional Assembly of Hybrid Polyurethane Nanocomposites Via Incorporation of Inorganic Building Blocks into Organic Polymer*. *Colloid & Polymer Science*, 2004. **283**(1): p. 66-73.
18. Brostow, W. and Datashvili, T., *Chemical Modification and Characterization of Boehmite Particles*. *Chemistry and Chemical Technology*, 2008. **2**(1): p. 27-32.
19. Liu, Y.-L., Hsu, C.-Y., Wang, M.-L., and Chen, H.-S., *A Novel Approach of Chemical Functionalization on Nano-Scaled Silica Particles*. *Nanotechnology*, 2003. **14**: p. 813-819.

20. Gatos, K.G., Martínez Alcázar, J.G., Psarras, G.C., Thomann, R., and Karger-Kocsis, J., *Polyurethane Latex/Water Dispersible Boehmite Alumina Nanocomposites: Thermal, Mechanical and Dielectrical Properties*. *Composites Science and Technology*, 2007. **67**(2): p. 157-167.
21. Guo, Z., Kim, T.Y., Lei, K., Pereira, T., Sugar, J.G., and Hahn, H.T., *Strengthening and Thermal Stabilization of Polyurethane Nanocomposites with Silicon Carbide Nanoparticles by a Surface-Initiated-Polymerization Approach*. *Composites Science and Technology*, 2008. **68**(1): p. 164-170.
22. Horch, R.A., Shahid, N., Mistry, A.S., Timmer, M.D., Mikos, A.G., and Barron, A.R., *Nanoreinforcement of Poly(Propylene Fumarate)-Based Networks with Surface Modified Alumoxane Nanoparticles for Bone Tissue Engineering*. *Biomacromolecules*, 2004. **5**(5): p. 1990-1998.
23. Mathieu, Y., Lebeau, B., and Valtchev, V., *Control of the Morphology and Particle Size of Boehmite Nanoparticles Synthesized under Hydrothermal Conditions*. *Langmuir*, 2007. **23**(18): p. 9435-9442.
24. Chattopadhyay, D.K., Muehlberg, A.J., and Webster, D.C., *Organic-Inorganic Hybrid Coatings Prepared from Glycidyl Carbamate Resins and Amino-Functional Silanes*. *Progress in Organic Coatings*, 2008. **63**(4): p. 405-415.

25. *Functional Particles*, Retrieved from <http://www.cmu.edu/maty/materials/properties-of-well-defined/functional-particles.html> Last Visited on 19/01/2011.
26. Alphonse, P. and Courty, M., *Structure and Thermal Behavior of Nanocrystalline Boehmite*. *Thermochimica Acta*, 2005. **425**(1-2): p. 75-89.
27. Chen, J.H., Rong, M.Z., Ruan, W.H., and Zhang, M.Q., *Interfacial Enhancement of Nano-SiO₂/Polypropylene Composites*. *Composites Science and Technology*, 2009. **69**: p. 252-259.
28. Zhang, J., Yu, J., and Guo, Z.X., *Modification of Nano-Alumina Surface by Michael Addition Reaction*. *Chinese Chemical Letters*, 2006. **17**(2): p. 251-252.
29. Guo, Z., Pereira, T., Choi, O., Wang, Y., and Hahn, H.T., *Surface Functionalized Alumina Nanoparticle Filled Polymeric Nanocomposites with Enhanced Mechanical Properties*. *Journal of Materials Chemistry*, 2006. **16**(27): p. 2800-2808.
30. Hozumi, A., Kim, B., and McCarthy, T.J., *Hydrophobicity of Perfluoroalkyl Isocyanate Monolayers on Oxidized Aluminum Surfaces*. *Langmuir*, 2009. **25**(12): p. 6834-6840.
31. Desset, S., Spalla, O., Lixon, P., and Cabane, B., *Variation of the Surface State of [Alpha]-Alumina through Hydrothermal Treatments*. *Colloids and Surfaces A: Physicochemical and Engineering Aspects*, 2002. **196**(1): p. 1-10.

32. Mousavand, T., Ohara, S., Umetsu, M., Zhang, J., Takami, S., Naka, T., and Adschiri, T., *Hydrothermal Synthesis and in Situ Surface Modification of Boehmite Nanoparticles in Supercritical Water*. *The Journal of Supercritical Fluids*, 2007. **40**(3): p. 397-401.
33. Kasprzyk-Hordern, B., *Chemistry of Alumina, Reactions in Aqueous Solution and Its Application in Water Treatment*. *Advances in Colloid and Interface Science*, 2004. **110**(1-2): p. 19-48.
34. *The Influence of Zeta Potential*, Retrieved from [Http://Www.Silver-Colloids.Com/tutorials/intropcs18.html](http://www.Silver-Colloids.Com/tutorials/intropcs18.html), Last Visited on 19/01/2011.
35. *Definitions and Categories of Hybrid Materials*, Retrieved from <http://www.nbtc.cornell.edu/facilities/downloads/zetasizer%20chapter%2016.Pdf>, Last Visited on 11/02/2011
36. *What Is Zeta Potential Explain in Detail*, Retrieved from <http://www.goiit.com/posts/list/physical-chemistry-what-is-zeta-potential-explain-in-detail-910458.htm>, Last Visited on 19/01/2011.
37. Awaja, F., Gilbert, M., Kelly, G., Fox, B., and Pigram, P.J., *Adhesion of Polymers*. *Progress in Polymer Science*, 2009. **34**(9): p. 948-968.
38. Rong, M.Z., Ji, Q.L., Zhang, M.Q., and Friedrich, K., *Graft Polymerization of Vinyl Monomers onto Nanosized Alumina Particles*. *European Polymer Journal*, 2002. **38**(8): p. 1573-1582.

39. Turri, S., Alborghetti, L., and Levi, M., *Formulation and Properties of a Model Two-Component Nanocomposite Coating from Organophilic Nanoclays*. Journal of Polymer Research, 2008. **15**(5): p. 365-372.
40. Wang, B., Liu, W., Zhu, Y., Yu, J., and Guo, Z., *A General Procedure for Surface Modification of Nano-Alumina and Its Application to Dendrimers*. Journal of Wuhan University of Technology--Materials Science Edition, 2007. **22**(3): p. 453-456.
41. Florjanczyk, Z., Debowski, M., Wolak, A., Malesa, M., and Plecha, J., *Dispersions of Organically Modified Boehmite Particles and a Carboxylated Styrene-Butadiene Latex: A Simple Way to Nanocomposites*. Journal of Applied Polymer Science, 2007. **105**(1): p. 80-88.
42. Perzyna, A., Zotto, C.D., Durand, J.O., Granier, M., Smietana, M., Melnyk, O., Stará, I.G., Starý, I., Klepetářová, B., and Šaman, D., *Reaction of Isocyanate-Functionalised Silicon Wafers with Complex Amino Compounds*. European Journal of Organic Chemistry, 2007. **2007**(24): p. 4032-4037.
43. Chen, S., Sui, J., Chen, L., and Pojman, J.A., *Polyurethane-Nanosilica Hybrid Nanocomposites Synthesized by Frontal Polymerization*. Journal of Polymer Science Part A: Polymer Chemistry, 2005. **43**(8): p. 1670-1680.
44. Nimbalkar, R. and Athawale, V., *Polyurethane Dispersions Based on Interesterification Product of Fish and Linseed Oil*. Journal of the American Oil Chemists' Society, 2010. **87**(9): p. 1035-1045.

45. Patel, A., Patel, C., Patel, M.G., Patel, M., and Dighe, A., *Fatty Acid Modified Polyurethane Dispersion for Surface Coatings: Effect of Fatty Acid Content and Ionic Content*. Progress in Organic Coatings, 2010. **67**(3): p. 255-263.
46. Athawale, V.D. and Nimbalkar, R.V., *Emulsifiable Air Drying Urethane Alkyds*. Progress in Organic Coatings, 2010. **67**(1): p. 66-71.
47. Çelebi, F., Aras, L., Gündüz, G., and Akhmedov, I., *Synthesis and Characterization of Waterborne and Phosphorus-Containing Flame Retardant Polyurethane Coatings*. Journal of Coatings Technology, 2003. **75**(944): p. 65-71.
48. Çelebi, F., Polat, O., Aras, L., Gündüz, G., and Akhmedov, I.M., *Synthesis and Characterization of Water-Dispersed Flame-Retardant Polyurethane Resin Using Phosphorus-Containing Chain Extender*. Journal of Applied Polymer Science, 2004. **91**(2): p. 1314-1321.
49. Choi, W.J., Kim, S.H., Jin Kim, Y., and Kim, S.C., *Synthesis of Chain-Extended Organifier and Properties of Polyurethane/Clay Nanocomposites*. Polymer, 2004. **45**(17): p. 6045-6057.
50. Awasthi, S. and Agarwal, D., *The Effect of Difunctional Acids on the Performance Properties of Polyurethane Coatings*. Journal of Coatings Technology and Research, 2009. **6**(3): p. 329-335.
51. Gündüz, G., *Boya Bilgisi*. 1st ed, Ankara: TMMOB Kimya Mühendisleri Odası. 184-199.

52. Takeichi, T., Guo, Y., and Agag, T., *Synthesis and Characterization of Poly(Urethane-Benzoxazine) Films as Novel Type of Polyurethane/Phenolic Resin Composites*. Journal of Polymer Science Part A: Polymer Chemistry, 2000. **38**(22): p. 4165-4176.
53. Maji, P.K., Guchhait, P.K., and Bhowmick, A.K., *Effect of the Microstructure of a Hyperbranched Polymer and Nanoclay Loading on the Morphology and Properties of Novel Polyurethane Nanocomposites*. ACS Applied Materials & Interfaces, 2008. **1**(2): p. 289-300.
54. Jena, K.K., Chattopadhyay, D.K., and Raju, K.V.S.N., *Synthesis and Characterization of Hyperbranched Polyurethane-Urea Coatings*. European Polymer Journal, 2007. **43**(5): p. 1825-1837.
55. Sharma, V. and Kundu, P.P., *Condensation Polymers from Natural Oils*. Progress in Polymer Science, 2008. **33**(12): p. 1199-1215.
56. Zilg, C., Thomann, R., Mülhaupt, R., and Finter, J., *Polyurethane Nanocomposites Containing Laminated Anisotropic Nanoparticles Derived from Organophilic Layered Silicates*. Advanced Materials, 1999. **11**(1): p. 49-52.
57. Li, G., Smith, R.L., Inomata, H., and Arai, K., *Synthesis and Thermal Decomposition of Nitrate-Free Boehmite Nanocrystals by Supercritical Hydrothermal Conditions*. Materials Letters, 2002. **53**(3): p. 175-179.

58. Zanganeh, S., Kajbafvala, A., Zanganeh, N., Mohajerani, M., Lak, A., Bayati, M., Zargar, H., and Sadrnezhad, S., *Self-Assembly of Boehmite Nanopetals to Form 3D High Surface Area Nanoarchitectures*. Applied Physics A: Materials Science & Processing, 2010. **99**(1): p. 317-321.
59. Mishra, D., Anand, S., Panda, R.K., and Das, R.P., *Hydrothermal Preparation and Characterization of Boehmites*. Materials Letters, 2000. **42**(1-2): p. 38-45.
60. Music, S., Dragcevic, Đ., and Popovic, S., *Hydrothermal Crystallization of Boehmite from Freshly Precipitated Aluminium Hydroxide*. Materials Letters, 1999. **40**(6): p. 269-274.
61. Liu, Y., Ma, D., Han, X., Bao, X., Frandsen, W., Wang, D., and Su, D., *Hydrothermal Synthesis of Microscale Boehmite and Gamma Nanoleaves Alumina*. Materials Letters, 2008. **62**(8-9): p. 1297-1301.
62. Brühne, S., Gottlieb, S., Assmus, W., Alig, E., and Schmidt, M.U., *Atomic Structure Analysis of Nanocrystalline Boehmite AlO(OH)*. Crystal Growth & Design, 2008. **8**(2): p. 489-493.
63. Tsai, M.-S., Yung, F.-H., and Yang, F.-H., *Boehmite Modification of Nano Grade [Alpha]-Alumina and the Rheological Properties of the Modified Slurry*. Ceramics International, 2007. **33**(5): p. 739-745.
64. Chen, Q., Udomsangpetch, C., Shen, S.C., Liu, Y.C., Chen, Z., and Zeng, X.T., *The Effect of AlOOH Boehmite Nanorods on*

Mechanical Property of Hybrid Composite Coatings. Thin Solid Films, 2009. **517**(17): p. 4871-4874.

65. Panda, P., Jaleel, V., and Usha Devi, S., *Hydrothermal Synthesis of Boehmite and α -Alumina from Bayer's Alumina Trihydrate*. Journal of Materials Science, 2006. **41**(24): p. 8386-8389.

66. Lepot, N., Van Bael, M.K., Van den Rul, H., D'Haen, J., Peeters, R., Franco, D., and Mullens, J., *Synthesis of Platelet-Shaped Boehmite and $[\gamma]$ -Alumina Nanoparticles Via an Aqueous Route*. Ceramics International, 2008. **34**(8): p. 1971-1974.

67. Inoue, M., *Glycothermal Synthesis of Metal Oxides*. Journal of Physics Condensed Matter, 2004. **16**: p. 1291-1303.

68. Mekasuwandumrong, O., Pavarajarn, V., Inoue, M., and Praserthdam, P., *Preparation and Phase Transformation Behavior of $[\chi]$ -Alumina Via Solvothermal Synthesis*. Materials Chemistry and Physics, 2006. **100**(2-3): p. 445-450.

69. Somiya, S. and Roy, R., *Hydrothermal Synthesis of Fine Oxide Powders*. Materials Science, 2000. **23**(6): p. 453-460.

70. Music, S., Dragcevic, D., Popovic, S., and Vdovic, N., *Microstructural Properties of Boehmite Formed under Hydrothermal Conditions*. Materials Science and Engineering B, 1998. **52**(2-3): p. 145-153.

71. Adschiri, T., Kanazawa, K., and Arai, K., *Rapid and Continuous Hydrothermal Synthesis of Boehmite Particles in Subcritical and Supercritical Water*. Journal of the American Ceramic Society, 1992. **75**(9): p. 2615-2618.
72. Buining, P.A., Pathmamanoharan, C., Bosboom, M., Jansen, J.B.H., and Lekkerkerker, H.N.W., *Effect of Hydrothermal Conditions on the Morphology of Colloidal Boehmite Particles: Implications for Fibril Formation and Monodispersity*. Journal of the American Ceramic Society, 1990. **73**(8): p. 2385-2390.
73. Hakuta, Y., Adschiri, T., Hirakoso, H., and Arai, K., *Chemical Equilibria and Particle Morphology of Boehmite (AlOOH) in Sub and Supercritical Water*. Fluid Phase Equilibria, 1999. **158-160**: p. 733-742.
74. Adschiri, T., Hakuta, Y., Sue, K., and Arai, K., *Hydrothermal Synthesis of Metal Oxide Nanoparticles at Supercritical Conditions*. Journal of Nanoparticle Research, 2001. **3**(2): p. 227-235.
75. Li, Y., Liu, J., and Jia, Z., *Fabrication of Boehmite AlOOH Nanofibers by a Simple Hydrothermal Process*. Materials Letters, 2006. **60**(29-30): p. 3586-3590.
76. Wei, S., Zhang, J., Elsanousi, A., Lin, J., Shi, F., Liu, S., Ding, X., Gao, J., Qi, S., and Tang, C., *From Al₄B₂O₉ Nanorods to AlOOH (Boehmite) Hierarchical Nanoarchitectures*. Nanotechnology, 2007. **18**(255605): p. 1-6.

77. Hakuta, Y., Ura, H., Hayashi, H., and Arai, K., *Effects of Hydrothermal Synthetic Conditions on the Particle Size of [Gamma]-AlO(OH) in Sub and Supercritical Water Using a Flow Reaction System*. *Materials Chemistry and Physics*, 2005. **93**(2-3): p. 466-472.
78. Liu, Y., Li, X., Xu, Z., and Hu, Z., *Preparation of Flower-Like and Rod-Like Boehmite Via a Hydrothermal Route in a Buffer Solution*. *Journal of Physics and Chemistry of Solids*, 2010. **71**(3): p. 206-209.
79. Zhang, J., Liu, S., Lin, J., Song, H., Luo, J., Elssfah, E.M., Ammar, E., Huang, Y., Ding, X., Gao, J., Qi, S., and Tang, C., *Self-Assembly of Flowerlike AlOOH (Boehmite) 3D Nanoarchitectures*. *The Journal of Physical Chemistry B*, 2006. **110**(29): p. 14249-14252.
80. Zhang, J., Wei, S., Lin, J., Luo, J., Liu, S., Song, H., Elawad, E., Ding, X., Gao, J., Qi, S., and Tang, C., *Template-Free Preparation of Bunches of Aligned Boehmite Nanowires*. *The Journal of Physical Chemistry B*, 2006. **110**(43): p. 21680-21683.
81. Liu, Q., Wang, A., Wang, X., and Zhang, T., *Morphologically Controlled Synthesis of Mesoporous Alumina*. *Microporous and Mesoporous Materials*, 2007. **100**(1-3): p. 35-44.
82. Sharma, P.K., Jilavi, M.H., Burgard, D., Nass, R., and Schmidt, H., *Hydrothermal Synthesis of Nanosize Alpha-Al₂O₃ from Seeded Aluminum Hydroxide*. *Journal of the American Ceramic Society*, 1998. **81**(10): p. 2732-2734.

83. Tsuchida, T., *Hydrothermal Synthesis of Submicrometer Crystals of Boehmite*. Journal of the European Ceramic Society, 2000. **20**(11): p. 1759-1764.
84. Kaya, C., He, J.Y., Gu, X., and Butler, E.G., *Nanostructured Ceramic Powders by Hydrothermal Synthesis and Their Applications*. Microporous and Mesoporous Materials, 2002. **54**(1-2): p. 37-49.
85. Zhu, H.Y., Gao, X.P., Song, D.Y., Ringer, S.P., Xi, Y.X., and Frost, R.L., *Manipulating the Size and Morphology of Aluminum Hydrous Oxide Nanoparticles by Soft-Chemistry Approaches*. Microporous and Mesoporous Materials, 2005. **85**(3): p. 226-233.
86. Jun-Cheng, L., Lan, X., Feng, X., Zhan-Wen, W., and Fei, W., *Effect of Hydrothermal Treatment on the Acidity Distribution of [Gamma]-Al₂O₃ Support*. Applied Surface Science, 2006. **253**(2): p. 766-770.
87. Cook, R.L., Elliott, B.J., Luebben, S.D., Myers, A.W., and Smith, B.M., *Surface Modified Particles by Multi-Step Addition and Process for the Preparation Thereof*. 2006, TDA Research: USA. p. 1-32.
88. Zhao, C., Ji, L., Liu, H., Hu, G., Zhang, S., Yang, M., and Yang, Z., *Functionalized Carbon Nanotubes Containing Isocyanate Groups*. Journal of Solid State Chemistry, 2004. **177**(12): p. 4394-4398.

89. Yoshinaga, K., *Functionalization of Inorganic Colloidal Particles by Polymer Modification*. Chemical Society of Japan, 2002. **75**: p. 2349-2358.
90. Krysztafkiewicz, A., Maik, M., and Rager, B., *Comparison of Waste Silica Fillers Modified with Various Proadhesive Compounds*. Journal of Materials Science, 1992. **27**(13): p. 3581-3588.
91. Fernández, L., Arranz, G., Palacio, L., Soria, C., Sánchez, M., Pérez, G., Lozano, A., Hernández, A., and Prádanos, P., *Functionalization of Γ -Alumina Cores by Polyvinylpyrrolidone: Properties of the Resulting Biocompatible Nanoparticles in Aqueous Suspension*. Journal of Nanoparticle Research, 2009. **11**(2): p. 341-354.
92. Kang, S., Hong, S.I., Choe, C.R., Park, M., Rim, S., and Kim, J., *Preparation and Characterization of Epoxy Composites Filled with Functionalized Nanosilica Particles Obtained Via Sol-Gel Process*. Polymer, 2001. **42**(3): p. 879-887.
93. Smuleac, V., Butterfield, D.A., Sikdar, S.K., Varma, R.S., and Bhattacharyya, D., *Polythiol-Functionalized Alumina Membranes for Mercury Capture*. Journal of Membrane Science, 2005. **251**(1-2): p. 169-178.
94. Zeng, Z., Yu, J., and Guo, Z.X., *Preparation of Functionalized Core-Shell Alumina/Polystyrene Composite Nanoparticles, 1*. Macromolecular Chemistry and Physics, 2005. **206**(15): p. 1558-1567.

95. Akram, D., Ahmad, S., and Sharmin, E., *Silica Reinforced Organic–Inorganic Hybrid Polyurethane Nanocomposites from Sustainable Resource*. *Macromolecular Chemistry and Physics*, 2010. **211**(4): p. 412-419.
96. Auxilio, A.R., Andrews, P.C., Junk, P.C., Spiccia, L., Neumann, D., Raverty, W., Vanderhoek, N., and Pringle, J.M., *Functionalised Pseudo-Boehmite Nanoparticles as an Excellent Adsorbent Material for Anionic Dyes*. *Journal of Materials Chemistry*, 2008. **18**(21): p. 2466-2474.
97. Mistry, A., Mikos, A., and Jansen, J., *Degradation and Biocompatibility of a Poly(Propylene Fumarate)-Based/Alumoxane Nanocomposite for Bone Tissue Engineering*. *Journal of Biomedical Materials Research Part A*, 2007. **83A**(4): p. 940-953.
98. Ding, Y., Xin, Z., Gao, Y., Yin, J., and Costa, G., *Functionalization of an Ethylene–Propylene Copolymer with Allyl(3-Isocyanate-4-Tolyl) Carbamate*. *Journal of Polymer Science Part B: Polymer Physics*, 2003. **41**(4): p. 387-402.
99. Braun, D. and Schmitt, M.W., *Functionalization of Poly(Propylene) by Isocyanate Groups*. *Polymer Bulletin*, 1998. **40**(2): p. 189-194.
100. Jiang, D., Xu, Y., Wu, D., and Sun, Y., *Isocyanate-Modified Tio₂ Visible-Light-Activated Photocatalyst*. *Applied Catalysis B: Environmental*, 2009. **88**(1-2): p. 165-172.

101. Cakic, S.M., Stamenkovic, J.V., Djordjevic, D.M., and Ristic, I.S., *Synthesis and Degradation Profile of Cast Films of Ppg-Dmpa-Ipdi Aqueous Polyurethane Dispersions Based on Selective Catalysts*. *Polymer Degradation and Stability*, 2009. **94**(11): p. 2015-2022.
102. Gündüz, G. and Kısakürek, R.R., *Structure–Property Study of Waterborne Polyurethane Coatings with Different Hydrophilic Contents and Polyols*. *Journal of Dispersion Science and Technology*, 2004. **25**(2): p. 217 - 228.
103. Vogt, H.C., Ile, G., Jr. Patton, J.T., and Wyandotte, M., *Process for the Preparation of Polyester Polyols*. 1977, BASF Wyandotte Corporation: USA. p. 1-6.
104. Pourjavadi, A., Rezai, N., and Zohuriaan-m, M.J., *A New Homologous Series of Linear Aliphatic Unsaturated Hydroxypolyesters a Polyol Soft Segments for Polyurethanes: Synthesis and Characterization*. *Journal of Applied Polymer Science*, 1998. **68**(2): p. 173-183.
105. Velayutham, T.S., Majid, W.H.A., Ahmad, A.B., Kang, G.Y., and Gan, S.N., *Synthesis and Characterization of Polyurethane Coatings Derived from Polyols Synthesized with Glycerol, Phthalic Anhydride and Oleic Acid*. *Progress in Organic Coatings*, 2009. **66**(4): p. 367-371.
106. Akram, D., Sharmin, E., and Ahmad, S., *Synthesis and Characterization of Boron Incorporated Polyester Polyol from*

Linseed Oil: A Sustainable Material. Macromolecular Symposia, 2009. **277**(1): p. 130-137.

107. Akram, D., Sharmin, E., and Ahmad, S., *Synthesis, Characterization and Corrosion Protective Properties of Boron-Modified Polyurethane from Natural Polyol*. Progress in Organic Coatings, 2008. **63**(1): p. 25-32.

108. Somani, K., Kansara, S., Parmar, R., and Patel, N., *High Solids Polyurethane Coatings from Castor-Oil – Based Polyester-Polyols*. International Journal of Polymeric Materials, 2004. **53**(3): p. 283 - 293.

109. Kısakürek, R.R., *Structure-Property Study of Waterborne Polyurethane Coatings Based on Different Hydrophilic Contents and Polyols*, in *Chemical Engineering*. 2001, Middle East Technical University: Ankara. p. 80.

110. Çelebi, F., *Synthesis and Characterization of Waterborne and Phosphorus Containing Flame-Retardant Polyurethane Coatings*, in *Chemistry*. 2002, Middle East Technical University: Ankara. p. 98.

111. Ramesh, S., Rajalingam, P., and Radhakrishnan, G., *Chain-Extended Polyurethanes—Synthesis and Characterization*. Polymer International, 1991. **25**(4): p. 253-256.

112. Kim, S.C., Klempner, D., Frisch, K.S., Radigan, W., and Frisch, H.L., *Polyurethane Interpenetrating Polymer Networks. I. Synthesis and Morphology of Polyurethane-Poly(Methyl*

Methacrylate) Interpenetrating Polymer Networks. *Macromolecules*, 1976. **9**(2): p. 258-263.

113. Lv, W., Luo, Z., Weng, W., and Yang, H., *Synthesis, Characterization and Performance of Nanosized $Bi_{0.1}Sn_{0.9}O_2$ -WPU Organic-Inorganic Hybrid Coatings*. *Journal of Sol-Gel Science and Technology*, 2009. **51**(1): p. 58-62.

114. Di Gianni, A., Bongiovanni, R., Turri, S., Deflorian, F., Malucelli, G., and Rizza, G., *Uv-Cured Coatings Based on Waterborne Resins and SiO_2 Nanoparticles*. *Journal of Coatings Technology and Research*, 2009. **6**(2): p. 177-185.

115. Vaia, R.A. and Maguire, J.F., *Polymer Nanocomposites with Prescribed Morphology: Going Beyond Nanoparticle-Filled Polymers*. *Chemistry of Materials*, 2007. **19**(11): p. 2736-2751.

116. Chen, W., Tao, X., and Liu, Y., *Carbon Nanotube-Reinforced Polyurethane Composite Fibers*. *Composites Science and Technology*, 2006. **66**(15): p. 3029-3034.

117. Yang, Y., Xie, X., Yang, Z., Wang, X., Cui, W., Yang, J., and Mai, Y.-W., *Controlled Synthesis and Novel Solution Rheology of Hyperbranched Poly(Urea-Urethane)-Functionalized Multiwalled Carbon Nanotubes*. *Macromolecules*, 2007. **40**(16): p. 5858-5867.

118. Ahmadi, B., Kassiriha, M., Khodabakhshi, K., and Mafi, E.R., *Effect of Nano Layered Silicates on Automotive Polyurethane Refinish Clear Coat*. *Progress in Organic Coatings*, 2007. **60**(2): p. 99-104.

119. Singh, D., Rai, K.N., Jayasimha, T., and Kumar, A., *Synthesis and Characterization of Nanoalumina Styrene Acrylonitrile High Impact Composite as a Plausible Civilian Armour Material*. Journal of Composite Materials, 2007. **41**(23): p. 2785-2805.

APPENDIX A

PROPERTIES OF USED MATERIALS IN THE EXPERIMENTS

General information about the used materials were tabulated in Table A.1.

Table A.1 List of chemicals.

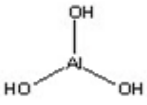
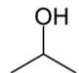
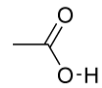
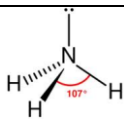
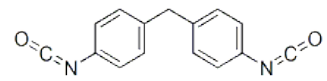
Chemical	Chemical Formula	Chemical Structure	MWt (g/mol)	Density (g/ml)	Purity	Firm	Usage
Aluminum Hydroxide (Al(OH) ₃)	Al(OH) ₃		78	-	extra pure	Merck	Production of boehmite
Isopropyl Alcohol (IPA)	C ₃ H ₈ O		60.1	0.786	≥99.5	Merck	wetting agent and solvent
Acetic Acid (AA)	CH ₃ COOH		60.05	1.049	Extra pure	Merck	peptization of Al(OH) ₃ plates
Ammonia Solution (AMM)	NH ₃		17.031	-	32%	Merck	adjusting the pH
4,4'-Methylene Diphenyl Diisocyanate (MDI)	C ₁₅ H ₁₀ N ₂ O ₂		250.25	1.230	98 %	Sigma-Aldrich	functionalization of boehmite and production of polyurethane

Table A.1 List of chemicals (continued).

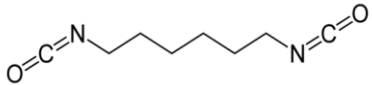
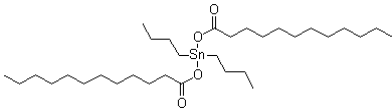
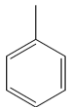
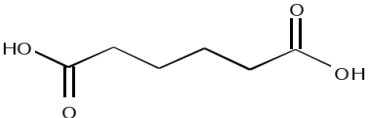
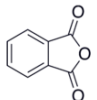
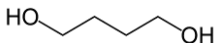
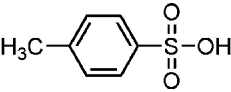
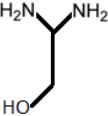
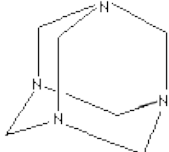
Chemical	Chemical Formula	Chemical Structure	MWt (g/mol)	Density (g/ml)	Purity	Firm	Usage
1,6-Hexamethylene Diisocyanate (HDI)	$C_8H_{12}N_2O_2$		168.2	1.047	98 %	Sigma-Aldrich	Surface modification of boehmite
Dibutyltin Dilaurate (DBTDL)	$C_{32}H_{64}O_4Sn$		631.56	1.066	95 %	Sigma-Aldrich	catalyst in the functionalization experiments
Toluene	$C_6H_5CH_3$		92.14	0.8669	≥99	Merck	Solvent
Adipic Acid (Ad.Ac.)	$(CH_2)_4(COOH)_2$		146.14	1.36	extra pure	Sigma-Aldrich	production of polyester polyol

Table A.1 List of chemicals (continued).

Chemical	Chemical Formula	Chemical Structure	MWt (g/mol)	Density (g/ml)	Purity	Firm	Usage
Phthalic Anhydride (PA)	$C_6H_4(CO)_2O$		148.1	1.53	≥98	Sigma-Aldrich	production of polyester polyol
1,4-Butanediol (BD)	$C_4H_{10}O_2$		90.121	1.0171	≥99	Merck	polyester polyol synthesis, and chain extender
p-Toluenesulfonic Acid (TSA)	$CH_3C_6H_4SO_3H$		172.20	-	≥99	Merck	catalyst in polyester polyol synthesis
Diaminoethanol (DAE)	$C_2H_3OH(NH_2)_2$		76.4	-	-	-	chain extender in polyurethane production
Hexamethylenetetramine (HMTA)	$(CH_2)_6N_4$		140.186	1.33	-	-	crosslinking agent in polyurethane production

APPENDIX B

CALCULATIONS OF THE EXPERIMENTS

B.1. PRE-GRINDING CALCULATION

$$W_{\text{balls}} = 622,9 \text{ g}$$

$$\text{Ball to particles ratio} = 12$$

$$W_{\text{particles}} = \frac{W_{\text{balls}}}{\text{Ball to particles ratio}} = \frac{622,9}{12} = 51,9 \text{ g} \quad (1)$$

$$\text{Liquid to solid molar ratio} = 0,5$$

$$V_{\text{liquid}} = (W_{\text{particles}} / \rho_{\text{particle}}) \times 0,5 = 28,8 \text{ ml} \quad (2)$$

$$W_{\text{liquid}} = \frac{28,8}{0,786} = 22,7 \text{ g}$$

Planetary Ball Milling Weight Balance Adjust;

$$W_{\text{empty_jar}} = 2700,0 \text{ g}$$

$$W_{\text{balls}} = 622,9 \text{ g}$$

$$W_{\text{particles}} = 51,9 \text{ g}$$

$$W_{\text{liquid}} = 22,7 \text{ g}$$

$$\begin{aligned} W_{\text{total}} &= W_{\text{empty_jar}} + W_{\text{balls}} + W_{\text{particles}} + W_{\text{liquid}} \\ &= 3397,6 \text{ g} \end{aligned} \quad (3)$$

B.2. GAP SOLUTION PREPARATION

$$V_{\text{total of the reactor}} = 1200 \text{ ml}$$

$$V_{\text{solution}} = 130 \text{ ml}$$

$$V_{\text{gap}} = 1070 \text{ ml}$$

Acetic acid amount;

$$\begin{aligned} V_{\text{AA in the gap}} &= \frac{V_{\text{AA in the solution}}}{V_{\text{solution}}} \times V_{\text{gap}} & (4) \\ &= (15/130) \times 1070 = 123.5 \text{ ml AA} \end{aligned}$$

Ammonia solution amount;

$$\begin{aligned} V_{\text{AMM in the gap}} &= \frac{V_{\text{AMM in the solution}}}{V_{\text{solution}}} \times V_{\text{gap}} & (5) \\ &= \{(15.84 \text{ g}/0.928)/130\} \times 1070 = 140.5 \text{ ml} \end{aligned}$$

Technical ammonia solution contains 25 % ammonia;

Therefore;

$$140.5 \text{ ml ammonia} \times 100 / 25 = 562.0 \text{ ml ammonia solution}$$

$$\begin{aligned} V_{\text{water}} &= V_{\text{total}} - V_{\text{AA}} - V_{\text{AMM}} & (6) \\ &= 1070 - 123.5 - 562.0 = 385.5 \text{ ml water} \end{aligned}$$

APPENDIX C

ACID NUMBER DETERMINATION

Acid number is the number of milligrams of potassium hydroxide required to neutralize the free acids in 1 gram of the tested material under test conditions. The acid number of varnishes or resin solutions should be expressed on the basis of solid components, not on the solution. Usually, the acidity is due to the presence of carboxylic groups from free fatty acids or acids used in polyester production.

Determination of acid number is made by titration of a mixture of sample and solvent with carefully standardized potassium or sodium hydroxide solution free from carbonates, using phenolphthalein as indicator, and a pink coloration as the end point. The acid number is calculated from the following equation:

$$\text{Acid Number} = \frac{V \times N \times 56.11}{W} \quad (7)$$

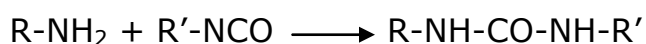
Where V is the volume of potassium hydroxide solution consumed, in ml, N is the normality of the solution, and W is the weight of the sample in gram, (solid basis).

APPENDIX D

DIBUTYLAMINE BACK TITRATION

This test method can be used to determine the NCO content in diisocyanate intermediate or the free (i.e. reactive) isocyanate available in a prepolymer.

Primary and secondary amines react with isocyanate to yield the corresponding urea.



This reaction is quite quantitative in the presence of an excess of the amine and is the basic reaction for most of the methods by which the isocyanate content of a sample is determined by back titration with an acid. The most widely used amine is dibutylamine, trichlorobenzene is used as a solvent.

The butylamine solution is prepared by dissolving 129 g of freshly distilled dibutylamine in 871 g of trichlorobenzene, and storing the resultant solution in the dark.

In the determination, about 2 g of the diisocyanate should be accurately weighed out into a conical flask and 5 ml of trichlorobenzene added. The mixture may be warmed to assist the solution. There is then added 25 ml of the standard dibutylamine

solution. The reaction is rapid and takes only a few minutes for complexation when a clear solution is obtained. After bromophenol blue and 100 ml of methanol, the excess dibutylamine can be titrated with 1 N HCl. The end point is reacted with the disappearance of the blue color and the appearance of a yellow color that persist for at least 15 seconds.

V1: Volume (in ml) of HCl solution is required for titration of the sample.

V2: Volume (in ml) of HCl solution is required for titration of 25 ml of dibutylamine solution (blank)

M: Molarity of HCl

Then,

$$NCO \% = 42 \times M \times \left[\frac{(V_2 - V_1)}{1000} \times W \right] \times 100 \quad (8)$$

APPENDIX E

MOLECULAR WEIGHT CALCULATION OF POLYESTER-POLYOL

Adjust the composition of the reaction mixture

A-A & B-B

$$N_A < N_B \quad \longrightarrow \quad r = \frac{N_A}{N_B}$$

$$\frac{N_A + N_B}{2} = \text{Total \# of monomer molecules present} = \frac{N_A(1 + 1/r)}{2} \quad (9)$$

At P (fraction of A groups reacted at time t) for B groups extent of reaction = rP

Therefore the total # of chain ends:

$$N_A(1 - P) + N_B(1 - rP) = N_A \left(1 - P + \frac{(1 - rP)}{r} \right) \quad (10)$$

Take 1/2 if number of molecules are needed

$$\bar{X}_n = \frac{\frac{N_A(1 + 1/r)}{2}}{\frac{N_A \left[1 - P + \frac{(1 - rP)}{r} \right]}{2}} = \frac{1 + r}{1 + r - 2rP} \quad (11)$$

$$= \frac{\text{total \# of A-A \& B-B molecules}}{\text{total \# of polymer molecules}} \quad (12)$$

APPENDIX F

INSTRUMENTAL INFORMATION

F.1. SEM (SCANNING ELECTRON MICROSCOPY) ANALYSIS

Morphologies and sizes of the produced boehmite nano-particles were characterized for comparing the differences between aluminum hydroxide, boehmite nano-particles, and functionalized boehmite nano-particles by Scanning Electron Microscopy in Central Laboratory at METU (Model No: Quanta 400 Field Emission SEM).

F.2. FTIR (FOURIER TRANSFORM INFRARED) SPECTROSCOPY

Boehmite nano-particles and synthesized polymers were analyzed for determining the molecular structure by FTIR spectroscopy in Mechanical Engineering Department at Hacettepe University (Model No: IR Prestige-21 SHIMADZU).

F.3. XRD (X-RAY DIFFRACTION) ANALYSIS

Structural characterization of aluminum hydroxide and the produced boehmite nano-particles were carried out by using X-ray Diffractometer in Metallurgical and Materials Engineering Department at METU (Model No: RIGAKU – D/Max-2200/PC) and

CuK α ($\lambda = 0.154$ nm) at 40 kV and 40 mA with a 2θ from 10° to 90° . Phase purities and crystallite sizes of the produced boehmite particles were calculated from XRD patterns. In addition, 100 % transition of aluminum hydroxide to boehmite nano-particles was proved by comparing the XRD patterns.

F.4. PCS (PHOTON CORRELATION SPECTROSCOPY)

The particle sizes of the produced particles were measured by using particle size analyzer in Chemical Engineering Department at METU (Malvern Zetasizer Nano Instrument – Model No: ZEN3500, Malvern Instruments Ltd.). The measurement range of the instrument is in between 1 nm and 5 μ m. Samples were prepared either in acetic acid or in IPA and 2-5 minutes ultrasonic mixing was applied to have better dispersion. The measurements were carried out by using zeta cells.

F.5. BET (BRUNAUER-EMMET-TELLER) ANALYSIS

Surface area of boehmite nano-particles was determined to see the change in the specific surface area of the samples by BET analysis in Central Laboratory at METU (Model No: Quantachrome Corporation, Autosorb-6).

Technical specifications:

Heating: Degas heating up to 350°C in steps of 1°C (physical adsorption)

Pressure: 1×10^{-5} - 1.0 atm. (Nitrogen)

Minimum Surface Area: 0.05 m²/g

Pore Diameter Interval: 5-500 Å

F.6. ELEMENTAL ANALYSIS

The analysis of nitrogen content of boehmite and functionalized boehmite particles was done to demonstrate the functionalization in Central Laboratory at METU (Model No: LECO, CHNS-932).

F.7. DTA-TGA (DIFFERENTIAL THERMAL ANALYSIS-THERMAL GRAVIMETRIC ANALYSIS)

Functionalization of the boehmite nano-particles was also checked by TGA/DTA analysis device in Central Laboratory at METU (Model No: Setaram Labsys TGA/DTA).

Technical Specifications:

Temperature Range: 170-1700 °C

Weight Accuracy: 0.4 µg

Measurement Range: ± 200 mg

Scanning Rate: 0.01-50 °C/min

F.8. MECHANICAL TESTS

F.8.1. FILM APPLICATION

The produced PU coatings were applied on a glass and metal plate surface by using a Braive Instrument casting knife film applicator with 50 μ m wet thickness (Chemical Engineering Department at METU). The metal plates were used for impact test while glass panels were used for pendulum hardness test, scratch resistance, abrasion resistance, adhesion test, and gloss test. Tests were applied to the specimens after 7 days of drying at room temperature.

F.8.2. PENDULUM HARDNESS TEST

Hardness of the samples was determined by Persoz Pendulum Hardness Tester in Chemical Engineering Department at METU (Braive Instruments Hardness Tester, Model 3034)). This method evaluates hardness by measuring the damping time of an oscillating pendulum. Pendulum hardness tester is shown in Figure F.1.

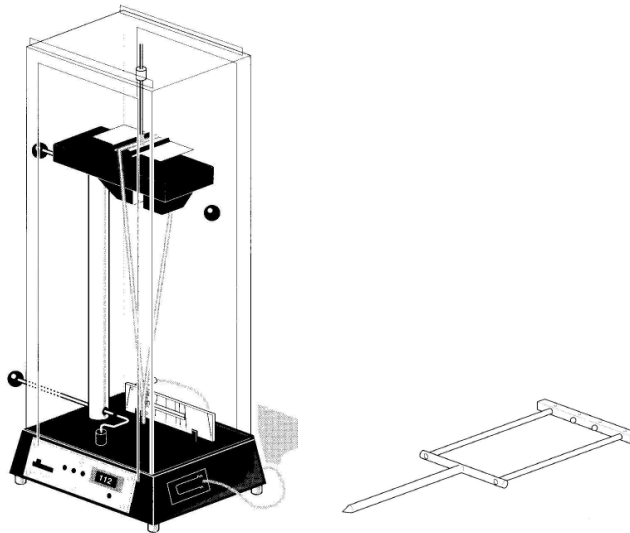


Figure F.1 Pendulum hardness tester and persoz pendulum.

F.8.3. IMPACT RESISTANCE TEST

Impact test is used to establish the stone-chip resistance of coatings which is the outstanding ability to impact with minimum damage. For this test a Gardner Impact Tester Chemical Engineering Department at METU (Model 5524) was used as shown in Figure F.2. The principle of test depends on the determination of potential energy needed to cause damage by drop weight (2 kg) released from a specified height. Impact resistance is determined when cracks first appeared in the coating. The potential energy is simply calculated from

$$\text{Impact Energy (J)} = m \cdot g \cdot h \quad (13)$$

m = weight of the dropweight (kg)

g = gravitational acceleration of the earth (m/sec^2)

h = height of dropweight (m)

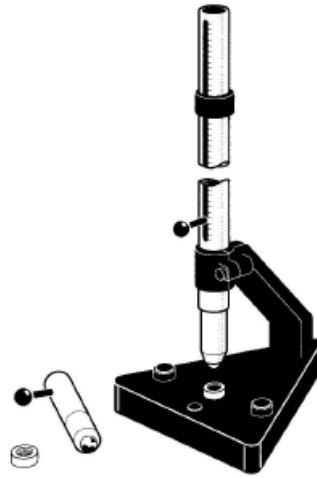


Figure F.2 Impact resistance tester.

The transfer of impact through the film is shown in Figure F.3 (a) and the result is shown in Figure F.3 (b). In debonding area, compression stress is present in the middle and the shear stress is in the annular region. Therefore debonding area is inversely proportional to the measure of the adhesion. The larger the debonding area means the lower the adhesion level of the coating

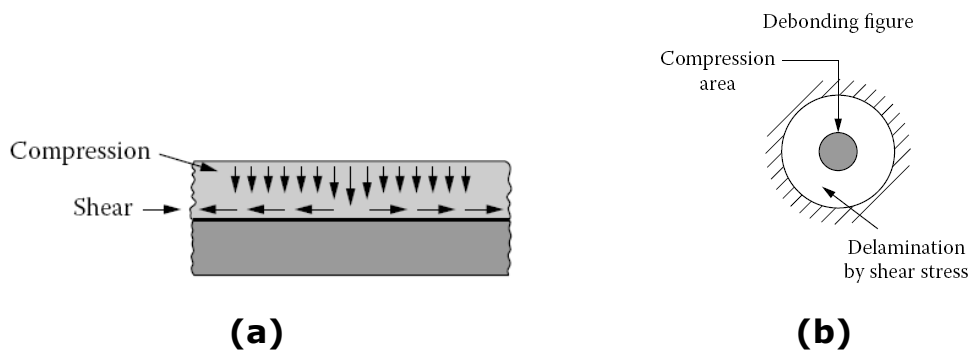


Figure F.3 (a) Transfer of impact, (b) result of impact.

F.8.4. SCRATCH RESISTANCE TEST

Scratch resistance of coating was measured by pencil with different hardness (2B, B, HB, H, and 2H). The compass used was adjusted to 45 ° of inclination, and the pencil was applied to the coating.

F.8.5. ABRASION RESISTANCE TEST

Abrasion resistance of coating was measured by sand-abrasion device Chemical Engineering Department at METU. The test specimen was placed at 45 ° inclination. Sand is poured down from a height of 91.5 cm height. The volume of standard size sand is recorded for certain abrasion of the film thickness. The test equipment is shown in Figure F.4.

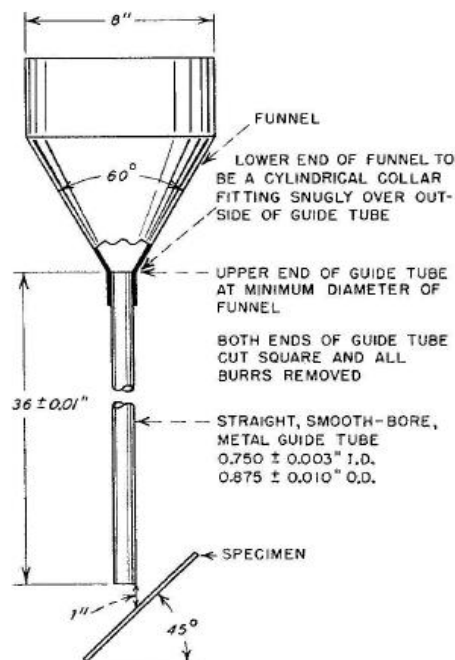


Figure F.4 Abrasion resistance tester.

F.8.6. SPECULAR GLOSS

Gloss of the paint samples were measured by a glossmeter (Rhopoint, Novo-Gloss) at different angles 25°, 60°, and 85°.

F.8.7. ADHESION TEST

This test was performed to measure the strength of the bonds formed by surface and coating material. Cross cut Test with ASTM D-3359 is the most common used adhesion test and the equipment is shown in Figure 3.23 (a). The classification is based on the percentage of paint flakes occurred in the surface and the levels are shown in Figure 3.23 (b)

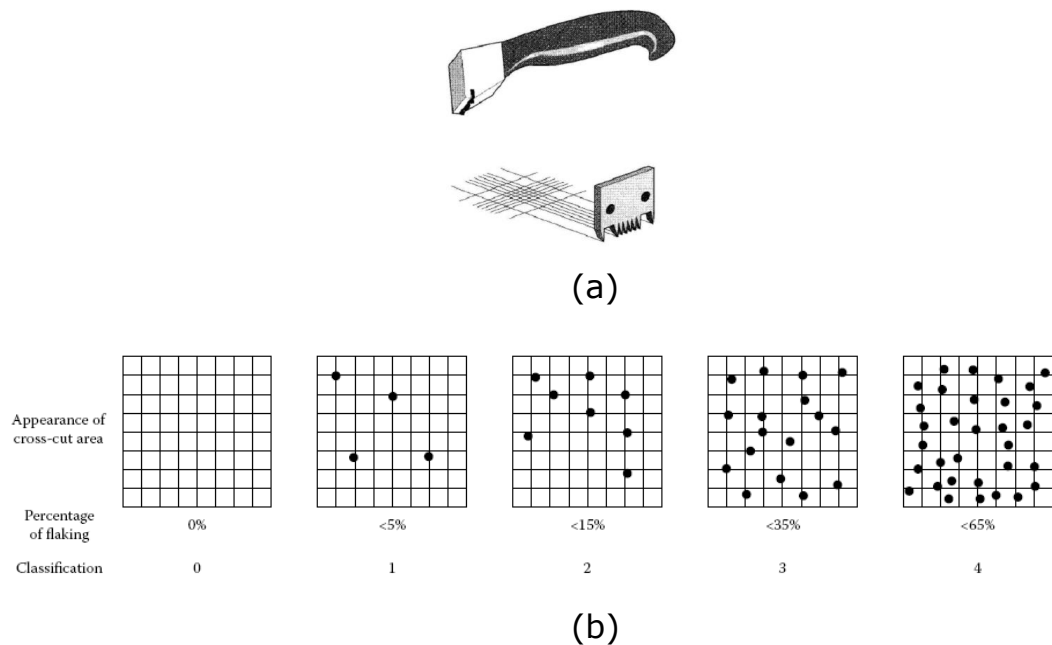


Figure 3.23 Cross-hatch cutter and levels for the classification of film.

APPENDIX G

MECHANICAL TESTS RESULTS

Table G.1 Hardness values of synthesized PUs.

Sample	Perso_z (s)
PU-1	40
PU-2	52
PU-3	30
PU-4	40
PU-5	60
PU-6	78
PU-7	75
PU-8	66
PU-9	32
PU-10	82
PU-11	98
PU-12	87

Table G.2 Abrasion resistance values of synthesized PUs.

Sample	Abrasion Resistance (I/μm)
PU-1	2
PU-2	12
PU-3	-
PU-4	-
PU-5	4
PU-6	14
PU-7	16
PU-8	20
PU-9	4
PU-10	2
PU-11	8
PU-12	10